EFFECT OF FALL RYE COVER CROP ON CO_2 AND N_2O FLUXES IN THE RED RIVER VALLEY, MANITOBA, CANADA

by

Kathryn E. Webb

A Thesis

Submitted to the Faculty of Graduate Studies of

The University of Manitoba

In partial fulfilment of the requirements for the degree of

MASTER OF SCIENCE

Department of Soil Science

University of Manitoba

Winnipeg, Manitoba

ABSTRACT

Webb, Kathryn Emily. M.Sc., The University of Manitoba, July, 2023. Effect of fall rye cover crop on CO_2 and N_2O fluxes in the Red River Valley, Manitoba, Canada. Supervisor: Mario Tenuta.

Cover crops can increase carbon (C) sequestration in soils. However, there is limited understanding of how cover crops affect carbon dioxide (CO_2) and nitrous oxide (N_2O) fluxes from agricultural soils in the Canadian Prairies. Research was conducted at the Trace Gas Manitoba (TGAS-MAN) long-term research site to determine the effect of a fall rye (*Secale cereale* L.) cover crop on spring-thaw and post-fertilizer N_2O emissions, CO_2 fluxes, and grain yield. Fluxes were measured over four years (2019-2022) from four 4-ha fields using the flux gradient method. In the fall of 2018 two fields were seeded no-till with fall rye and two were cultivated and left into winter. The cover crop was terminated the following spring with an herbicide application and the cash crops oats (*Avena sativa*), canola (*Brassica napus*), and spring wheat (*Triticum aestivum* L.) were grown in 2019, 2020, 2021, and 2022. 2020 and 2021 CO_2 fluxes were removed due to unreliable data caused by flux measurement equipment. In 2019, C assimilation by the cover crop resulted in the system being a C sink of 424 kg C ha^{-1} after accounting for harvest removals, and the conventional system was a C source of 248 kg C ha^{-1}. In 2022, wet growing conditions resulted in both cropping systems being a C source, with the conventional and cover crop system losing 1,366 kg C ha^{-1} and 1,558 kg C ha^{-1}, respectively. The cover crop fields saw lower spring-thaw N_2O emissions during years of good cover crop establishment. N_2O emissions following fertilizer application and cumulative N_2O fluxes were lower in cover crop fields in all study years. Combining cumulative CO_2 fluxes and N_2O emissions in CO_2-equivalents (CO_2-eq) in 2019 and 2022, the cover crop system was a net greenhouse gas source of 5,665 CO_2-eq ha^{-1} and the

conventional system was a source of 7,653 CO_2-eq ha^{-1}. The cover crop did not significantly affect crop yields.

FOREWARD

This thesis has been developed in adherence with the manuscript guidelines established by the University of Manitoba's Department of Soil Science. Versions of Chapters 2 and 3 will be submitted for publication in the future.

The data, results, and contents of this thesis were collected, analyzed and written by Kathryn Webb. Data bias analysis of data collected in 2020 and 2021, as well as analysis of previous data to determine appropriate field comparisons from the TGAS-MAN site, were performed by Dr. Brian Amiro. The protocol to correct the data bias in 2020 and 2021 was proposed by Dr. Amiro and implemented by Kathryn Webb under the advisement of Dr. Mario Tenuta. Original versions of the bias correction protocol and field variability analysis written by Dr. Brian Amiro have been included in the Appendix of this thesis with permission from the author Dr. Brian Amiro and thesis advisor Dr. Mario Tenuta.

ACKNOWLEDGEMENTS

Thank you to my advisor, Dr. Mario Tenuta, for providing me with this opportunity and challenging me throughout my degree. Thank you for sharing your passion for soil ecology with me. A special thank you to the beloved technician, Dr. Brian Amiro, for your countless hours of help with the flux data, Matlab code, and having impromptu meetings with me to discuss and resolve the numerous issues I ran into. I am forever grateful! Thank you to Matt Gervais and Krista Hanis-Gervais for looking after the TGAS-MAN site prior to me coming onto the project and for taking the time to meet with me in the early stages of my program from Scotland. I appreciate you taking the time out of your evenings to answer my questions! Thank you to Marcus and Paul Loeppky for conducting all the agronomic field operations at the site. Thank you to Brad Sparling, Emma Unruh and Trevor Fraser for technical help in and out of the field and to Zhe Song and Mervin Bilous for analyzing samples in the laboratory. Thank you to the numerous technicians and summer students that helped with field work and sample processing. This project would not have been possible without you! Thank you to Dr. Francis Zvomuya for helping me with the statistics for my project, and thank you to my committee members, Dr. Xiaopeng Gao and Dr. Tim Papakyriakou, for guiding and supporting me through my degree.

Thank you to my family and friends who supported me and kept me sane throughout this adventure. A special thank you to my TGAS-MAN successor and friend, Shannon Mustard, for making my challenging 2022 field season a more enjoyable experience. I will cherish the many wild memories we made together in the field!

Funding for this project was provided by General Mills and NSERC Discovery. Thank you for this opportunity.

TABLE OF CONTENTS

Page

LIST OF TABLES

Table **Page**

LIST OF FIGURES

Figure **Page**

LIST OF ABBREVIATIONS

a.i.	active ingredient
a.s.l	above sea level
C	carbon
C/N	carbon to nitrogen ratio
cm	centimeter
CO_2	carbon dioxide
cv	cultivar
°C	degrees Celsius
d	zero-plane displacement
$\Delta[CO_2]$	carbon dioxide vertical concentration gradient
$\Delta[N_2O]$	nitrous oxide vertical concentration gradient
F_C	carbon flux
$F_{ECOSYSTEM}$	carbon balance
$F_{HARVEST}$	carbon removals
F_N	nitrous oxide flux
$F_{N\text{-}FERTILIZER}$	post-fertilizer nitrous oxide flux
$F_{N\text{-}SPRING\text{-}THAW}$	spring-thaw nitrous oxide flux
$\sum F_{GHG}$	cumulative net greenhouse gas flux equivalents
$\sum F_{GPP}$	gap-filled cumulative gross photosynthetic production
$\sum F_N$	cumulative gap-filled study year nitrous oxide flux
$\sum F_{NEP}$	cumulative net ecosystem production
$\sum F_{N\text{-}FERTILIZER}$	cumulative gap-filled post-fertilizer nitrous oxide flux

$\sum F_{N\text{-}SPRING\text{-}THAW}$	cumulative gap-filled spring-thaw nitrous oxide flux
$\sum F_R$	gap-filled cumulative respiration
GHG	greenhouse gases
GMC	gravimetric moisture content
GPP	gross photosynthetic production
GWP	global warming potential
ha	hectare
Hz	hertz
φ_1	stability correction factor for lower intake
φ_2	stability correction factor for upper intake
K	degrees Kelvin
k	von Karmann constant
K	turbulent transfer coefficient
KCl	potassium chloride
kg	kilogram
km	kilometer
L	litre
m	meter
M	molar concentration
m	autotropic respiration over gross photosynthetic production (1 – slope)
mA	milliampere
mb	millibar
Mg	megagram

mg	milligram
min	minute
ml	millilitre
mm	millimeter
N	nitrogen
N_2O	nitrous oxide
NEP	net ecosystem production
NH_4^+	ammonium
NO_2^-/NO_3^-	nitrate
PAR	photosynthetically active radiation
ppb	parts per billion
PPFD	photosynthetic photon flux density
ppm	parts per million
R	respiration
R_a	autotrophic respiration
R_h	heterotrophic respiration
TC	total carbon
TGAS-MAN	Trace Gas Manitoba
TN	total nitrogen
u_*	friction velocity
VMC	volumetric moisture content
WFPS	water-filled pore space
z	vertical height difference

z_1	lower intake height above zero-plane displacement
z_2	upper intake height above zero-plane displacement

1. INTRODUCTION

1.1 Greenhouse Gas Emissions from Agricultural Cropping Systems

Agricultural soils are a major source of greenhouse gases (GHGs), carbon dioxide (CO_2) and nitrous oxide (N_2O), which have and continue to contribute to climate change (Smith et al., 2018). Since the clearing and cultivation of soils for agricultural production began over a century ago, agricultural soils have lost significant amounts of soil carbon (C) as CO_2 to the atmosphere by decomposing soil organic matter by soil microorganisms (Glenn et al., 2010). In Canada, it is believed that up to 90% of the soil organic carbon that has been lost from agricultural soils has been lost from the Prairies (Glenn et al., 2010). Nitrous oxide (N_2O) is a potent GHG that is produced by agricultural soils and, while produced in lower quantities than CO_2, is of particular concern as it destroys stratospheric ozone and has a warming potential of nearly 300 times that of CO_2 (Smith et al., 2018; Tenuta et al., 2016). It is believed that approximately 6% of the anthropogenic radiative forcing experienced globally is attributed to N_2O, of which agricultural soils are a major contributor (Tenuta et al., 2019).

Agriculturally managed soils can be a source or sink of CO_2 depending on the balance between CO_2 assimilation by plants via photosynthesis, decomposition of plant residues and soil organic matter by soil microbes, and the amount of C removed from fields with harvest removals, all influenced by agronomic practices and management (Amiro et al., 2017; Maas et al., 2013; Smith et al., 2018). The assimilation of CO_2 by crops depends on crop physiology and environmental conditions during crop growth (Tausz et al., 2013). Different crops species accumulate different amounts of biomass by the end of their growth and allocate different amounts of photosynthetic products to root, shoot, and reproductive tissues, affecting the amount of biomass that is remaining following crop harvest (Hakala et al., 2009; Tausz et al., 2013). While soils can be a C sink, it is currently believed that the soil organic C balance of agricultural soils in western Canada is approximately neutral, with C gains from crop growth matching losses from soil respiration and harvest removals (Amiro et al., 2017; Glenn et al., 2010). Therefore, there is a significant challenge to increase C sequestration in soils with the management practices currently used in agricultural production in the Canadian Prairies. Nevertheless, there is optimism that soil organic C stocks can be restored to their historical levels in agricultural soils and that cropland soils can be used as a climate change mitigation strategy to sequester atmospheric CO_2 by utilizing management strategies that increase C returns to the soil (Chahal et al., 2020; Glenn et al., 2010).

N_2O production in agricultural soils occurs through two microbial processes, nitrification and denitrification (Smith et al., 2018). Nitrification is an aerobic process where ammonium is converted to nitrite and eventually nitrate (Smith et al., 2018). While nitrification is aerobic, when the oxygen supply in soil is limited nitrifying bacteria can utilize nitrite as an electron acceptor and reduce nitrite to nitric oxide and N_2O, which can be lost to the atmosphere (Smith et al., 2018). Alternatively, denitrification is an anaerobic process where nitrate is reduced to nitrite, then nitric oxide, followed by N_2O, before being reduced to atmospheric nitrogen gas (N_2) (Smith et al., 2018). N_2O can be consumed in soil (Liu et al., 2022; Smith et al., 2018; Wu et al., 2013). However, the consumption rates are insignificant compared to the rates of production and emission to the atmosphere. The production of N_2O via nitrification and denitrification is driven mainly by soil water-filled pore space (WFPS), soil structure, and temperature (Smith et al., 2018). Rates of N_2O production via nitrification increase with increased WFPS as more water in soil pores reduces oxygen supply and makes conditions more conducive for nitric oxide and N_2O production (Smith et al., 2018). The same is true for denitrification, which requires anaerobic soil conditions, however, soil structure and location of denitrification on soil aggregates become important (Smith et al., 2018). Extremely saturated soil conditions reduce the ability of newly formed N_2O to diffuse to air-filled pores and escape from the soil profile to the atmosphere, making N_2O much more likely to be reduced all the way to N_2 gas (Smith et al., 2018). Temperature also significantly affects N_2O production, with higher microbial activity and oxygen consumption occurring with increased soil temperatures, leading to an increase in anaerobic conditions in the soil (Smith et al., 2018).

N_2O emissions from agricultural soils are primarily produced during the spring-thaw of soils and following synthetic nitrogen fertilizer application. Applying synthetic nitrogen fertilizer increases the amount of nitrogen available to soil microbes to produce N_2O and when soil moisture conditions are high enough, from either a precipitation event or from moist soil conditions when fertilizer is applied, substantial N_2O emissions occur (Tenuta et al., 2019). N_2O emissions from spring-thaw are driven by denitrification and freeze-thaw cycles, which are important contributors to emissions due to increased anaerobiosis and substrate availability, changes in activity and structure of denitrifying enzymes, and the release of previously produced N_2O trapped under snow and ice cover (Wagner-Riddle et al., 2017).

Some recommended management practices to increase C sequestration in agricultural soils and reduce N_2O emissions have been reduced or no-tillage, incorporating perennial forages into crop rotations, and utilizing the “4Rs” of nitrogen fertilizer application. Reduced or no-tillage has seen mixed results in increasing C sequestration and reducing N_2O emissions (Asgedom and Kebreab, 2011; Glenn et al., 2010; Glenn et al., 2012; Wagner-Riddle et al., 2007). Glenn et al. (2010) found that converting from intensive to reduced tillage at a site in Manitoba did not increase C sequestration in those soils. Wagner-Riddle et al. (2007) found that spring-thaw N_2O emissions were reduced with no-tillage as insulation from increased snow cover reduced the intensity of soil freezing. Alternatively, Glenn et al. (2012) found that reduced tillage did not affect N_2O emissions compared to conventionally managed soils. Maas et al. (2013) found that incorporating perennial forages into a crop rotation significantly increased C sequestration and decreased N_2O emissions in the first two years of establishment compared to an annual crop rotation. However, following the plow down of the perennial forages, the C sequestered was lost and N_2O emissions significantly increased from the perennial forage fields compared to the annual-only crop rotation (Amiro et al., 2017; Tenuta et al., 2019). The "4Rs" of fertilizer management, which refer to the right source, placement, timing and rate, have reduced N_2O emissions (Asgedom and Kebreab, 2011; Snyder et al., 2009; Tenuta et al., 2016). However, reductions in N_2O emissions in a single growing season may not result in multi-year reductions in N_2O emissions (Tenuta et al., 2019). With extreme weather events from climate change already impacting communities and ecosystems globally and projected to do so with increased frequency and severity well into the future, implementing agronomic practices that reduce GHG emissions, sequester C from the atmosphere, and make farms more resilient to the effects of climate change will be essential in combating the worst effects of climate change and ensuring food security in the future (IPCC, 2022).

1.2 Cover Crops in Agricultural Production

One management practice that has been gaining popularity in agricultural production has been the use of cover crops. Cover crops are defined as plant species or mixes of species that are grown to improve environmental and/or soil health rather than be harvested and are often grown between growing seasons when fields would be left in fallow (Darapuneni et al., 2021; Frick et al., 2017; Hartwig and Ammon, 2002). Some of the reasons cover crops are utilized in agricultural production include providing a biological source of nitrogen for cash crop production, reducing nitrogen leaching, reducing soil erosion, increasing the biodiversity of cropping systems, increasing C sequestration in soils, and potentially reducing nitrous oxide (N_2O) emissions to name a few (Blesh, 2018; De Baets et al., 2011; Frick et al., 2017; Perrone et al., 2020; Poeplau and Don, 2015). Research into the ability of cover crops to increase C sequestration in soils has shown that cover crops are an effective management strategy to improve C sequestration in agricultural soils (Poeplau and Don, 2015; Tellatin and Myers, 2018). The concept behind growing cover crops to increase C sequestration in soils is to replace the fallow period, where cash crops are not being grown, with an additional period of C assimilation, increasing the amount of C returned to the soil and subsequently increasing C gains to the cropping system (Maas et al., 2013; Poeplau and Don, 2015). Analysis by Tellatin and Myers (2018) in the United States has shown that the potential for cover crops to increase C sequestration in soils is quite substantial if widely adopted and that cover crops could sequester an average of 1.38 t CO_2-equivalent ha^{-1} y^{-1} (Tellatin and Myers, 2018). There is uncertainty about how effective cover crops would be at increasing C sequestration in cropland soils in northern latitudes where frost-free periods are relatively short.

Planting cover crops during non-growing fallow seasons has been suggested as a potential method to reduce spring-thaw N_2O emissions (Dietzel et al., 2011; Reicks et al., 2021). However, cover crop species and cover crop residue management significantly affect overall N_2O emissions during cover crop growth and after its termination. A meta-analysis by Basche et al. (2014) found that non-legume cover crops generally reduced N_2O emissions while legume cover crops increased N_2O emissions and that incorporating cover crop residues after termination increased N_2O emissions further compared to residues left unincorporated. Reicks et al. (2021) reported reduced N_2O emissions in spring from soils seeded with a fall rye cover crop the fall prior. However, they did not look into the difference in N_2O emissions between the cover crop and conventionally managed soils after cover crop termination and synthetic nitrogen fertilizer application. Cover crops can change soil physical properties compared to conventionally managed soils, such as altering C and nitrogen sources for soil microbial communities, soil structure, and soil moisture, which can have effects on soil conditions and N_2O emissions following fertilizer application (Fiorini et al., 2020; Kahimba et al., 2008; Reicks et al., 2021). Cover crop residues provide C to soil microorganisms which can increase rates of nitrification and denitrification as C additions promote the growth and activity of N_2O-producing bacteria, which subsequently increases the consumption of oxygen in the soil and can potentially increase N_2O production (Tenuta et al., 2019). The effect of cover crop residues on N_2O production can be further complicated as carbon to nitrogen (C/N) ratios of residues affect the movement of N in the soil, with C/N ratios greater than 20 favouring immobilization and C/N ratios less than 20 favouring mineralization and release of N into the soil solution, subsequently affecting N_2O production (Basche et al., 2014; Fiorini et al., 2020; Hunter et al., 2019; Liebman et al., 2018; Pimentel et al., 2015). N_2O response to cover crop residues can be further affected by residue management, with the incorporation of residues increasing microbial access and reducing residue particle size compared to residues being left intact on the soil surface (Basche et al., 2014; Fiorini et al., 2020; Liebman et al., 2018). The response of N_2O emissions following cover crop termination and fertilizer application has been mixed (Basche et al., 2014; Fiorini et al., 2020), and needs to be further investigated if cover crops are to be recommended as a GHG mitigation strategy.

An important aspect when considering the usage of cover crops in agricultural production is the impact on subsequent cash crop yields. The impact of cover crop species and residue C/N ratio on cash crop grain yields has seen varying results, with some studies reporting increased yields and others reporting decreased yields (Finney et al., 2016; Fiorini et al., 2020; Hunter et al., 2019; Liebman et al. 2018). Suppose cover crops are to be utilized as a management strategy to increase C sequestration and reduce spring-thaw N_2O emissions. In that case, the N_2O emissions following cover crop termination and synthetic nitrogen fertilizer application must be considered to ensure that cumulative GHG emissions do not increase. Further, the effects of these cover crops on cash crop grain yield must be investigated if cover crops are widely recommended as a management strategy, as reductions in grain yield will increase yield-scaled emissions and reduce farm profitability.

1.3 Long-Term GHG Monitoring at the Trace Gas Manitoba Research Site

The Trace Gas Manitoba (TGAS-MAN) research site has continuously monitored CO_2 and N_2O fluxes between agroecosystems and the atmosphere for over a decade (Amiro et al., 2017; Tenuta et al., 2019). Since its establishment in the fall of 2005, the site has conducted research looking at the effects of different agricultural management practices commonly used in the Canadian prairies on CO_2 and N_2O fluxes by measuring fluxes from four 4-ha field plots (Amiro et al., 2017; Glenn et al., 2010; Glenn et al., 2012; Maas et al., 2013; Tenuta et al., 2016; Tenuta et al., 2019). The site uses the flux gradient micrometeorology method to determine CO_2 and N_2O fluxes from each field. While large field plots limit the number of replicates and treatments that can be done, it allows for better quantification of fluxes as they can capture field variability that might be missed using small plots and other methods, such as static-vented chambers that are commonly used in GHG flux research (Chadwick et al., 2014; Glenn et al., 2012; Hutchinson and Livingston, 1993).

Since its establishment, the site has addressed multiple research questions regarding agricultural practices that are typically utilized in the Canadian Prairies over the short term and put them into context over the long term, as continuous data collection allows the cessation of the practice also to be assessed. Previous research at the site has shown that the utilization of certain agronomic practices, such as inclusion of perennial forages in crop rotations, implementing reduced tillage practices, and timing of nitrogen fertilizer application, can have considerable effects on CO_2 and N_2O fluxes in the short term while other agronomic practices have no effect (Glenn et al., 2010; Glenn et al., 2012; Maas et al., 2013; Tenuta et al., 2016). When looking at the effects of these short-term management changes on long-term CO_2 and N_2O fluxes for the different crop rotations at the site, increasing long-term C sequestration and reducing N_2O emissions has been a challenge (Amiro et al., 2017; Tenuta et al., 2019). Amiro et al. (2017) looked at the long-term impact of incorporating a perennial forage into the crop rotation on cumulative CO_2 fluxes compared to the annual-only crop rotation from 2006-2016 at the site and found that the two cropping systems were not different from each other and were C neutral over the long-term. Similarly, Tenuta et al. (2019), looking at N_2O fluxes from 2006-2016, found that while the perennial phase of the annual-perennial crop rotation at the site had significantly lower N_2O emissions, after the perennials were terminated N_2O emissions over the 11 years were not different from the annual rotation (Tenuta et al., 2019).

The following research goal at TGAS-MAN was to assess the effect of fall rye (*Secale cereale* L.) cover crop seeded no-till on CO_2 and N_2O fluxes, as cover crops have been increasing in popularity as a strategy to increase C sequestration in soils and potentially reduce cumulative N_2O emissions (Basche et al., 2014; Poeplau and Don, 2015). Usage of the flux gradient method utilized at TGAS-MAN allows for better temporal coverage of CO_2 and N_2O fluxes which will be important in determining the effect of a fall rye cover crop on C dynamics and N_2O fluxes during its growth and after its termination. The objectives of the study were to, (1) assess the effect of no-till fall rye cover crop on spring and growing season carbon dynamics, (2) assess the effect of the no-till fall rye cover crop on cumulative carbon balance from January to harvest, (3) assess the effect of a no-till fall rye cover crop on spring-thaw and post-fertilizer N_2O emissions, (4) assess the effect of a no-till fall rye cover crop on net GHG balance, and (5) assess the effect of the no-till fall rye cover crop on cash crop grain yields.

1.4 Thesis Organization

The format of this thesis following this general introduction is two chapters prepared in a manuscript format to be submitted to the journal Agricultural and Forest Meteorology. Data for this study were collected over four years, from 2018 to 2022. The first chapter (Chapter 2) reports two seasons (2019 and 2022) of net ecosystem production measurements made over a conventionally managed cropping system and a cover crop no-till cropping system. The second chapter (Chapter 3) reports on four years of N_2O flux measurements made over conventional and cover crop no-till cropping systems and combines the results from the first chapter to make net GHG flux equivalent estimates from January to harvest for the two cropping systems in 2019 and 2022. Following the two data chapters is a synthesis chapter that integrates the results of the two data chapters, highlights important findings and their implications, recommends study improvements, and outlines suggestions for future work.

1.5 References

Amiro, B.D., Tenuta, M., Gervais, M., Glenn, A.J., and Gao, X. 2017. A decade of carbon flux measurements with annual and perennial crop rotations on the Canadian Prairies. Agricultural and Forest Meteorology. **247**: 491-502.

Asgedom, H. and Kebreab, E. 2011. Beneficial management practices and mitigation of greenhouse gas emissions in the agriculture of the Canadian Prairie: a review. Agronomy for Sustainable Development. **31**: 433-451.

Basche, A.D., Miguez, F.E., Kaspar, T.C., and Castellano, M.J. 2014. Do cover crops increase or decrease nitrous oxide emissions? A meta-analysis. Journal of Soils and Water Conservation. **69**: 471-482.

Blesh, J. 2018. Functional traits in cover crop mixtures: Biological nitrogen fixation and multifunctionality. Journal of Applied Ecology. **55**: 38-48.

Chadwick, D.R., Cardenas, L., Misselbrook, T.H., Smith, K.A., Rees, R.M., Watson, C.J., McGeough, K.L., Williams, J.R., Clow, J.M., Thorman, R.E., and Dhanoa, M.S. 2014. Optimizing chamber methods for measuring nitrous oxide emissions from plot-based agricultural experiments. European Journal of Soil Science. **65**: 295-307.

Chahal, I., Vyn, R.J., Mayers, D., and Van Eerd, L.L. 2020. Cumulative impact of cover crops on soil carbon sequestration and profitability in a temperate humid climate. Scientific Reports. **10**: 13381.

Darapuneni, M.K., Idowu, O.J., Sarihan, B., DuBois, D., Grover, K., Sanogo, S., Djaman, K., Lauriault, L., Omer, M., and Dodla, S. 2021. Growth characteristics of summer cover crop grasses and their relation to soil aggregate stability and wind erosion control in arid southwest. Applied Engineering in Agriculture. **37**: 11-23.

De Baets, S., Poesen, J., Meersmans, J., and Serlet, L. 2011. Cover crops and their erosion-reducing effects during concentrated flow erosion. Catena. **85**: 237-244.

Dietzel, R., Wolfe, D., and Thies, J.E. 2011. The influence of winter soil cover on spring nitrous oxide emissions from an agricultural soil. Soil Biology and Biochemistry. **43**: 1989-1991.

Finney, D.M., White, C.M., and Kaye, J.P. 2016. Biomass production and carbon/nitrogen ratio influence ecosystem services from cover crop mixtures. Agronomy Journal. **108**: 39-52.

Fiorini, A., Maris, S.C., Abalos, D., Amaducci, S., and Tabaglio, V. 2020. Combining no-till with rye (*Secale cereale L.*) cover crop mitigates nitrous oxide emissions without decreasing yield. Soil and Tillage Research. **196**: 104442.

Frick, B., Telford, L., and Thiessen Martens, J. 2017. Organic Field Crop Handbook (J. Wallace (Ed). Third Edition. Canadian Organic Growers.

Glenn, A.J., Amiro, B.D., Tenuta, M., Stewart, S.E., and Wagner-Riddle, C. 2010. Carbon dioxide exchange in a northern Prairie cropping system over three years. Agricultural and Forest Meteorology. **150**: 908-918.

Glenn, A.J., Tenuta, M., Amiro, B.D., Maas, S.E., and Wagner-Riddle, C. 2012. Nitrous oxide emissions from an annual crop rotation on poorly drained soil on the Canadian Prairies. Agricultural and Forest Meteorology. **166-167**: 41-49.

Hakala, K., Keskitalo, M., Eriksson, C., and Pitkänen, T. 2009. Nutrient uptake and biomass accumulation for eleven different field crops. Agricultural and Food Science. **18**: 366-387.

Hartwig, N.L. and Ammon, H.U. 2002. Cover crops and living mulches. Weed Science. **50**: 688-699.

Hunter, M.C., Schipanski, M.E., Burgess, M.H., LaChance, J.C., Bradley, B.A., Barbercheck, M.E., Kaye, J.P., and Mortensen, D.A. 2019. Cover crop mixture effects on maize, soybean, and wheat yield in rotation. Agricultural and Environmental Letters. **4**: 180051.

Hutchinson, G.L. and Livingston, G.P. 1993. Use of chamber systems to measure trace gas fluxes. *In*: Harper, L.A., Mosier, A.R., Duxbury, J.M., and Rolston, D.E. (Eds.). Agricultural Ecosystem Effects on Trace Gases and Global Climate Change. Agronomy Society of America, Inc. ASA Special Publication Number 55. Madison, WI. pp. 63-78.

IPCC. 2022. Summary for Policymakers. Pörtner, H.-O., Roberts, D.C., Poloczanska, E.S., Mintenbeck, K., Tignor, M., Alegría, A., Craig, M., Langsdorf, S., Löschke, S., Möller, V., and Okem, A. (eds.). *In*: Climate Change 2022: Impacts, Adaptation and Vulnerability. Contribution of Working Group II to the Sixth Assessment Report of the Intergovernmental Panel on Climate Change. Pörtner, H.-O., Roberts, D.C., Tignor, M., Poloczanska, E.S., Mintenbeck, K., Alegría, A., Craig, M., Langsdorf, S., Löschke, S., Möller, V., Okem, A., and Rama, B. (Eds.). Cambridge University Press. Cambridge, UK and New York, NY, USA. pp. 3-33, doi:10.1017/9781009325844.001.

Kahimba, F.C., Sri Ranjan, R., Froese, J., Entz, M., and Nason, R. 2008. Cover crop effects on infiltration, soil temperature, and soil moisture distribution in the Canadian Prairies. Applied Engineering in Agriculture. **24**: 321-333.

Liebman, A.M., Grossman, J., Brown, M., Scott Wells, M., Reberg-Horton, S.C., and Shi, W. 2018. Legume cover crops and tillage impact nitrogen dynamics in organic corn production. Agronomy Journal. **110**: 1046-1057.

Liu, H., Li, Y., Pan, B., Zheng, X., Yu, J., Ding, H., and Zhang, Y. 2022. Pathways of soil N_2O uptake, consumption, and its driving factors: a review. Environmental Science and Pollution Research. **29**: 30850-30864.

Maas, S.E., Glenn, A.J., Tenuta, M., and Amiro, B.D. 2013. Net CO_2 and N_2O exchange during perennial forage establishment in an annual crop rotation in the Red River Valley, Manitoba. Canadian Journal of Soil Science. **93**: 639-652.

Perrone, S., Grossman, J., Liebman, A., Sooksa-nguan, T., and Gutknecht, J. 2020. Nitrogen fixation and productivity of winter annual legume cover crops in Upper Midwest organic cropping systems. Nutrient Cycling in Agroecosystems. **117**: 61-76.

Pimentel, L.G., Weiler, D.A., Pedroso, G.M., and Bayer, C. 2015. Soil N_2O emissions following cover-crop residues application under two soil moisture conditions. Journal of Plant Nutrition and Soil Science. **178**: 631-640.

Poeplau, C. and Don, A. 2015. Carbon sequestration in agricultural soils via cultivation of cover crops – A meta-analysis. Agriculture, Ecosystems and Environment. **200**: 33-41.

Reicks, G.W., Clay, D.E., Clay, S.A., Joshi, D.R., Moriles-Miller, J., Westhoff, S., Daigh, A.L.M., and Bruggeman, S.A. 2021. Winter cereal rye cover crop decreased nitrous oxide emissions during early spring. Agronomy Journal. **113**: 3900-3909.

Smith, K.A., Ball, T., Conen, F., Dobbie, K.E., Massheder, J., and Rey, A. 2018. Exchange of greenhouse gases between soil and atmosphere: interactions of soil physical factors and biological processes. European Journal of Soil Science. **69**: 10-20.

Snyder, C.S., Bruulsema, T.W., Jensen, T.L., and Fixen, P.E. 2009. Review of greenhouse gas emissions from crop production systems and fertilizer management effects. Agriculture, Ecosystems and Environment. **133**: 247-266.

Tausz, M., Tausz-Posch, S., Norton, R.M., Fitzgerald, G.J., Nicolas, M.E., and Seneweera, S. 2013. Understanding crop physiology to select breeding targets and improve crop management under increasing atmospheric CO_2 concentrations. Environmental and Experimental Botany. **88**: 71-80.

Tellatin, S. and Myers, R.L. 2018. Cover crop impacts on US cropland carbon sequestration. Journal of Soil and Water Conservation. **73**: 117A-121A.

Tenuta, M., Gao, X., Flaten, D.N., and Amiro, B.D. 2016. Lower nitrous oxide emissions from anhydrous ammonia application prior to soil freezing in late fall than spring pre-plant application. Journal of Environmental Quality. **45**: 1133-1143.

Tenuta, M., Amiro, B.D., Gao, X., Wagner-Riddle, C., and Gervais, M. 2019. Agricultural management practices and environmental drivers of nitrous oxide emissions over a decade for an annual and an annual-perennial crop rotation. Agricultural and Forest Meteorology. **276-277**: 107636.

Wagner-Riddle, C., Furon, A., McLaughlin, N.L., Lee, I., Barbeau, J., Jayasundara, S., Parkin, G., von Bertoldi, P., and Warland, J. 2007. Intensive measurement of nitrous oxide emissions from a corn-soybean-wheat rotation under two contrasting management systems over 5 years. Global Change Biology. **13**: 1722-1736.

Wagner-Riddle, C., Congreves, K.A., Abalos, D., Berg, A.A., Brown, S.E., Ambadon, J.T., Goa, X., and Tenuta, M. 2017. Globally important nitrous oxide emissions from croplands induced by freeze-thaw cycles. Nature Geoscience. **10**: 279-283.

Wu, D., Dong, W., Oenema, O., Wang, Y., Trebs, I., and Hu, C. 2013. N_2O consumption by low-nitrogen soil and its regulation by water and oxygen. Soil Biology and Biochemistry. **60**: 165-172.

2. EFFECT OF FALL RYE COVER CROP ON SPRING AND GROWING SEASON CO_2 FLUXES IN THE RED RIVER VALLEY, MANITOBA, CANADA

2.1 Abstract

While cover crops have been found to increase carbon (C) sequestration in soils, there is little understanding of their effects on CO_2 fluxes and short-term C dynamics during their growth and following their termination. The objectives of this study were to determine the effect of a no-till fall rye (*Secale cereale* L.) cover crop on spring and growing season CO_2 fluxes and cumulative C balance by cash crop harvest in the Red River Valley, Manitoba, Canada. CO_2 fluxes were measured in 2019 and 2022 from four 4-ha fields using the flux gradient method to determine net ecosystem production (*NEP*). A tunable-diode laser analyzer measured the CO_2 gradient from each field, and sonic anemometer-thermometers determined the transfer coefficient. In the fall of 2018 and 2021, two fields were seeded no-till with fall rye and two fields were cultivated and left fallow. The fall rye was terminated the following spring with an herbicide application and oats (*Avena sativa*) and spring wheat (*Triticum aestivum* L.) were seeded in 2019 and 2022, respectively. In both years, the cover crop assimilated C in spring prior to seeding and increased respiration (*R*) during the growing season by approximately 7 kg ha^{-1} day^{-1} compared to the conventional fields. Analysis of the relationship between growing season *NEP* and Gross Photosynthetic Production (*GPP*) indicated that increased *R* from the cover crop fields in 2019 was from heterotrophic respiration and in 2022 was from autotrophic respiration when *GPP* < 40 and from heterotrophic respiration when *GPP* > 40. In 2019, the cover crop system was a C sink following harvest removals of 424 kg C ha^{-1} and the conventional system was a C source of 248 kg C ha^{-1}. In 2022,

both systems were a C source (> 1300 kg C ha^{-1}) due to saturated soil conditions in spring and during the growing season.

2.2 Introduction

The clearing and cultivation of soils for agricultural production, which began over a century ago, has resulted in significant amounts of soil carbon (C) being decomposed by soil microorganisms and lost to the atmosphere as carbon dioxide (CO_2) (Glenn et al., 2010). It is estimated that up to 90% of the soil organic C in Canada has been lost from the Prairie region (Glenn et al., 2010). Agricultural soils can be a source or sink of CO_2 depending on the agronomic practices that are utilized and how they influence the C balance of the cropping system (Amiro et al., 2017; Maas et al., 2013; Smith et al., 2018). The C balance of an agroecosystem can be determined as the sum of CO_2 assimilated by plants via photosynthesis during growth, CO_2 respired and returned to the atmosphere by soil microbes decomposing soil organic matter and plant residues, and the amount of C removed from fields with harvest (Maas et al., 2013). There is optimism that utilizing management strategies in agricultural production that increase carbon sequestration in soils can help mitigate climate change's effects, as soils have a significantly higher potential to store C than the atmosphere (Chahal et al., 2020). However, previous research in the Red River Valley in Manitoba has shown that annual crop rotations that utilize practices, such as reduced tillage and incorporating perennial forages into crop rotations, in the short-term are C neutral (Amiro et al., 2017). There is, therefore, a significant challenge in increasing C sequestration in agricultural soils in this region with currently promoted practices.

Cover crops, which are defined as plants grown on agricultural soils to improve environmental and/or soil health instead of being harvested for economic purposes, can provide numerous benefits and have been shown to increase C sequestration in soils (Frick et al., 2017; Perrone et al., 2020; Poeplau and Don, 2015; Tellatin and Myers, 2018). One practice that has been suggested to increase carbon sequestration in agricultural soils is growing cover crops during non-cropping fallow periods (Darapuneni et al., 2021; Frick et al., 2017; Hartwig and Ammon, 2002). The notion behind growing cover crops is to replace the fallow period, where no crops are grown and heterotrophic respiration dominates, with a period of additional C assimilation, which increases C returns to the soil and alters the overall C balance of the system (Maas et al., 2013; Poeplau and Don, 2015).

Previous studies have shown significant potential for cover crops to increase soil C sequestration (Chahal et al., 2020; Chahal et al., 2021; Poeplau and Don, 2015; Tellatin and Myers, 2018). However, most of the research on cover crops and C sequestration has not been done in croplands in northern latitudes. There is limited understanding of how successful cover crops would be sequestering C during fallow periods when the number of frost-free days is limited. In Manitoba, frost-free periods are relatively short, ranging from 75 to 135 days depending on the year and region of the province, leaving a short period for cover crops to establish and accumulate biomass (Government of Manitoba, 2023*a*). Days for the establishment and biomass accumulation can be shortened further if cash crop species are grown with longer days to maturity.

As a solution, fall rye (*Secale cereale* L.) has been recommended as a crop species to be used as a cover crop in this region as it can establish quickly in fall, survive during the winter months where air and soil temperatures are below 0°C, and continue to grow the following spring (Larsen et al., 2018). Fall rye is also suited to be grown in soils managed under no-tillage or no-till, as intact crop residues help to trap snow and increase the insulation and survival rate of fall rye in spring (Larsen et al., 2018). While in some regions, no-till or reduced tillage has been found to increase C sequestration in soils (Asgedom and Kebreab, 2011; Chahal et al., 2021), previous research in Manitoba saw no effect of reduced tillage on C sequestration (Glenn et al., 2010). However, there are soil health benefits associated with no-till and combining cover cropping with no-till practices could provide increased soil health benefits, such as improving water use efficiency, reducing soil erosion, improving snow trapping and water conservation, and potentially increasing C sequestration, which could help make cropping systems more resilient to the effects of climate change (Asgedom and Kebreab, 2011; Chahal et al., 2021; Larsen et al., 2018; Liu and Lobb, 2021). However, questions remain regarding the ability of a cover crop to affect carbon fluxes and overall C balance by the end of the growing season in northern latitude croplands when the establishment and biomass accumulation periods are limited. Further, the effects of the cover crop on the following cash crop carbon uptake and soil respiration after its termination need to be determined to understand the cover crop's effect on the cropping system's ecosystem C balance.

Continuous monitoring of CO_2 fluxes can distinguish how environmental and agronomic events affect the C dynamics of the two cropping systems at different times of the year. Micrometeorological monitoring of CO_2 fluxes offers an opportunity to determine the effects of no-till fall rye cover crop cropping systems on short-term C dynamics and ecosystem C balance at the end of the growing season compared to conventional soils. This study's CO_2 flux data were collected from the Trace-Gas Manitoba (TGAS-MAN) long-term research site in the Red River Valley in Manitoba, Canada. TGAS-MAN has been monitoring CO_2 and N_2O fluxes since its establishment in 2005. Numerous studies assessing the effects of different management strategies, such as reduced tillage and perennial forages, on CO_2 fluxes have been conducted at the site (Glenn et al., 2010; Maas et al., 2013). The most recent study at the site looked at the effect of these different crop rotations and management strategies on CO_2 fluxes over a decade (Amiro et al., 2017). The present study assessed the difference in field scale CO_2 fluxes from January to cash crop harvest from a cropping system managed with conventional tillage practices to a cropping system that received no-tillage and was seeded with a fall rye cover crop after cash crop harvest in fall. CO_2 flux data, weather data, cover crop and cash crop biomass samples, and soil samples were collected in 2019 and 2022 from the site to assess the effect of the cover crop on soil conditions and CO_2 fluxes. The objectives of this study were to (1) assess the effect of a no-till fall rye cover crop system on spring and growing season C dynamics compared to a conventional cropping system and (2) assess the effect of a no-till fall rye cover crop system on cumulative C balance from January to harvest in each study year compared to a conventional cropping system.

2.3 Materials and Methods

2.3.1 Site Description

The study was conducted at the University of Manitoba's TGAS-MAN research site (49.64N 97.16W, 235m a.s.l), located in Glenlea, Manitoba, approximately 16km south of Winnipeg, Manitoba, in the flat (<2% slope) Red River Valley floodplain. The experimental fields were situated on glaciolacustrine clay with an extremely humid-continental climate and had soils that consisted of gleyed humic vertisols (Canadian system) or typic humicryerts (U.S system) of the Osborne and Red River Series (Ehrlich et al., 1953; Michalyna et al., 1975). The soil texture at the site was approximately 60% clay, 35% silt, and 5% sand and soil drainage ranged from poorly to imperfectly. The site experienced poor to imperfect drainage under saturated conditions from high precipitation levels or slow drainage in spring and formed large cracks under drought conditions.

2.3.2 Site Design and Agronomic History

The TGAS-MAN research site has been continuously monitoring N_2O and CO_2 trace gas fluxes since its establishment in 2005 using the flux gradient method (Amiro et al., 2017; Glenn et al., 2010; Maas et al., 2013; Tenuta et al., 2019). The site consists of four 4-ha plots (each 200m by 200m) arranged in a 2x2 grid situated in a larger 30 ha field (Figure 2.1). Detailed agronomic history from 2006 to 2016 can be found in Amiro et al. (2017). In 2017 the site was seeded with corn (*Zea mays*) and received no experimental manipulations. Experimental manipulations for this study started in the fall of 2018. For each year of this study, two plots were treated as controls and were managed with conventional tillage practices and left in fallow during non-cropping periods, and two plots were seeded with fall rye in the fall following harvest and received no-tillage.

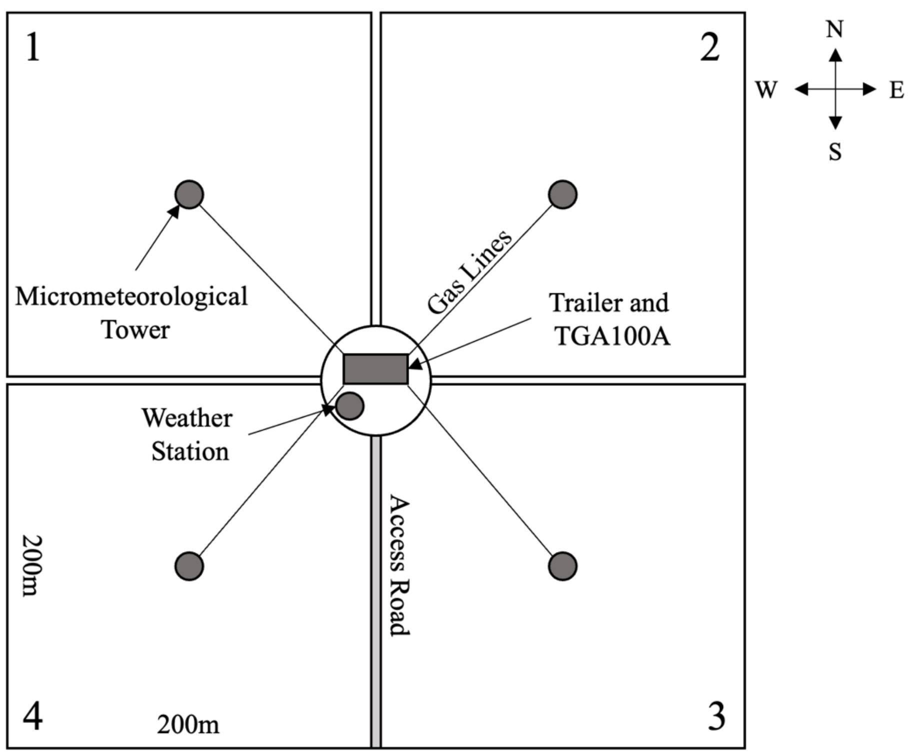

Figure 2.1 TGAS-MAN experimental site layout. The conventional treatment was on Fields numbered 1 and 4 on the west side of the site, and the cover crop no-till treatment was on Fields 2 and 3 on the site's east side.

Following the harvest of canola (*Brassica napus*, cv 'L233P' (InVigor®), BASF) on August 24, 2018, fall rye cover crop was direct seeded into canola stubble with a Case IH SDx30 seeder at a rate of 63 kg ha^{-1} on the two east fields (Fields 2 and 3) on August 29, 2018. On August 30, the two west fields (Fields 1 and 4) were cultivated with a JD 1610 deep tiller to approximately 13cm depth. On May 13, 2019, all fields at the site were seeded with oats (*Avena sativa,* cv 'AC® Summit') at a rate of 108 kg ha^{-1} and banded with a granular fertilizer blend (N-P-K-S) of 78 kg ha^{-1} ESN®, 17 kg ha^{-1} P, 6 kg ha^{-1} K, and 17 kg ha^{-1} S. On May 14, 2019, the site was sprayed with Roundup Transorb (1.65 L ha^{-1}; a.i. glyphosate) to terminate the cover crop on the east fields and kill any volunteer weeds on the west fields. An additional herbicide application of Roundup Transorb (1.65 L ha^{-1}) was made on the east fields on May 20 to terminate the remaining cover crop. The herbicide Outshine (applied according to the product label; a.i. florasulam/fluroxypyr + MCPA ester) and the fungicide Twinline (applied according to the product label; a.i. pyraclostrobin and metconazole) were applied on June 5 and July 1, 2019, respectively, to all fields. On August 19, the oats were desiccated with Roundup Transorb (1.65 L ha-1) application and harvested on September 9, 2019. Straw from the crop was not removed from the field after harvest. The cover crop and conventional comparison continued for the 2020 and 2021 growing seasons. However, issues with micrometeorological equipment caused the flux data from 2020 and 2021 to be eliminated. An explanation and description of the flux corrections can be found in Section 2.3.5 below. Detailed agronomic information from fall 2019 until fall 2021 can be found in Table 5.1 in APPENDIX A.

In fall 2021, following the harvest of wheat (*Triticum aestivum* L., cv 'AAC Starbuck VB') on August 16, a fall rye cover crop was direct seeded into the wheat residue on the east fields (Fields 2 and 3) with a Case IH SDx30 seeder at a rate of 63 kg ha^{-1} on August 30, 2021. On

September 1, 2021, and October 5, 2021, the west fields (Fields 1 and 4) were cultivated with a Summers chisel plow to approximately 13cm depth. Additional cultivation passes were made on the west fields on November 9, 2021, with a disc cultivator to terminate small patches of volunteer wheat germinating underneath micrometeorological equipment in the field. On June 10, 2022, the cover crop was terminated on Fields 2 and 3 with an herbicide application of Roundup Transorb (1.65 L ha^{-1}). Under normal weather conditions, seeding and termination of the cover crop were coordinated to occur close to or at the same time as seeding. However, precipitation shortly after the herbicide application to terminate the cover crop in 2022 and saturated soil conditions delayed seeding at the site. On June 20, 2022, the site was seeded with wheat (*Triticum aestivum* L. cv 'AAC Viewfield') at a rate of 135 kg ha^{-1}. A starter fertilizer blend was banded with the seed at 22 kg ha^{-1} N, 22 kg ha^{-1} P, and 11 kg ha^{-1} S. Two different fertilizer treatments were applied at seeding for a subsequent fertilizer study at the site. On June 20, 2022, eNtrench™ coated urea was applied to the two north fields (Fields 1 and 2) at an intended rate of 118 kg ha^{-1}. However, flowability issues with the applicator caused approximately half of the intended rate to be applied, resulting in an estimated 56 kg ha^{-1} of eNtrench™ coated urea to be applied. As a result, 56kg ha^{-1} UAN (28%) treated with Centuro® was applied with a Case IH 3230 patriot sprayer with 100' boom and tri-tip streamers on June 22, 2022, to the two north fields to make up for the half rate of eNtrench™. On June 20, 2022, the two south fields (Fields 3 and 4) were fertilized with 118 kg ha^{-1} urea. On July 13, 2022, all fields were sprayed with Velocity (988 ml ha^{-1}; a.i. thiencarbazone, bromoxynil and pyrasulfotole). The site was harvested on October 5, 2022.

2.3.3 Micrometeorological Instrumentation and Carbon Dioxide Flux Measurements

A detailed description of the research site and equipment used for flux measurements for 2019 can be found in Glenn et al. (2010). CO_2 fluxes were measured at the site using the micrometeorological flux gradient method. Micrometeorology equipment used to measure net CO_2 fluxes was mounted onto towers at the center of the four fields. A Tunable Diode Laser absorption spectrophotometer (Model TGA100A, Campbell Scientific Inc., Logan, UT, USA) trace gas analyzer (TGA) and associated hardware and electronics was housed at the junction of the four fields in an insulated and temperature-controlled trailer and continuously measured CO_2 and N_2O concentrations of gas samples from the fields. The lead-salt tunable diode laser100A (Model IR-N2O/CO2, Laser Components GmbH., Olching, Germany) was operated in dual-ramp, jump scanning mode at 84K (-189°C) and was cooled with liquid nitrogen and set to measure both CO_2 and N_2O concentrations simultaneously at 10Hz frequency. The first ramp of the TGA laser was set to scan a $^{14}N_2O$ absorption line peak at a frequency of 2243.110 cm^{-1} by applying a DC current of ~563 mA, while the second ramp was set to scan $^{13}CO_2$ absorption line peak at a frequency of 2243.585 cm^{-1} at a DC current of ~589 mA. Using a beam splitter, a non-reflecting laser beam in the TGA was deflected onto two detectors, one in a sample cell and one in a reference cell. Reference gas with concentrations of approximately 2000 ppm N_2O and 300,000 ppm CO_2 (0.2% and 30% by volume N_2O and CO_2, respectively) was continuously drawn through the reference cell of the TGA at a rate of 10 ml min^{-1}. Sample pressure within the TGA was maintained at 30 mb.

The net exchange of CO_2 between the cropping systems and the lower atmosphere was determined using the flux-gradient micrometeorology method (Amiro et al., 2017; Denmead, 2008; Pattey et al., 2006). Carbon flux (F_C) was determined as:

$$F_C = -K\frac{\Delta[CO_2]}{\Delta z}$$

where K is the turbulent transfer coefficient, $\Delta[CO_2]$ is the vertical concentration gradient, and Δz is the vertical height difference.

To determine K, 3-D sonic anemometer-thermometers (CSAT-3, Campbell Scientific Inc.) were mounted at 2m to the towers in the south fields (Fields 3 and 4). An additional sonic was added in the summer of 2022 in the northwest field (Field 1). The K data collected from the different fields were averaged to give one K value. Corrections to K for atmospheric stability were determined as:

$$K = u_* k\ (z_2 - z_1) / [\ln (z_2 / z_1) - \varphi_2 + \varphi_1]$$

where u_* is the friction velocity, k is the von Karmann constant of 0.4, z_2 is the upper intake height above the zero-plane displacement (d), z_1 is the lower intake height above d, and φ_2 and φ_1 are stability correction factors for the upper and lower intakes, respectively (Amiro et al., 2017). d was estimated by measuring the crop height during the growing season and snow depth during winter. Crop heights and snow depth were measured approximately once every two weeks for the growing season following crop emergence and during winter when snow was present. Crop height and snow depth were interpolated between measurements. During the growing season, d was assumed to be 0.66 of crop height, while during the non-growing season, it was presumed to be at the soil or snow surface (Amiro et al., 2017; Denmead, 2008; Garratt, 1992; Glenn et al., 2010). Large experimental field size and location of micrometeorological towers at the center of each field allowed fetch to effective observation height ratios of approximately 100:1 to be maintained for all fields in all directions during the study (Glenn et al., 2010).

To measure $\Delta[CO_2]$ and Δz, gas sample intakes were mounted to each micrometeorology tower at the center of each field. The intakes were moved up as necessary during the growing season as the crop grew and snow started approaching the height of the lower intake. The lower intake height was 0.66 of the crop height plus 60cm, and the upper intake height was the lower intake height plus 50cm. Before November 2019, the site used the hardware and sampling system described by Glenn et al. (2010) to collect gas samples from towers, transport them to the analyzer for analysis, and record gas samples. Briefly, gas samples were taken using two stainless steel intakes, with each intake being sampled for 12 seconds before switching to the other intake at that tower. Fields were sampled for 30 minutes to determine the concentration gradient before moving to the next field in the sequence. A one-way solenoid valve at the tower controlled switching between the intakes. Gas samples from the intakes were drawn through an air dryer and filter located at the tower prior to being transported down approximately 150 m of tubing (4.3 mm i.d., Model P, Synflex, St-Gobain Performance Plastics, Wayne, New Jersey, USA) to the instrumentation trailer by a rotary vacuum pump (Model RB0021, Busch Vacuum Technics, Boisbriand, Quebec, Canada) at a rate of 20 L min^{-1} (5 L min^{-1} per field). Once in the trailer, four 3-way solenoid valves directed the gas sample from the tower being sampled through another air dryer, removing water vapour from the sample, bringing the sample to a constant temperature before being sent to the TGA, and discarding the samples from the other towers using a purge line. The switching of the solenoid valves in the trailer and at the towers was controlled by a datalogger (Model CR1000, Campbell Scientific Inc.) which relayed activation signals to a modified 16-channel DC controller. Since only one gas line was used to transport samples from the towers to the trailer, gas concentration data from the mixing of gases in the lines was omitted from calculating the 30-minute concentration gradient. Following sampling a field for 30 minutes, the following field in the sequence would be sampled, yielding an average of 12 half-hour gradients per day from each field. Sampling rotated through the fields clockwise and lagged at midnight daily to prevent a time-of-day bias over four days.

In November 2019, the sampling system and data collection equipment were upgraded. The stainless-steel intakes were replaced with heated sample intakes (Model 27693, Campbell Scientific Inc.) at all the towers and an additional gas line was added so each intake had a gas line to transport samples from the towers to the analyzer. The solenoid valve system in the trailer was replaced with a 16-inlet TGA sampling manifold (Model 30497, Campbell Scientific Inc.). The manifold contained a datalogger (Model CR3000, Campbell Scientific Inc.) which controlled the switching of the sampling intakes and recorded the gas concentration data and diagnostics from the TGA. Samples were drawn from each gas sample intake at each of the towers through approximately 150 m of tubing (4.3 mm i.d, Model varied by field, Synflex, St-Gobain Performance Plastics, Wayne, NJ, USA) by a diaphragm pump (Model DOA-V502A-FB, Gast Manufacturing Inc., Benton Harbor, MI, USA) to the manifold in the instrumentation trailer. The selected samples were directed from the manifold through an air dryer line and to the TGA by a diaphragm pump (XDD 1 115/230 V Diaphragm Pump, Edwards Vacuum, West Sussex, UK). The other gas samples not being sampled were discarded using the bypass system in the manifold. The sample flow to the TGA was manually set by a needle valve between the manifold and TGA and was maintained between 175 – 220 ml min^{-1}. Excess flow, which is the excess gas from the sample that is not being taken to the TGA for analysis and acts as a buffer to maintain sample flow and pressure, was maintained between 50 – 75 ml min^{-1}. The sample flow was adjusted to keep the excess flow within the operating range. Sample and bypass pressure in the manifold were set at 400 mb and TGA pressure was set at 30 mb. The intakes were switched every 15 seconds for the 30-minute sampling period. Data was shifted to adjust for the lag time from the valves switching in the manifold and the gas samples arriving at the TGA. Gas data from samples mixing in the line from the manifold to the TGA was omitted to give clean gradient data for CO_2 and N_2O. After data collection, shift and omit corrections were made in Matlab (The MathWorks Inc., Natick, MA, USA). From January 1, 2020, until November 23, 2021, the sampling sequence was Field 1, Field 2, Field 4, Field 3. For the remainder of 2021 and 2022, the sampling sequence rotated through the fields in a clockwise rotation. The manifold did not lag at midnight as the other system did, so there was a potential for time-of-day sampling bias. High-frequency data from the sonic anemometers and TGA were stored on compact flash data cards in TOB1 format in the data loggers and converted to IEEE binary table format using LoggerNet software (Campbell Scientific Inc.) and then processed using Matlab.

2.3.4 Supporting Environmental, Soil, and Biomass Data

Environmental conditions for the duration of the study were monitored using the on-site weather station located at the junction of the four fields south of the instrumentation trailer in an undisturbed grassed area. The instrumentation to measure air temperature and relative humidity (Model HMP45C, Vaisala Inc., Woburn, MA, USA), photosynthetic photon flux density (PPFD) (Model PAR LITE, Kipp & Zonen, Delft, the Netherlands), incoming solar radiation (Model SP-LITE Silicon Pyranometer, Kipp & Zonen), wind speed and direction (Model 05103-10 Wind Monitor, R.M. Young Company, Traverse City, MI, USA), and barometric pressure (Model 61205, R.M. Young Company) were mounted to a tripod. Total precipitation was measured using a precipitation gauge (Model T-200B Series Precipitation Gauge, Geonor, Inc., Milford, PA, USA) approximately 3 m from the weather station tripod. At the base of the tripod, soil temperature was measured at 2, 5, 10, 20, 50 and 100 cm depths using soil temperature thermistors (Model 107 and

107B Thermistors, Campbell Scientific Inc.) and volumetric soil moisture probes (Model EC-10 ECH2O Dielectric Aquameter, Decagon Devices Inc., Pullman, WA, USA) was positioned at 10 and 30 cm depths to measure soil moisture content. Weather station data was recorded at 0.1 Hz with a datalogger (Model CR1000, Campbell Scientific Inc.) and stored in TOB5 format at 30-minute, 60-minute, and daily intervals. 30-year climate normals from 1981-2010 for Glenlea, Manitoba, were obtained from Environment Canada (Environment Canada, 2023*a*).

Soil samples were taken approximately once a month from soil thaw in spring to freeze in fall each study year at six random locations within each field. The sampling locations were determined at the beginning of the study and repeatedly sampled (± 5 m radius) during each sampling. Four samples were taken at 0-15 cm and 15-30 cm depths at each sampling location and combined to make a single composite sample for each depth for each sampling location. Samples were stored in an insulated cooler on ice while being collected in the field until they were transported back to the laboratory, where they were stored in a walk-in freezer at approximately -20°C until analysis. Before analysis, samples were thawed, homogenized and broken down until the soil particle size for the sample was approximately ≤ 1 cm in diameter. Samples were analyzed for gravimetric moisture content (GMC), ammonium (NH_4^+), and nitrate (NO_2^-/NO_3^-). GMC was determined by oven-drying sub-samples at 105°C for 24 hours. NH_4^+ and NO_2^-/NO_3^- of samples were determined using a 2 M KCl extraction at a 1:5 soil-to-extractant ratio and a Technicon Autoanalyzer II colorimetry (Pulse Instrumentation Ltd., Saskatoon, SK). Samples were not dried prior to NH_4^+ and NO_2^-/NO_3^- analysis. Minimum reportable limits were set at 0.02 mg L^{-1} and 0.2 mg L^{-1} for NH_4^+ and NO_2^-/NO_3^-, respectively. Results below reportable limits were set to 0 mg L^{-1} when determining averages for a field.

Cover crop biomass, cash crop harvest removals and grain yield were determined by taking hand-clipped aboveground biomass samples prior to termination of the cover crop and harvest of the cash crop in each of the fields at the site. Samples were taken from the same six random sampling locations to collect soil samples from the site. 1 m of biomass from two adjacent rows was sampled twice at each sampling location, yielding 4 m of biomass total from each location. Plants were clipped approximately 2 cm from the soil surface. Samples were weighed following sampling and then stored in a drying room at approximately 32.2°C until they reached an equilibrium air-dry weight. Once the equilibrium weight was established, cash crop biomass was stationary combined (Wintersteiger Classic Combine, Ried, Austria) to determine air-dry grain yield and straw weight. Grain and straw samples taken in the fall and cover crop samples taken in spring were dried in an oven at approximately 60°C for 24 hours to determine oven dry weight. Samples were then ground using a Wiley mill (Wiley Laboratory Mill, Model 4 3375-E10, Thomas Scientific, Swedesboro, NJ, USA) with a 2 mm screen size and analyzed for total carbon (TC), total nitrogen (TN) and carbon to nitrogen ratio (C/N) using a vario MAX cube analyzer (vario MAX cube, Elementar, Langenselbold, Germany).

2.3.5 Data Quality Control

The data collected at the TGAS-MAN site was processed in Matlab. Parameters were set in the manifold data logger program to ensure high-quality data was maintained during data collection. Station flags were issued and data was removed if the TGA pressure was ± 1 mb from the set point and if the sample and bypass pressure were ± 10 mb from the set point. Following data collection, half-hourly data was removed during site visits from power interruptions, human interference, and during field operations (seeding, spraying, harvesting, cultivating). The 30-

minute period where liquid nitrogen fills were performed, which occurred biweekly, and the next 30 minutes following were removed to prevent inaccurate gas concentration measurements from possible vibrations and temperature changes of the analyzer (Edwards et al., 2003).

Quality control parameters were set when processing fluxes and data was discarded if it was outside the acceptable range. Gas concentration data was removed if the TGA temperature was > 84.5K or < 83.5K. Gas data where the sample flow > 250 ml min^{-1} or < 135 ml min^{-1} or where the excess flow < 30 ml min^{-1} or > 90 ml min^{-1} was discarded. Fluxes were discarded if the standard deviation of the CO_2 concentrations over the 30-minute sampling period were greater than 20 ppm, a parameter also used by Maas et al. (2013), who conducted previous research at the site. Fluxes were also discarded when $u_* < 0.15$ m s^{-1} as insufficient atmospheric mixing caused unreliable K data. This u_* threshold was also used in previous flux research conducted at the site (Amiro et al., 2017; Glenn et al., 2010; Maas et al., 2013; Tenuta et al., 2019).

Following the system upgrades in 2019, a bias in N_2O and CO_2 concentration gradients was observed from all the fields. In the summer of 2021, field tests were conducted to determine the cause of the gradient bias and it was determined that the bias was caused by mismatched line types (one intake having one line material type and the other intake having another line material type). A defect in the sampling system manifold also affected the data collected from Field 3. In the fall of 2021, the gas lines and manifold were replaced and zero gradient tests, where the gas sample intakes were set at the same height ($\Delta z = 0$), were performed in the field at each tower to ensure that there was no longer a bias in the gas concentration gradients. The intakes were returned to their normal sampling heights at each tower in December 2021. The Matlab protocol set by Amiro (2021) was used to correct the bias in the flux data for 2020 and 2021. The protocol can be found in the APPENDIX B of this thesis. After the carbon fluxes were corrected for 2020 and 2021, negative night-time respiration data during some periods of the year at each site indicated that the uncertainty in the quality of the carbon flux data was too high. Thus, the CO_2 flux data collected for 2020 and 2021 are not reported.

2.3.6 Gap-Filling

Gap-filling of carbon fluxes and partitioning of flux data was done using the Fluxnet Canada Research Network protocol to determine net ecosystem production (*NEP*), gross photosynthetic production (*GPP*), and respiration (*R*) using measured F_C data. A positive NEP flux indicates a gain of C to the agroecosystem, while a negative NEP flux indicates a loss of C to the atmosphere. Small gaps of 2 hours or less were interpolated. Gaps larger than 2 hours were filled using a 5 cm soil temperature function to determine *R* and photosynthetically active radiation (PAR) relationship to determine *GPP* using a 100-data-point moving window (Amiro et al., 2017; Barr et al., 2004).

Missing air temperature data from the on-site weather station was gap-filled using the air temperature data from the sonic anemometer thermometers located at the towers. Missing precipitation data was gap-filled using data from Winnipeg's James Armstrong Richardson International Airport Winnipeg A CS weather station (Environment Canada, 2023*b*).

2.3.7 Cumulative Net Ecosystem Production and Carbon Budget

To determine the effect of the cropping system on carbon balance ($F_{ECOSYSTEM}$), the *NEP* of the two treatment fields was averaged and summed for each study year. A study year was defined as January 1 to harvest for each year, respectively. To compare the difference in *NEP* between the two treatments in spring before seeding, *NEP* was assessed from the start of spring-thaw until its termination. The start of spring-thaw was defined as the first date of daily average air temperature above 0°C (Tenuta et al., 2019). TC and biomass weight results were used to determine carbon removals ($F_{HARVEST}$) from grain harvest, which were subsequently used to determine $F_{ECOSYSTEM}$ for each cropping system. $F_{ECOSYSTEM}$ was determined as the sum of cumulative net ecosystem production ($\sum F_{NEP}$) for the study year minus $F_{HARVEST}$, with positive $F_{ECOSYSTEM}$ indicating a net ecosystem gain in C and negative values indicating net ecosystem loss of C. To compare the difference in *GPP* and *R* for the cover crop and conventional cropping systems, *GPP* and *R* were summed for each study year to give gap-filled cumulative gross photosynthetic production ($\sum F_{GPP}$) and gap-filled cumulative respiration ($\sum F_R$).

The relationship of *NEP* vs. *GPP* was compared to assess the difference in *NEP*, autotrophic respiration (R_a) and the contribution of the cover crop residues to heterotrophic respiration (R_h) from each cropping system during the growing season. The protocol used by Amiro et al. (2017) was used to determine the relationship between *NEP*, *GPP*, and *R*, such that:

$$NEP = GPP - R_a - R_h = (1 - m)\ GPP - R_h$$

where m is R_a / GPP or "1 – slope" and R_h is the intercept. The growing season was defined as days with $GPP > 5$ kg ha^{-1} day^{-1} following seeding (Amiro et al., 2017). Each treatment field's *NEP* and *GPP* values (cover crop and conventional, respectively) were averaged to give one value for each treatment.

2.3.8 Statistical Analysis

Statistical analysis of the data collected was performed in Matlab. Linear regression analysis (Matlab, "regstats") was used to test the relationship between *NEP vs. GPP* for each of the treatments during the growing season. In 2022, linear regression analysis of *NEP vs. GPP* for each treatment was conducted twice, when *GPP* < 40 and when *GPP* > 40, due to the distribution of the data. Significance of the linear regression models was set at P < 0.05. *NEP* from the conventional and cover crop treatments during the growing season were compared in both study years using a two-sample t-test (Matlab, "ttest2"). The two-sample t-test was performed on *NEP* data in 2022 when *GPP* < 40 and *GPP* > 40 separately. Significance was set with P < 0.05. Growing season *NEP* for both years met normality assumptions with the confidence interval set at 95%.

Analysis of variance was performed using the biomass sample locations as replicates for each treatment, yielding 12 samples total for each treatment for each year, to compare treatment effects on grain yield for each of the study years (Matlab, "anova1"). Significance was determined as P < 0.05. An Anderson-Darling test (Matlab, "adtest") determined that the yield data were not different from the normal distribution (P = 0.18 – 0.98). Differences in 0-30 cm soil GMC from the two cropping systems during the growing season were evaluated using analysis of variance (Matlab, "anova1") and results were deemed significant when P < 0.05. Anderson-Darling test (Matlab, "adtest") was performed on data from each treatment from each sampling. Data from the cover crop fields did not meet normal distribution from June 12, 2019 (P = 0.01) and May 11, 2022 (P = 0.04) sampling dates. Data from the conventional fields did not meet normal distribution on June 13, 2022 (P = 0.007). Data from both treatments at all the other sampling dates were not different from normal (P = 0.10 – 0.91).

2.4 Results

2.4.1 Weather and Soil Conditions

The average air temperature during the month of cover crop seeding in both 2018 and 2021 was close to the 30-year normal for the area (Table 2.1). Air temperature during cover crop emergence and establishment in September and October was lower than the 30-year normal in 2018 and higher than normal in 2021 (Table 2.1). The total precipitation from August to October during the cover crop seeding and establishment period was lower than the 30-year normal in 2018 and 2021, 93 mm and 140 mm for 2018 and 2021, respectively, compared to the 30-year normal of 165 mm (Table 2.1). The average air temperature from January to the month of harvest for 2019 and 2022 was lower than the 30-year normal of 5.3°C from January to September and January to October (Table 2.1). The air temperature was 4.0°C from January to September 2019, and 3.9° C from January to October 2022 (Table 2.1). Total precipitation from January to September 2019 was 394 mm, lower than the 30-year normal of 452 mm for the same period. Total precipitation in 2022 from January to October was more than 200 mm higher than the 30-year normal at 701 mm, compared to the normal of 495 mm (Table 2.1).

Ammonium and nitrate concentrations followed similar patterns for both cropping systems in both study years, starting low in spring, peaking following fertilization, and then decreasing for the rest of the growing season (Figure 2.2). In 2019, soil nitrate was similar for the two cropping systems except in April and May, when the cover crop fields' nitrate was lower than the conventional fields (Figure 2.2). In 2019, only the cover crop fields saw a slight increase in ammonium concentrations following fertilization (Figure 2.2). In 2022, both systems saw an increase in ammonium concentrations following fertilization, with the conventional fields seeing a slightly larger increase than the cover crop fields (Figure 2.2). In 2022, soil nitrate was slightly higher at all samplings in the conventional fields than in the cover crop fields (Figure 2.2). GMC was consistently lower in the cover crop fields at all samplings compared to the conventional fields in 2022 (Figure 2.2). GMC was lower in all sampling dates in 2019 except for April and June, where they were similar (Figure 2.2). However, the differences were insignificant (P = 0.06-0.85). Differences were significant in 2022 from samples collected on June 29, 2022 (P = 0.01) and September 9, 2022 (P = 0.046). Differences were not significant from the other samplings in 2022 (P = 0.059 – 0.18).

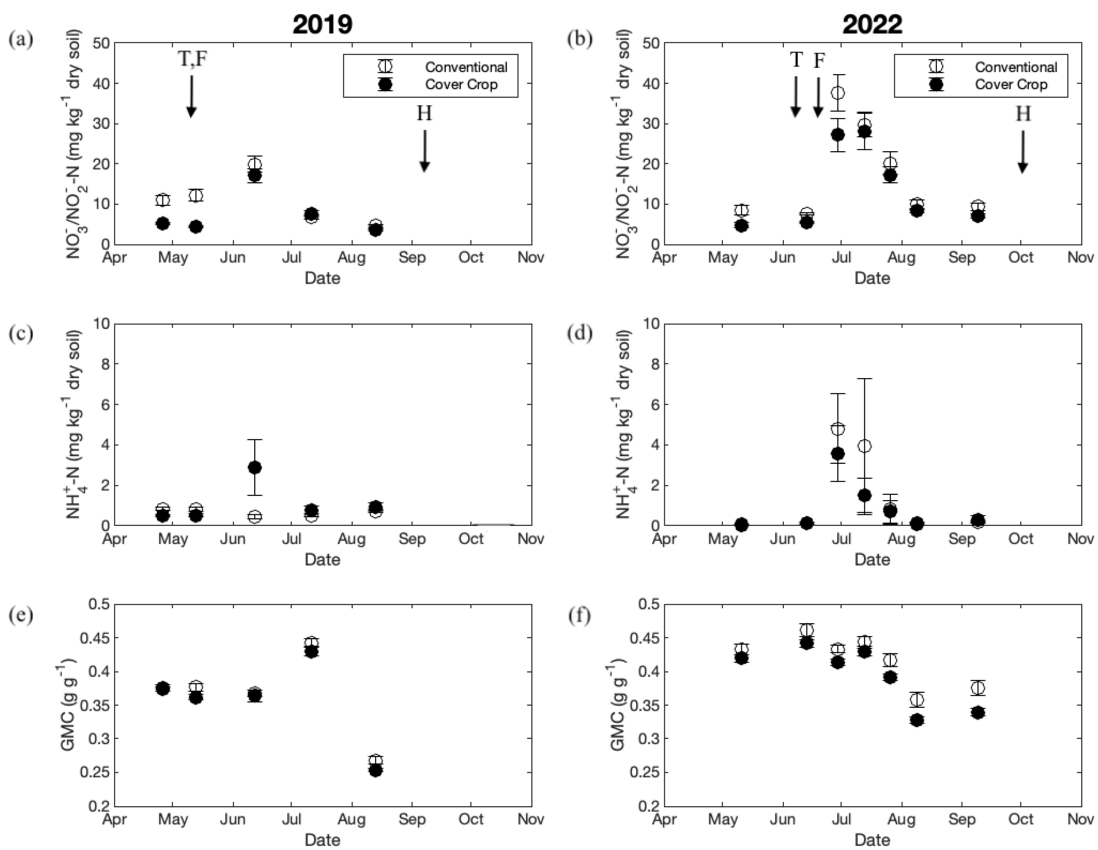

Figure 2.2 Concentrations of NO_3^-/NO_2^-, NH_4^+, and gravimetric moisture content (GMC) from 0 to 0.3m soil depth from the conventional and cover crop fields for (a, c, e) 2019 and (b, d, f) 2022. Cover crop termination (T), fertilizer application (F), and harvest (H) are denoted by arrows at the top of the figures. Open circles correspond to the conventional treatment; closed circles correspond to the cover crop treatment. Soil samples were collected from six locations in each of the two replicate fields for each treatment (n=12). ± 1 SE as error bars are shown.

Table 2.1 Air temperature and precipitation from month of cover crop seeding until harvest the following year during the two study years compared with the 30-year (1981-2010) Canadian Climate Normal for Glenlea, Manitoba (Environment Canada, 2023*a*).

	Aug	Sep	Oct	Nov	Dec	Jan	Feb	Mar	Apr	May	Jun	Jul	Aug	Sep	Oct
Average Air Temperature (°C)															
2018/2019	19.0	10.9	2.6	-7.9[a]	-11.3[a]	-17.9	-20.0	-8.3	4.2	10.0	17.6	19.6	17.9	13.2	-
2021/2022	18.8	16.0	8.6	-2.8	-13.4	-19.5[a]	-20.1	-8.4	-0.3	10.3[a]	17.8[a]	20.0[a]	19.0	13.9	5.9
30 Year Normal	18.8	12.5	4.9	-5.3	-14.3	-17.2	-13.3	-6.0	4.4	12.2	17.0	19.4	18.8	12.5	4.9
Standard Deviation	1.8	1.6	1.4	4.1	4.6	3.9	4.4	3.3	2.6	1.8	2.2	1.4	1.8	1.6	1.4
Total Precipitation (mm)															
2018/2019	19	53	21	4[b]	10[b]	1	0	0	6	28	47	119	53	139	-
2021/2022	80	8	52	20	9	21[b]	36	40	98	147[b]	85[b]	112[b]	85	62	15
30 Year Normal	72	49	43	27	22	16	13	21	28	62	100	92	72	49	43

[a] Missing temperature data from the on-site weather station was gap-filled with air temperature data from the sonic anemometer thermometers

[b] Missing precipitation data from the weather station was gap-filled using data from Winnipeg's James Armstrong Richardson International Airport Winnipeg A CS weather station, located approximately 35km from the site (Environment Canada, 2023*b*)

2.4.2 Carbon Dioxide Fluxes

The study year length was 252 days and 279 days for 2019 and 2022, respectively. The percent of CO_2 fluxes that were captured by flux measurements following data filtering was 46% from January 1 to harvest in both study years. In both study years, ideal weather conditions at cover crop establishment in the fall resulted in good cover crop biomass accumulation the following spring before seeding. The length of biomass accumulation from spring-thaw until cover crop termination differed between the two years due to varying soil conditions in spring at seeding, resulting in different accumulated amounts of biomass (Table 2.2).

In 2019, biomass accumulation was 49 days, with spring-thaw starting on March 27, 2019, and termination occurring on May 13, 2019. Cover crop biomass was similar for the two fields in 2019, with Field 2 yielding 489 kg dry weight ha^{-1} and Field 3 yielding 452 kg dry weight ha^{-1}, resulting in an average of 470 kg dry weight ha^{-1} (Table 2.2). The period of biomass accumulation from spring-thaw until termination in 2022 was significantly longer than in 2019 at 83 days, with spring-thaw starting on March 20, 2022, and cover crop termination on June 10, 2022. The more extended accumulation period in 2022 was caused by intermittent flooding and prolonged saturated soil conditions in spring which delayed field operations and resulted in nearly four times as much biomass being accumulated in 2022 compared to 2019 (Table 2.2). Field 2 amassed considerably more biomass than Field 3 in 2022, accumulating 2,198 kg dry weight ha^{-1} compared to 1,324 kg dry weight ha^{-1} for Field 3. The average biomass accumulation in 2022 was 1,761 kg dry weight ha^{-1} (Table 2.2).

Table 2.2 Average biomass and C/N ratio of cover crop in spring at termination. Biomass was collected from six locations in each field, yielding 12 samples per treatment per year (n=12).

Year	Cover Crop Biomass (kg dry weight ha^{-1})	Biomass S.D.	C/N ratio	C/N ratio S.D.
2019	470	192	19.2	2.4
2022	1,761	948	26.9	4.3

NEP and *R* were temporally variable between the two cropping systems and the two study years. In both study years, daily average *NEP* was similar for the two cropping systems from January 1 until a few weeks after the start of the spring-thaw, after which the *NEP* for the two systems started to diverge, with the conventional system being a consistent C source, and the cover crop system being approximately neutral and eventually a C sink (Figure 2.3 a,b). In both study years, growth of the cover crop in spring resulted in uptake of C and positive daily *NEP* prior to its termination (Figure 2.3 a,b).

In 2019, the cover crop fields were consistently a C sink from April 22 until seeding and cover crop termination on May 13, with maximum C uptake occurring on May 9 at 13 kg C ha^{-1} (Figure 2.3 a). After cover crop termination, the cover crop fields were a C source until June 15, 2019. The conventional system did not become a C sink until June 11, 2019. Daily C uptake peak occurred on July 21, 2019, at 104 kg C ha^{-1} for the cover crop system and July 22, 2019, at 83 kg C ha^{-1} for the conventional system (Figure 2.3 a). Both cropping systems became a C source again in mid-August when the cash crop started desiccating (Figure 2.3 a).

In 2022, the cover crop fields started to become a daily C sink periodically starting May 15 and were consistently a C sink on May 31 (Figure 2.3 b). Peak C uptake by the cover crop fields occurred on June 4, 2022, at 43 kg C ha^{-1} (Figure 2.3 b). Following the cover crop termination on June 10, 2022, the two systems saw similar daily *NEP* until seeding on June 20, 2022, after which the cover crop system started to see larger daily losses of C compared to the conventional system until mid-July, where they were similar (Figure 2.3 b). The conventional system became a daily C sink starting July 2, 2022, and the cover crop system became a daily C sink starting July 10, 2022 (Figure 2.3 b). Maximum daily C uptake of 47 kg C ha^{-1} and 45 kg C ha^{-1} occurred on July 20 and July 23, 2022, for the conventional and cover crop systems, respectively (Figure 2.3 b). Both systems became a periodic source of C starting August 15, 2022 and were consistently a source as of September 25, 2022 (Figure 2.3 b).

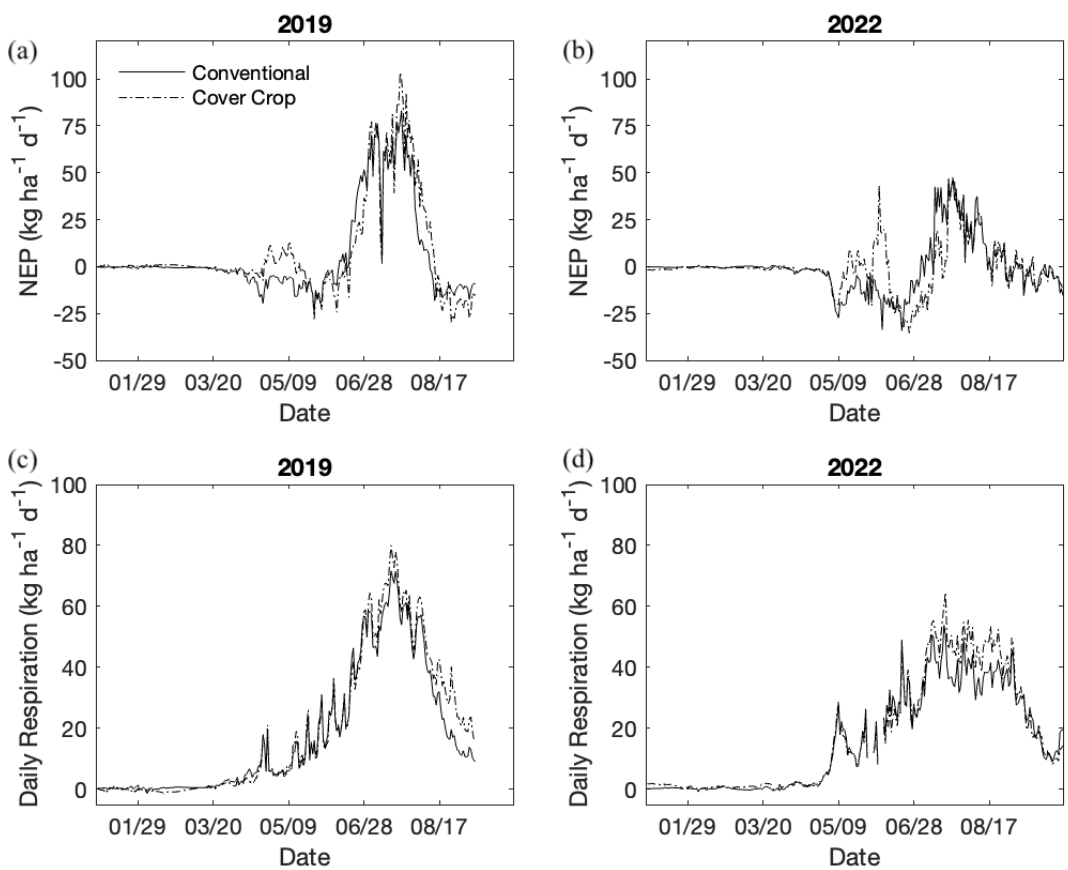

Figure 2.3 Gap-filled daily average net ecosystem production (F_{NEP}) for (a) 2019 and (b) 2022, and gap-filled daily average respiration (F_R) for (c) 2019 and (d) 2022 from January to harvest for both fields from each treatment.

Respiration from the two cropping systems was similar in both study years until late June when the two systems started to deviate (Figure 2.3 c, d). After June 29, 2019, R was consistently higher for the cover crop fields compared to the conventional fields until harvest, with a maximum difference of approximately 21 kg C ha^{-1} occurring on August 24, 2019, and a mean difference of approximately 7 kg C ha^{-1} day^{-1} for the period (Figure 2.3 c). In 2022, daily R was consistently higher for the cover crop system from June 22 until September 7, with a maximum difference of approximately 14 kg C ha^{-1} occurring on July 18, 2022, and a mean difference of approximately 7 kg C ha^{-1} day^{-1} for the period (Figure 2.3 d).

The effect of the cover crop on cumulative gap-filled *NEP* ($\sum F_{NEP}$) differed for each study year (Figure 2.4). In 2019, the C uptake by the cover crop had a short-term effect on spring $\sum F_{NEP}$ and $\sum F_{NEP}$ by harvest (Figure 2.4). Growth of the cover crop in the spring of 2019 resulted in the cropping system becoming a net C sink by May 4 (Figure 2.4). On the same date, the conventional cropping system was a net source of 301 kg C ha^{-1} (Figure 2.4). C uptake by the cover crop resulted in the cover crop fields being a cumulative C sink of 50 kg C ha^{-1} during spring-thaw until cover crop termination and the conventional fields being a C source of 316 kg C ha^{-1} in 2019. Following the termination of the cover crop at seeding, the cover crop fields became a cumulative source of C from May 24, 2019, until cash crop emergence and growth resulted in the system becoming a net sink again by June 20, 2019. The conventional system was a net C source until July 3, 2019, after which it was a sink. By harvest on September 9, 2019, the cover crop fields had a cumulative *NEP* of 1,941 kg C ha^{-1} and the conventional fields had a cumulative *NEP* of 1,445 kg C ha^{-1}.

The C uptake by the cover crop in 2022 did not have the same effect on $\sum F_{NEP}$ by harvest as in 2019. While there was C uptake by the cover crop in spring 2022, both cropping systems were a cumulative C source from spring-thaw until cover crop termination (Figure 2.4). However, the cover crop fields had significantly less C losses of 47 kg C ha^{-1} during that period than the conventional fields with losses of 649 kg C ha^{-1} (Figure 2.4). While this had an effect in the short term, increased respiration from the cover crop fields following termination resulted in similar $\sum F_{NEP}$ by harvest of -153 kg C ha^{-1} and -182 kg C ha^{-1} (Figure 2.4).

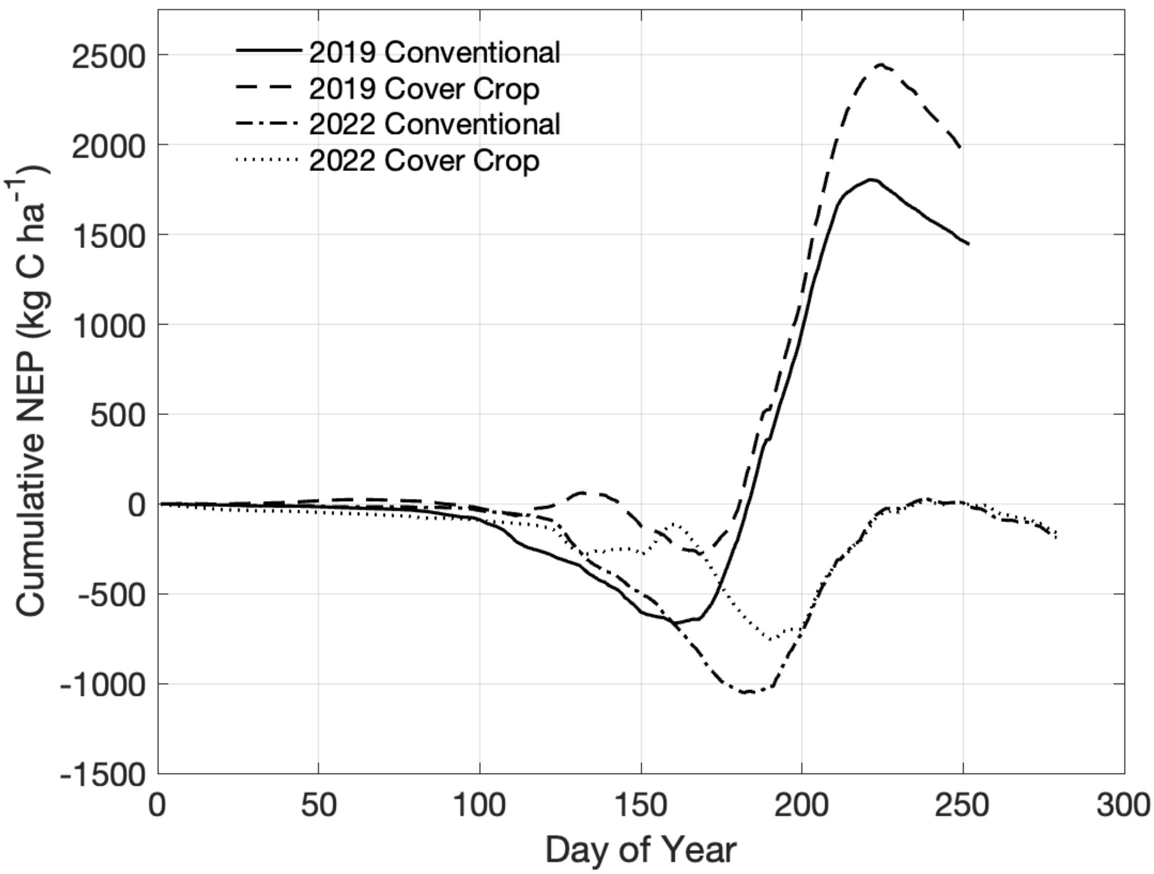

Figure 2.4 Average cumulative gap-filled net ecosystem production ($\sum F_{NEP}$) for both replicate fields from January to harvest for each treatment for the two study years.

The effect of the cover crop on grain yield compared to the conventional cropping system differed between 2019 and 2022. In 2019, both conventional fields had higher grain yields than the cover crop fields, with the mean grain yield of the conventional system being approximately 400 kg ha^{-1} greater than the grain yield of the cover crop system (Table 2.3). Compared to the average yield of 3,860 kg ha^{-1} for oats in Manitoba in 2019 (Government of Manitoba, 2023*b*), the conventional system was approximately 100 kg ha^{-1} greater than the provincial average yield for oat yield in 2019, while the grain yield from the cover crop system was 92% of the provincial average (Table 2.3). Alternatively, in 2022 the cover crop fields yielded, on average, nearly 500 kg ha^{-1} more grain than the conventional fields, with the highest yield from the site coming from Field 2 at 3,382 kg ha^{-1} (Table 2.3). Mean grain yield from the conventional and cover crop fields was 70% and 83% of the provincial average grain yield for wheat in 2022 at 3,910 kg ha^{-1}, respectively (Government of Manitoba, 2023*c*). Differences in grain yield between the treatments were not significantly different in both study years ($P = 0.27$ in 2019; $P = 0.41$ in 2022).

Table 2.3 Air dry grain yield from each cropping system for each study year. Biomass samples were collected from six locations in each field (n=6).

		Cropping System					
		Conventional			**Cover Crop No Till**		
Year	**Location**	**Field 1**	**Field 4**	**Mean**	**Field 2**	**Field 3**	**Mean**
2019	Grain Yield (kg ha^{-1})	3,667	4,247	3,957	3,496	3,616	3,556
	Standard Deviation	1,251	701	1,013	639	782	684
2022	Grain Yield (kg ha^{-1})	2,287	3,213	2,750	3,382	3,101	3,242
	Standard Deviation	1,756	1,139	1,492	1,192	1,678	1,395

By harvest in 2019, both cropping systems were a significant C sink. After factoring in harvest removals, the conventional cropping system was a source of approximately 250 kg C ha^{-1}, due to lower $\sum F_{NEP}$ and higher grain yields, while the cover crop system was a cumulative sink of approximately 400 kg C ha^{-1}, derived from higher $\sum F_{NEP}$ and lower grain yields (Table 2.4). In 2022, both cropping systems were slight C sources before factoring in carbon removals. After factoring in harvest removals, both systems were a significant source of C, with the cover crop system having greater losses due to higher grain yields (Table 2.4). Combining the $F_{ECOSYSTEM}$ from both study years for each cropping system, both systems were a C source, with the conventional system losing 1,614 kg C ha^{-1} and the cover crop system losing 1,134 kg C ha^{-1}.

Table 2.4 Carbon balance components of the two study years (January 1 to harvest for each year respectively) for the two cropping systems: gap-filled cumulative gross photosynthetic production ($\sum F_{GPP}$), gap-filled cumulative respiration ($\sum F_R$), gap-filled cumulative net ecosystem production ($\sum F_{NEP}$), C harvest removal ($F_{HARVEST}$), and C balance ($F_{ECOSYSTEM} = \sum F_{NEP} - F_{HARVEST}$). Positive net ecosystem values indicate an ecosystem gain; negative indicates an ecosystem loss.

		Year					
Cropping System		2019			2022		
Conventional	Location	Field 1	Field 4	Mean	Field 1	Field 4	Mean
	$\sum F_{GPP}$, kg C ha^{-1}	4,496	7,243	5,869	3,959	4,488	4,224
	$\sum F_R$, kg C ha^{-1}	3,032	5,761	4,396	4,195	4,417	4,306
	$\sum F_{NEP}$, kg C ha^{-1}	1,446	1,444	1,445	-297	-66	-182
	$F_{HARVEST}$, kg C ha^{-1}	1,570	1,815	1,693	984	1,385	1,185
	$F_{ECOSYSTEM}$, kg C ha^{-1}	-124	-372	-248	-1,281	-1,451	-1,366
Cover Crop No-Till	Location	Field 2	Field 3	Mean	Field 2	Field 3	Mean
	$\sum F_{GPP}$, kg C ha^{-1}	7,349	6,227	6,788	4,390	4,645	4,518
	$\sum F_R$, kg C ha^{-1}	5,284	4,404	4,844	4,648	4,916	4,782
	$\sum F_{NEP}$, kg C ha^{-1}	2,062	1,820	1,941	-178	-128	-153
	$F_{HARVEST}$, kg C ha^{-1}	1,488	1,547	1,517	1,480	1,331	1,406
	$F_{ECOSYSTEM}$, kg C ha^{-1}	575	273	424	-1,658	-1,459	-1,558

2.4.3 Relationship Between NEP and GPP

NEP vs. *GPP* showed a strong relationship between the cover crop and conventional cropping systems in 2019 with $R^2 > 0.95$ (Figure 2.5). In 2022, *NEP vs. GPP* when $GPP < 40$ showed a weak relationship, with R^2 values of 0.032 and 0.219 for the cover crop and conventional systems, respectively (Figure 2.5). *NEP vs GPP* when $GPP > 40$ in 2022 had a stronger relationship with R^2 values of 0.845 and 0.877 for the cover crop and conventional systems, respectively (Figure 2.5). The relationship of *NEP vs. GPP* was significant ($P < 0.05$) from all linear regression analyses except for the cover crop system when $GPP < 40$ in 2022 ($P = 0.297$).

R_h, calculated from the intercept of the linear regression equations, varied between the cropping system and year. In 2019, the cover crop system had R_h of approximately 5 kg C ha^{-1} greater than the conventional system during the growing season (Figure 2.5). R_h in 2022 when

GPP < 40 was similar between the two cropping systems at 8.6 kg C ha^{-1} and 8.4 kg C ha^{-1} for the cover crop and conventional systems, respectively (Figure 2.5). R_h differed between the two cropping systems in 2022 when *GPP* > 40, with the cover crop system having a R_h approximately 9.4 kg C ha^{-1} greater than the conventional system (Figure 2.5).

R_a/GPP was similar for both cropping systems in 2019, with approximately 28% and 31% of *GPP* respired autotrophically in the cover crop and conventional systems, respectively. R_a/GPP in 2022 differed between the two cropping systems when *GPP* < 40, with approximately 89% and 79% of *GPP* respired autotrophically in the cover crop and conventional systems, respectively. R_a/GPP when *GPP* > 40 in 2022 was similar between the two cropping systems at 2% and 5% for the cover crop and conventional systems, respectively. The growing season *NEP* from the cover crop and conventional cropping systems were not statistically different in both study years (P = 0.59 in 2019; P = 0.13 when *GPP* < 40 in 2022; P = 0.06 when *GPP* > 40 in 2022).

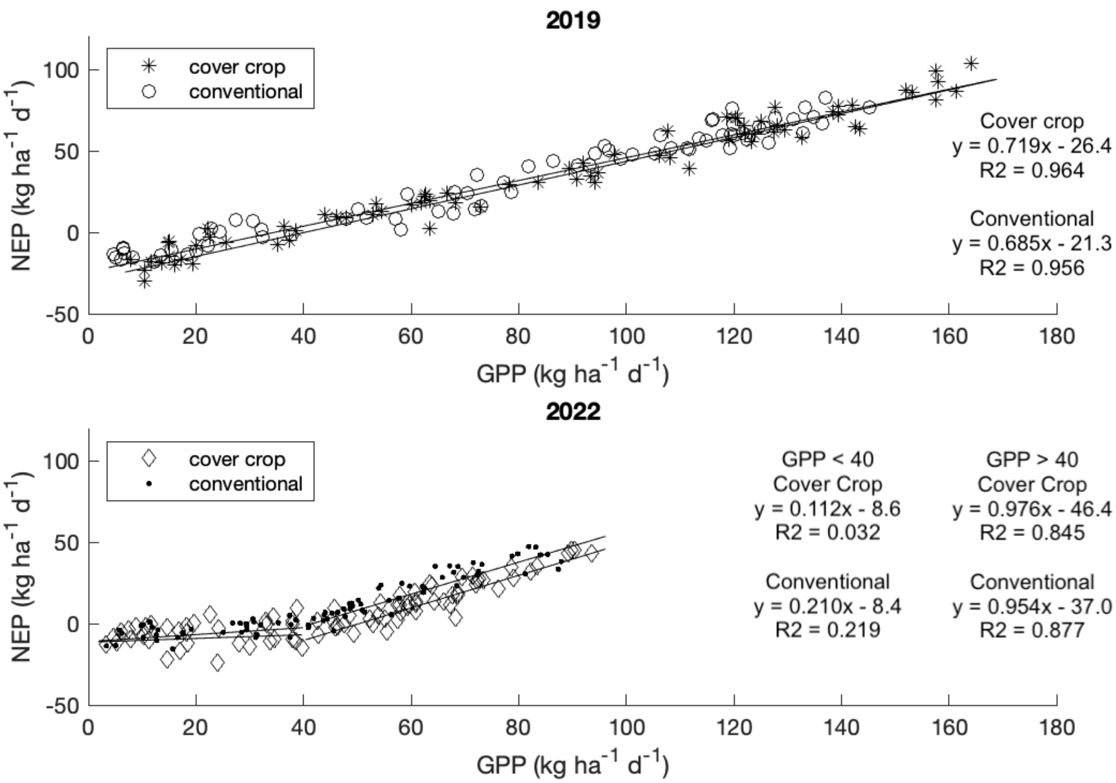

Figure 2.5 Daily *NEP* vs. *GPP* during the growing season for 2019 and 2022. The growing season was defined as *GPP* > 5 kg ha^{-1} day^{-1} following seeding and cover crop termination. Linear regressions of cover crop and conventional treatments are shown.

2.5 Discussion

2.5.1 Cover Crop Impacts on Soil Moisture

Differences in soil GMC in the two study years showed that the cover crop had a minimal effect on soil moisture under lower than normal precipitation amounts in 2019 and a greater effect under saturated soil conditions and high precipitation experienced in 2022. Total precipitation from January to September 2019 was lower than the 30-year normal in all months except July and September. Similar GMC values from both treatments in 2019 showed that the use of soil moisture by the cover crop during growth in spring did not affect soil GMC compared to conventional fields.

A similar response was seen by Rosario-Lebron et al. (2019) in a study in Maryland, USA, who reported no difference in soil moisture from cover crops following termination and cash crop planting under average rainfall conditions for the region. In 2022 however, under prolonged saturated soil conditions and higher than normal amounts of precipitation, the cover crop appeared to influence soil moisture as soil GMC was lower at all samplings in the cover crop fields compared to the conventional fields and was significantly lower in June and September. Lower soil GMC from the cover crop fields was potentially due to water usage and transpiration from the cover crop, as well as improved soil physical structure from the cover crop roots and no-tillage practices. Chakraborty et al. (2022) reported lower early-season soil moisture from cover-cropped soils compared to non-cover cropped soils due to water usage and transpiration and improved soil water status for the subsequent cash crop by improving soil physical properties. Kahimba et al. (2008) found that a berseem clover cover crop inter-seeded with an oat crop reduced excess soil moisture during the growing season and Acharya et al. (2019) found that no-till increased water percolation at 20 to 40 cm soil depth compared to conventional tillage. The lower GMC observed in 2022 was likely a result of water usage by the cover crop and improved soil physical structure.

2.5.2 Carbon Dioxide Fluxes

Good cover crop establishment in the fall of 2018 and 2021 resulted in good biomass accumulation the following spring. However, environmental conditions from January to harvest varied significantly between the two study years resulting in different conditions during cover crop and cash crop growth. Precipitation was generally lower than the 30-year normal from cover crop seeding in August 2018 until termination in May 2019 (Table 2.1), resulting in fair cover crop growth and cash crop seeding occurring close to the recommended seeding date for oats for the region (MASC, 2023). Alternatively, precipitation was higher than the 30-year normal every month from January to August 2022, except for June, which was slightly below normal (Table 2.1). This resulted in prolonged flooding in spring 2022, which delayed field operations and seeding until June 20, over a month later than the recommended seeding date for spring wheat for the region (MASC, 2023). Varying environmental conditions in spring affected the length of cover crop biomass accumulation and, thus, total cover crop biomass accumulation at termination, with nearly four times the amount of biomass accumulated in 2022 compared to 2019 (Table 2.2). However, increased biomass accumulation did not result in increased cumulative C uptake in both years as weather and saturated soil conditions delayed cover crop growth and C uptake in 2022, resulting in more C being lost from respiration before it was assimilated by cover crop growth. In both study years, the cover crop fields were consistently a C sink for spring before termination, affecting cumulative *NEP* for the spring-thaw to cover crop termination compared to the conventional cropping system. Similar early season C uptake was observed by Maas et al. (2013), who observed differences in spring C assimilation and cumulative net ecosystem exchange from an established perennial forage crop compared to an annual cropping system where soils were in fallow, with the perennial system having earlier C assimilation and being a cumulative C sink earlier than the annual system. Peak C uptake varied between the two years and was the result of differences in physiological maturity due to the length of biomass accumulation of the cover crop, with the cover crop approaching maturity in 2022 when peak uptake of 43 kg C ha^{-1} occurred on June 4, 2022, compared to peak uptake in 2019 of 13 kg C ha^{-1} which occurred on May 9, 2019.

The cover crop increased *R* in both years by approximately 7 kg C ha^{-1} day^{-1} compared to the conventional fields from late June until early September (Figure 2.3). Increased respiration and CO_2 emissions from soils with the adoption of cover crops have been seen in other studies (Bavin et al., 2009; Muhammad et al., 2019; Negassa et al., 2015; Sanz-Cobena et al., 2014), as cover crop residues increase C inputs to soil, increasing the amount of C available to soil microbes. $\sum F_R$ was similar for both cropping systems in both study years, despite the study year in 2022 being over a month longer than 2019, with mean $\sum F_R$ of 4,396 kg C ha^{-1} and 4,306 kg C ha^{-1} for the conventional system in 2019 and 2022, respectively, and mean $\sum F_R$ of 4,844 kg C ha^{-1} and 4,782 kg C ha^{-1} for the cover crop system in 2019 and 2022, respectively (Table 2.4). Cumulative C loss experienced in 2022 thus resulted from lower *GPP* and not increased *R* (Table 2.4).

$\sum F_{NEP}$ by harvest varied between the two study years and treatments. In 2019 both cropping systems were a *NEP* sink, whereas, in 2022, both were a slight source (Table 2.4). Glenn et al. (2010) observed that a spring wheat crop grown in 2008 at the site was a net C sink prior to factoring in harvest removals, similar to what was observed in our study in 2019. Alternatively, Amiro et al. (2017) found similar responses in *NEP* to what was observed in our study in 2022 during wheat and barley growth at the site in 2010, 2011, and 2014, with *NEP* being close to neutral or a slight source. Growing conditions in 2010 during barley growth at the site were similar to those in 2022 in our study, with high precipitation levels (Amiro et al., 2017), which may partially explain the lower *NEP* in 2022 compared to 2019. Lower *NEP* in 2022 could have also resulted from poorer crop performance from late seeding, as the spring wheat was seeded over a month later than the recommended seeding date (MASC, 2023). Differences in $\sum F_{NEP}$ between the cover crop and conventional fields were observed in 2019, with C uptake by the cover crop persisting until harvest. However, the C sequestered by the cover crop in 2022 did not affect $\sum F_{NEP}$ by harvest compared to the conventional fields, with $\sum F_{NEP}$ being similar for the two cropping systems and a slight C source.

Cash crop yield response varied between the two study years, with the cover crop fields having lower yields than the conventional fields in 2019 and higher yields than the conventional fields in 2022, which affected overall $F_{ECOSYSTEM}$ for each of the cropping systems in both study years (Table 2.3). While the conventional system was a $\sum F_{NEP}$ sink in 2019, it was a C source after factoring in harvest removals ($F_{ECOSYSTEM}$ = -248 kg C ha-1). Net C losses with positive *NEP* have occurred in other flux studies (Amiro et al., 2017; Aubinet et al., 2009; Béziat et al., 2009; Ceschia et al., 2010; Dold et al., 2017; Glenn et al., 2010; Kutsch et al., 2010; Maas et al., 2013), highlighting that harvest removals are an important component in determining the overall C balance of cropping systems. The cover crop system was both a $\sum F_{NEP}$ and $F_{ECOSYSTEM}$ sink after factoring in harvest removals in 2019. This resulted from increased *NEP* from cover crop growth and slightly lower harvest removals compared to the conventional system. In 2022, both systems were a slight $\sum F_{NEP}$ source and a significant C source after factoring in harvest removals. Similar results for the conventional fields have been seen at the site in previous research (Amiro et al., 2017; Glenn et al., 2010; Maas et al., 2013), however $F_{ECOSYSTEM}$ for the cover crop system was considerably different in 2022 compared to 2019. Baker and Griffis (2005) found similar results when an oat cover crop was seeded in spring before soybean planting. The oats increased C sequestration prior to soybean planting but increased respiration following its termination, resulting in both the conventional and alternative management practices having nearly identical C balance after harvest C removals were accounted for (Baker and Griffis, 2005). Cates and Jackson (2018) also found no difference between the net ecosystem carbon balance of a corn silage crop managed conventionally versus being seeded with a rye cover crop, even though the cover increased net primary productivity compared to the conventional system. In our study, decreased

GPP, increased *R,* and increased harvest removals for the cover crop fields in 2022 resulted in the system being a $F_{ECOSYSTEM}$ source.

2.5.3 *NEP vs GPP*

R^2 values from the relationship of *NEP vs. GPP* differed between the two study years and different periods in 2022. In 2019 and 2022 when *GPP* > 40, R^2 values were within the range of R^2 values reported by Amiro et al. (2017) for other cereal crops grown at the site ($R^2 = 0.52 – 0.95$) (Amiro et al., 2017) and the relationship between *NEP* and *GPP* was significant (P < 0.05). In 2022 when *GPP* < 40 however, R^2 values were lower than all values reported by Amiro et al. (2017), and the P value of the linear regression analysis for the cover crop system was insignificant (P > 0.05). The low R^2 values when *GPP* < 40 and weak P value from the cover crop system in 2022 could have been the result of prolonged saturated soil conditions experienced at the site and potentially from late seeding affecting crop performance. The lowest R^2 value from *NEP vs. GPP* analysis by Amiro et al. (2017) was from a wheat crop in 2011 which was seeded on June 10, close to when the spring wheat was seeded in 2022 in our study. While statistical analysis showed that the cover crop did not significantly affect growing season *NEP* compared to the conventional fields in both study years, poor growing conditions and late seeding may have affected the relationship between *NEP vs. GPP* when *GPP* < 40, resulting in an insignificant relationship for the cover crop system and low R^2 values.

R_a values from the relationship of *NEP vs. GPP* in 2019 were within the range of values reported by Amiro et al. (2017) for other cereal crops grown at the site in previous years ($R_a = 0.21 – 0.52$) (Amiro et al., 2017). R_a values from the relationship of *NEP vs. GPP* in 2022 differed compared to 2019 and when *GPP* > 40 and when *GPP* < 40. When *GPP* < 40, R_a values were higher than the R_a values from 2019 and all values reported by Amiro et al. (2017) in previous years at the site. When $GPP > 40$, R_a values were substantially lower compared to R_a values from 2019 and values reported by Amiro et al. (2017). Differences in R_a between the two cropping systems were also observed in 2022 when $GPP < 40$, with the cover crop system having approximately 10% higher R_a than the conventional system, which was not observed in 2019 or in 2022 when $GPP > 40$. Low R_a values when $GPP > 40$ may have been due to saturated soil conditions at the site during the growing season. The lowest R_a value reported by Amiro et al. (2017) was observed in 2008 when precipitation levels were more than 700 mm, similar to precipitation levels experienced in our study in 2022. The difference in R_a in 2022 when $GPP < 40$ could have been from reduced soil moisture from the cover crop utilizing available soil water compared to the conventional system. Reduced autotrophic respiration from high soil moisture was reported by Zhang et al. (2013), who found that autotrophic respiration was suppressed for a period under waterlogged soil conditions in a corn crop. While the site received higher than normal amounts of precipitation in 2022, soil GMC was lower in the cover crop fields than in the conventional fields, potentially resulting in better growing conditions for the wheat crop and higher R_a for the cover crop system when $GPP < 40$.

The cover crop fields had higher R_h values than the conventional fields in 2019 and in 2022 when $GPP > 40$, indicating that the cover crop increased heterotrophic respiration during the growing season compared to the conventional fields. The increase in R_h from the cover crop system compared to the conventional system was greater in 2022 than in 2019 at approximately 10 kg C ha^{-1} increase compared to approximately 5 kg C ha^{-1}. Differences in R_h values between the two study years was likely the result of biomass accumulation, with substantially more cover crop biomass being accumulated in 2022 compared to 2019, providing more C substrates to soil microbes and increasing respiration. Overall, analysis of the relationship of *NEP vs. GPP* suggests that increased *R* in both study years from the cover crop fields was primarily from increased heterotrophic respiration in 2019 and 2022 when *GPP* > 40 and from increased autotrophic respiration in 2022 when *GPP* < 40.

2.5.4 Cover Crop and Cash Crop Variability

Cover crop and cash crop variability between fields at the site were lower in 2019 than in 2022 due to better weather and soil conditions during growth. Cover crop biomass was similar between the two fields in 2019. Cash crop yields in 2019 were similar between Fields 1, 2 and 3 but higher in Field 4, as observed in previous research at the site (Amiro et al., 2017), and increased mean grain yield for the conventional fields.

Saturated soil conditions in 2022 resulted in higher cover crop and cash crop growth variability. Cover crop biomass was considerably higher in Field 2 than in Field 3 due to a drainage ditch that ran through Field 3, drowning some of the cover crop in that field in spring. Grain yield was similar between Fields 2, 3 and 4 in 2022 and lowest in Field 1, which was partially flooded for most of 2022, resulting in large bare patches during cash crop growth and lowering yields.

2.5.5 Uncertainty

Following data filtering, flux measurements captured 46% of the CO_2 fluxes at the site. Data gaps were filled using the FCRN model using the moving-window technique (Amiro et al., 2017; Barr et al., 2004). However, uncertainty in flux measurements and gap-filling could have been introduced during our study. Early research at the site by Glenn et al. (2010) estimated that random errors during the growing season were approximately 10% and that uncertainty increased to 18-35% following gap-filling from systematic errors. Random and systematic errors were likely similar in our study. The error may have been introduced during our study from *K* values, as *K* values from each sonic were averaged to give one *K* value which was used for flux calculations. Uncertainty in flux calculations due to time-of-day bias could have been introduced in 2022 as the logger program that came with the system upgrades in 2019 did not include a lag at midnight to avoid time-of-day bias.

Uncertainty existed in soil GMC and biomass estimations as samples that were collected during the study were collected from only six locations within each field. There is also uncertainty in cover crop biomass accumulation and $F_{HARVEST}$ as both were determined from hand-clipped biomass samples. Further, cash crop biomass samples were threshed with different equipment than what was used to harvest the cash crop from the field, which could have caused over or underestimations of harvest removals depending on the differences in equipment and grain losses during harvest.

2.5.6 Implications for Agricultural System Management

Utilizing cover crops in agricultural production has been found to increase soil organic carbon (SOC) in agricultural soils (Firth et al., 2022; Poeplau and Don, 2015; Tellatin and Myers; 2018; Thapa et al., 2019). However, changes are often assessed over multiple years or following long-term implementation. This study provides insight into the short-term impact of converting to a no-till cover crop system on CO_2 fluxes in northern latitude soils compared to a conventional cropping system and the effects of cover crop growth on C dynamics in spring and following cover crop termination. Uptake of CO_2 in the spring of 2019 resulted in differences in cumulative C flux by harvest and led to the cropping system being a net C sink once harvest removals were included, demonstrating that cover crops can increase C sequestration in soils in the short-term in the Canadian Prairies. However, the cover crop did not increase C sequestration in both study years, with 2022 being a significant C loss with harvest removals. In both study years, *GPP* was the driver of differences in cumulative *NEP* as *R* was similar for each cropping system for both years, even with varying monitoring lengths. While increased *GPP* resulted in higher *NEP* in the cover crop fields in 2019, the cover crop increased *R* compared to the conventional system in both study years and needs to be considered in future research that aims to increase *GPP* in agricultural production.

Our study did not look at the prolonged use of cover crops on C balance, differences in CO_2 fluxes during establishment in fall, or the effects of discontinuing the use of cover crops on C fluxes. Amiro et al. (2017) found that terminating a perennial forage crop at the site resulted in the loss of the C that was gained during the forage phase of the crop rotation as residues were decomposed by soil microbes. Discontinuation of cover cropping could have similar impacts on the following growing season *NEP* as the decomposition of cover crop residues could increase soil respiration the following growing season. Increased respiration often occurs in maize-soybean rotations during the soybean year of the rotation as remaining maize residues are respired the following year during soybean growth (Suyker and Verma, 2012). Therefore, the effects of the cover crop no-till systems on long-term C dynamics in the Canadian Prairies and following cessation of the practice needs to be investigated to understand the full effect of cover crops on C dynamics.

While the cover crop did not result in the cropping system being a net C sink after harvest removals in both study years, other benefits of cover crops were demonstrated in this study, particularly in 2022 under prolonged saturated soil conditions where the cover crop fields had higher grain yield and lower soil moisture than the conventional fields. The frequency and severity of extreme weather events are projected to increase as GHG emissions continue and climate change worsens, destabilizing food production (IPCC, 2022). Fall rye cover crops can provide security in food production as they can be harvested as a cash crop if allowed to reach maturity, offering a way to diversify and increase security in cropping systems. Long-term cover crop studies will be necessary to fully assess the impact of cover crops on C sequestration in agricultural soils in Canada.

2.6 Conclusion

A no-till fall rye cover crop cropping system increased C assimilation in spring prior to cash crop seeding in 2019 and 2022. C assimilation in 2019 resulted in the cropping system being a net C sink of 424 kg C ha^{-1} compared to the conventional cropping system, which was a C source of 248 kg C ha^{-1} following harvest removals. In 2022 however, the cover crop no-till and conventional systems were a large C source of 1,558 kg C ha^{-1} for the cover crop system and 1,366 kg C ha^{-1} for the conventional system, respectively, demonstrating that cover crops do not necessarily increase C sequestration by harvest compared to conventional cropping systems. However, the cover crop did result in lower soil moisture and increased yields in 2022, highlighting other agronomic benefits of cover crops. The cover crop no-till system increased soil respiration during the growing season following cover crop termination in both study years by approximately 7 kg ha^{-1} day^{-1} compared to the conventional cropping system. The relationship between *NEP* and *GPP* showed that the increase in respiration in 2019 was due to increased heterotrophic respiration, and in 2022 it was due to increased autotrophic respiration when $GPP < 40$ and from increased heterotrophic respiration when $GPP > 40$. To fully understand the effect of no-till cover crop systems on C balance in the Canadian Prairies, the effect of cover crops on fall C dynamics during establishment and use over the long term needs to be determined. Our study helps further the understanding of cover crop use on seasonal CO_2 fluxes, C dynamics during the growing season, and C balance up to cash crop harvest.

2.7 References

Acharya, B.S., Dodla, S., Gaston, L.A., Darapuneni, M., Wang, J.J., Sepat, S., and Bohara, H. 2019. Winter cover crops effect on soil moisture and soybean growth and yield under different tillage systems. Soil and Tillage Research. **195**: 104430.

Amiro, B.D. 2021. Corrections for bias in gradients caused by mis-matched lines in 2020 and 2021 at TGAS-MAN. APPENDIX B.

Amiro, B.D., Tenuta, M., Gervais, M., Glenn, A.J., and Gao, X. 2017. A decade of carbon flux measurements with annual and perennial crop rotations on the Canadian Prairies. Agricultural and Forest Meteorology. **247**: 491-502.

Asgedom, H. and Kebreab, E. 2011. Beneficial management practices and mitigation of greenhouse gas emissions in the agriculture of the Canadian Prairie: a review. Agronomy for Sustainable Development. **31**: 433-451.

Aubinet, M., Moureaux, C., Bodson, B., Dufranne, D., Heinesch, B., Suleau, M., Vancutsem, F., and Vilret, A. 2009. Carbon sequestration by a crop over a 4-year sugar beet/ winter wheat/ seed potato/ winter wheat rotation cycle. Agricultural and Forest Meteorology. **149**: 407-418.

Baker, J.M. and Griffis, T.J. 2005. Examining strategies to improve the carbon balance of corn/soybean agriculture using eddy covariance and mass balance techniques. Agricultural and Forest Meteorology. **128**: 163-177.

Barr, A.G., Black, T.A., Hogg, E.H., Kljun, N., Morgenstern, K., and Nesic, Z. 2004. Inter-annual variability in the leaf area index of a boreal aspen-hazelnut forest in relation to net ecosystem production. Agricultural and Forest Meteorology. **126**: 237-255.

Bavin, T.K., Griffis, T.J., Baker, J.M., and Venterea, R.T. 2009. Impact of reduced tillage and cover cropping on the greenhouse gas budget of a maize/soybean rotation ecosystem. Agriculture, Ecosystems and Environment. **134**: 234-242.

Béziat, P., Ceschia, E., and Dedieu, G. 2009. Carbon balance of a three crop sucession over two cropland sites in South West France. Agricultural and Forest Meteorology. **149**: 1628-1645.

Cates, A.M. and Jackson, R.D. 2018. Cover crop effects on net ecosystem carbon balance in grain and silage maize. Agronomy Journal. **110**: 30-38.

Ceschia, E., Béziat, P., Dejoux, J.F., Aubinet, M., Bernhofer, Ch., Bodson, B., Buchmann, N., Carrara, A., Cellier, P., Di Tommasi, P., Elbers, J.A., Eugster, W., Grünwald, T., Jacobs, C.M.J., Jans, W.W.P., Jones, M., Kutsch, W., Lanigan, G., Magliulo, E., Marloie, O., Moors, E.J., Moureaux, C., Olioso, A., Osborne, B., Sanz, M.J., Saunders, M., Smith, P., Soegaard, H., and Wattenbach, M. 2010. Management effects on net ecosystem carbon and GHG budgets at European crop sites. Agriculture, Ecosystems and Environment. **139**: 363-383.

Chahal, I., Hooker, D.C., Deen, B., Janovicek, K., and Van Eerd, L.L. 2021. Long-term effects of crop rotation, tillage, and fertilizer nitrogen on soil health indicators and crop productivity in a temperate climate. Soil and Tillage Research. **213**: 105121.

Chahal, I., Vyn, R.J., Mayers, D., and Van Eerd, L.L. 2020. Cumulative impact of cover crops on soil carbon sequestration and profitability in a temperate humid climate. Scientific Reports. **10**: 13381.

Chakraborty, P., Singh, J., Singh, N., and Kumar, S. 2022. Assessing the influence of cover crop on soil water dynamics using soil moisture measurements and hydrus-1D simulations. Soil Science Society of America Journal. **86**: 1538-1552.

Darapuneni, M.K., Idowu, O.J., Sarihan, B., DuBois, D., Grover, K., Sanogo, S., Djaman, K., Lauriault, L., Omer, M., and Dodla, S. 2021. Growth characteristics of summer cover crop grasses and their relation to soil aggregate stability and wind erosion control in arid southwest. Applied Engineering in Agriculture. **37**: 11-23.

Denmead, O.T. 2008. Approaches to measuring fluxes of methane and nitrous oxide between landscapes and the atmosphere. Plant and Soil. **309**: 5-24.

Dold, C., Büyükcangaz, H., Rondinelli, W., Prueger, J.H., Sauer, T.J., and Hatfield, J.L. 2017. Long-term carbon uptake of agro-ecosystems in the Midwest. Agricultural and Forest Meteorology. **232**: 128-140.

Edwards, G.C., Thurtell, G.W., Kidd, G.E., Dias, G.M., and Wagner-Riddle, C. 2003. A diode laser based gas monitor suitable for measurement of trace gas exchange using micrometeorological techniques. Agricultural and Forest Meteorology. **115**: 71-89.

Ehrlich, W.A., Poyser, E.A., Pratt, L.E., and Ellis, J.H. 1953. MB-5 Report of Reconnaissance Soil Survey of Winnipeg and Morris Map Sheet Areas. Manitoba Soil Survey, Winnipeg, MB. https://sis.agr.gc.ca/cansis/publications/surveys/mb/mb5/mb5_report.pdf (accessed March 21, 2022).

Environment Canada. 2023*a*. Canadian Climate Normals 1981-2010 Station Data. Government of Canada. https://climate.weather.gc.ca/climate_normals/results_1981_2010_e.html?searchType=stnName&txtStationName=Glenlea&searchMethod=contains&txtCentralLatMin=0&txtCentralLatSec=0&txtCentralLongMin=0&txtCentralLongSec=0&stnID=3599&dispBack=1 (accessed March 25, 2023).

Environment Canada. 2023*b*. Historical Data. Government of Canada. https://climate.weather.gc.ca/climate_data/hourly_data_e.html?hlyRange=2013-12-10%7C2023-01-03&dlyRange=1996-10-01%7C2023-01-03&mlyRange=1996-10-01%7C2007-11-01&StationID=27174&Prov=MB&urlExtension=_e.html&searchType=stnName&optLimit=yearRange&StartYear=1840&EndYear=2023&selRowPerPage=25&Line=0&searchMethod=contains&txtStationName=Winnipeg+A+CS&timeframe=1&time=LST&time=LST&Year=2022&Month=8&Day=28# (accessed March 25, 2023).

Firth, A.G., Brooks, J.P., Locke, M.A., Morin, D.J., Brown, A., and Baker, B.H. 2022. Dynamics of soil organic carbon and CO_2 flux under cover crop and no-till management in soybean cropping systems of the Mid-South (USA). Environments. **9**, 109. https://doi.org/10.3390/environments9090109.

Frick, B., Telford, L., and Thiessen Martens, J. 2017. Organic Field Crop Handbook (J. Wallace (Ed). Third Edition. Canadian Organic Growers.

Garratt, J.R. 1992. The atmospheric boundary layer. Cambridge Atmospheric and Space Science Series. Cambridge University Press. New York, NY.

Glenn, A.J., Amiro, B.D., Tenuta, M., Stewart, S.E., and Wagner-Riddle, C. 2010. Carbon dioxide exchange in a northern Prairie cropping system over three years. Agricultural and Forest Meteorology. **150**: 908-918.

Government of Manitoba. 2023*a*. Agricultural Climate of Manitoba. Government of Manitoba. https://www.gov.mb.ca/agriculture/weather/agricultural-climate-of-mb.html (accessed April 4, 2023).

Government of Manitoba. 2023*b*. Manitoba Markets – November Estimates of Crop Production 2019. Government of Manitoba. https://www.gov.mb.ca/agriculture/markets-and-statistics/pubs/estimates-of-production.pdf (accessed March 29, 2023).

Government of Manitoba. 2023*c*. Manitoba Markets – Estimates of Field Crop Production 2022. Government of Manitoba. https://www.manitoba.ca/agriculture/markets-and-statistics/crop-statistics/pubs/estimates_of_field_crop_production-2022.pdf (accessed March 29, 2023).

Hartwig, N.L. and Ammon, H.U. 2002. Cover crops and living mulches. Weed Science. **50**: 688-699.

IPCC. 2022. Summary for Policymakers. Pörtner, H.-O., Roberts, D.C., Poloczanska, E.S., Mintenbeck, K., Tignor, M., Alegría, A., Craig, M., Langsdorf, S., Löschke, S., Möller, V., and Okem, A. (eds.). *In*: Climate Change 2022: Impacts, Adaptation and Vulnerability. Contribution of Working Group II to the Sixth Assessment Report of the Intergovernmental Panel on Climate Change. Pörtner, H.-O., Roberts, D.C., Tignor, M., Poloczanska, E.S., Mintenbeck, K., Alegría, A., Craig, M., Langsdorf, S., Löschke, S., Möller, V., Okem, A., and Rama, B. (Eds.). Cambridge University Press. Cambridge, UK and New York, NY, USA. pp. 3-33, doi:10.1017/9781009325844.001.

Kahimba, F.C., Sri Ranjan, R., Froese, J., Entz, M., and Nason, R. 2008. Cover crop effects on infiltration, soil temperature, and soil moisture distribution in the Canadian Prairies. Applied Engineering in Agriculture. **24**: 321-333.

**Kutsch, W.L., Aubinet, M., Buchmann, N., Smith, P., Osborne, B., Eugster, W., Wattenbach, M., Schrumpf, M., Schulze, E.D., Tomelleri, E., Ceschia, E., Bernhofer, C., Béziat, P., Carrara, A., Di Tommasi, P., Grünwald, T., Jones, M., Magliulo, V., Marloie, O., Moureaux,

C., Olioso, A., Sanz, M.J., Saunders, M., Søgaard, H., and Ziegler, W. 2010. The net biome production of full crop rotations in Europe. Agriculture, Ecosystems and Environment. **139**: 336-345.

Larsen, R.J., Beres, B.L., Blackshaw, R.E., and Graf, R.J. 2018. Extending the growing season: winter cereals in western Canada. Canadian Journal of Plant Science. **98**: 267-277.

Liu, J. and Lobb, D.A. 2021. An overview of crop and crop residue management impacts on crop water use and runoff in the Canadian Prairies. Water. **13**: 2929.

Maas, S.E., Glenn, A.J., Tenuta, M., and Amiro, B.D. 2013. Net CO_2 and N_2O exchange during perennial forage establishment in an annual crop rotation in the Red River Valley, Manitoba. Canadian Journal of Soil Science. **93**: 639-652.

MASC (Manitoba Agricultural Services Corporation). 2023. MMPP – Seeding Dates and Yield Information. https://www.masc.mb.ca/masc.nsf/mmpp_seeding_dates.html (Accessed April 10, 2023).

Michalyna, W., Gardiner, W.M., and Podolsky, G. 1975. Soils of the Winnipeg Region Study Area. Canada-Manitoba Soil Survey. Prepared for: Province of Manitoba, Department of Municipal Affairs Municipal Planning Branch. https://sis.agr.gc.ca/cansis/publications/surveys/mb/mbd14/mbd14_report.pdf (accessed March 21, 2022).

Muhammad, I., Sainju, U.M., Zhao, F., Khan, A., Ghimire, R., Fu, X., and Wang, J. 2019. Regulation of soil CO_2 and N_2O emissions by cover crops: A meta-analysis. Soil and Tillage Research. **192**: 103-112.

Negassa, W., Price, R.F., Basir, A., Snapp, S.S., and Kravchenko, A. 2015. Cover crop and tillage systems effect on soil CO_2 and N_2O fluxes in contrasting topographic positions. Soil and Tillage Research. **154**: 64-74.

Pattey, E., Edwards, G., Strachan, I.B., Desjardins, R.L., Kaharabata, S., and Wagner-Riddle, C. 2006. Towards standards for measuring greenhouse gas fluxes from agricultural fields using instrument towers. Canadian Journal of Soil Science. **86**: 373-400.

Perrone, S., Grossman, J., Liebman, A., Sooksa-nguan, T., and Gutknecht, J. 2020. Nitrogen fixation and productivity of winter annual legume cover crops in Upper Midwest organic cropping systems. Nutrient Cycling in Agroecosystems. **117**: 61-76.

Poeplau, C. and Don, A. 2015. Carbon sequestration in agricultural soils via cultivation of cover crops – A meta-analysis. Agriculture, Ecosystems and Environment. **200**: 33-41.

Rosario-Lebron, A., Leslie, A.W., Yurchak, V.L., Chen, G., and Hooks, C.R.R. 2019. Can winter cover crop termination practices impact weed suppression, soil moisture, and yield in no-till soybean [*Glycine max* (L.) Merr.]? Crop Protection. **116**: 132-141.

Sanz-Cobena, A., García-Marco, S., Quemada, M., Gabriel, J.L., Almendros, P., and Vallejo, A. 2014. Do cover crops enhance N_2O, CO_2 or CH_4 emissions from soil in Mediterranean arable systems? Science of the Total Environment. **466-467**: 164-174.

Smith, K.A., Ball, T., Conen, F., Dobbie, K.E., Massheder, J., and Rey, A. 2018. Exchange of greenhouse gases between soil and atmosphere: interactions of soil physical factors and biological processes. European Journal of Soil Science. **69**: 10-20.

Suyker, A.E. and Verma, S.B. 2012. Gross primary production and ecosystem respiration of irrigated and rainfed maize-soybean cropping systems over 8 years. Agricultural and Forest Meteorology. **165**: 12-24.

Tellatin, S. and Myers, R.L. 2018. Cover crop impacts on US cropland carbon sequestration. Journal of Soil and Water Conservation. **73**: 117A-121A.

Tenuta, M., Amiro, B.D., Gao, X., Wagner-Riddle, C., and Gervais, M. 2019. Agricultural management practices and environmental drivers of nitrous oxide emissions over a decade for an annual and an annual-perennial crop rotation. Agricultural and Forest Meteorology. **276-277**: 107636.

Thapa, V.R., Ghimire, R., Duval, B.D., and Marsalis, M.A. 2019. Conservation systems for positive net ecosystem carbon balance in semiarid drylands. Agrosystems, Geosciences and Environment. **2**: 190022.

Zhang, Q., Lei, H-.M., and Yang, D-.W. 2013. Seasonal variations in soil respiration, heterotrophic respiration and autotrophic respiration of a wheat and maize rotation cropland in the North China Plain. Agricultural and Forest Meteorology. **180**: 34-43.

3. EFFECT OF FALL RYE COVER CROP ON SPRING-THAW AND POST-FERTILIZER N_2O FLUXES IN THE RED RIVER VALLEY, MANITOBA, CANADA

3.1 Abstract

While cover crops have been gaining popularity in increasing carbon (C) sequestration in soils, the understating of their effects on N_2O fluxes in the Canadian Prairies is limited. The objectives of this study were to assess the effect of a fall rye (*Secale cereale* L.) cover crop on spring-thaw and post-fertilizer N_2O emissions, net greenhouse gas (GHG) balance by harvest, and cash crop grain yield. Fluxes were measured over four years (2019-2022) from January to August 15 from four 4-ha fields using the flux gradient method. A tunable-diode laser analyzer was used to determine the gas concentration gradient and sonic anemometer-thermometers were used to determine the transfer coefficient. In fall 2018, two fields were seeded no-till with fall rye and two fields were cultivated and left fallow. The fall rye was terminated with an herbicide application in spring and the cash crops oats (*Avena sativa*), canola (*Brassica napus*), and spring wheat (*Triticum aestivum* L.) were grown in 2019, 2020, 2021, and 2022, respectively. The cover crop decreased spring-thaw N_2O emissions in years with the good establishment. In all study years, the cover crop fields saw lower initial peak N_2O emissions and lower cumulative emissions than the conventional fields following termination and herbicide application. The cover crop fields reduced N_2O emissions by an average of 25% during the duration of the study. Both cropping systems were a GHG source after combining cumulative CO_2 fluxes and N_2O emissions in CO_2-equivalents (CO_2-eq) in 2019 and 2022, with the conventional system being a source of 7,653 CO_2-eq ha^{-1} and the cover crop system being a source of 5,665 CO_2-eq ha^{-1}. Cash crop yields were not significantly different in all years of the study.

3.2 Introduction

Nitrous oxide (N_2O) is a greenhouse gas (GHG) produced by agricultural soils that destroys stratospheric ozone and has a warming potential of almost 300 times that of carbon dioxide (CO_2) (Smith et al., 2018; Tenuta et al., 2016). It is believed that N_2O is responsible for approximately 6% of the anthropogenic radiative forcing experienced globally (Tenuta et al., 2019). In Canada, agricultural soils are accountable for approximately 70% of anthropogenic N_2O emissions, with the majority of emissions being produced following synthetic nitrogen fertilizer application and during the spring-thaw of soils (Environment Canada, 2018; Tenuta et al., 2019; Wagner-Riddle et al., 2017).

The production of N_2O in soil occurs due to the microbial processes of nitrification and denitrification (Smith et al., 2018). Nitrification and denitrification are aerobic and anaerobic processes, respectively, and rates of N_2O production by these microbial processes are affected by temperature, soil moisture, and soil structure (Smith et al., 2018). Emissions following synthetic nitrogen fertilizer application result from increased nitrogen substrate availability, utilized by N_2O-producing soil microbes, and increases in soil moisture, typically following a precipitation event (Tenuta et al., 2019). The use of synthetic nitrogen fertilizers in crop production has allowed for significant increases in global crop yields over the last century and it is not currently possible to reduce its use without severe negative consequences to crop yields, crop nutrition, and soil health (Zhang et al., 2015). Concern regarding N_2O production following fertilizer application has led to the development of the “4Rs” of nutrient management, referring to the right source, timing, rate, and placement when applying fertilizer, which has been shown to decrease N_2O emissions with fertilizer application (Snyder et al., 2009; Tenuta et al., 2016; Tenuta et al., 2019). The other significant source of N_2O emissions from agricultural soils in northern latitudes comes from the spring-thaw of frozen soils, which can account for over half of annual N_2O fluxes in some cases (Tenuta et al., 2019; Wagner-Riddle et al., 2017). Spring-thaw N_2O emissions are regulated by denitrification and freeze-thaw cycles, which affect emissions by increasing anaerobic conditions and substrate availability, changing the structure and activity of denitrifying enzymes, and releasing previously produced N_2O that is trapped under snow and ice cover (Wagner-Riddle et al., 2017). Reducing spring-thaw N_2O emissions is thus directed at altering the conditions that make N_2O production ideal during spring-thaw. Suggested management practices in agricultural production to reduce spring-thaw have been directed at reducing the intensity of freeze-thaw cycles and reducing the amount of nitrate available in soils so there is less available in spring for denitrification (Dietzel et al., 2011; Reicks et al., 2021; Wagner-Riddle et al., 2007). No-till reduced freeze-thaw intensities and subsequent N_2O emissions during spring-thaw in a study in Ontario, Canada, as intact crop residues increased snow trapping and insulation of soils (Wagner-Riddle et al., 2007). However, a study conducted in Manitoba, Canada, found that implementing reduced tillage practices did not affect spring-thaw N_2O emissions (Glenn et al., 2012).

Reducing soil nitrate concentrations in soils by planting cover crops during non-cropping periods is a proposed strategy to reduce spring-thaw N_2O emissions (Basche et al., 2014; Dietzel et al., 2011; Reicks et al., 2021). Non-legume cover crop species can reduce soil nitrate concentrations by utilizing available nitrogen in the soil for growth (Basche et al., 2014; Dietzel et al., 2011; Reicks et al., 2021). In northern latitude cropland soils, the winter cereal fall rye (*Secale cereale* L.) has been recommended to be used as a cover crop to reduce spring-thaw N_2O emissions as it can establish in a short time following cash crop harvest, overwinter long periods where soil and air temperatures are below 0°C, and continue to grow the following spring (Larsen et al., 2018). A recent study by Reicks et al. (2021) conducted in South Dakota, USA, found that a fall rye cover crop reduced soil nitrate concentrations and spring-thaw N_2O emissions compared to soils left in fallow. There is less understanding, however, of how cover crops will affect N_2O emissions following synthetic nitrogen fertilizer application. Cover crops can change soil physical properties, such as soil moisture and structure, and provide a carbon (C) source to soil microorganisms which can increase microbial activity and production of N_2O (Fiorini et al., 2020; Kahimba et al., 2008; Reicks et al., 2021; Tenuta et al., 2019). Therefore, spring-thaw and post-fertilizer N_2O emissions must be considered when assessing the impact of fall rye cover crops on N_2O emissions. Further, the effect of implementing these practices on cash crop yield must be considered if fall rye cover crops are going to be recommended as a management strategy, as a reduction in grain yield could potentially increase yield-scaled emissions.

Monitoring N_2O fluxes using micrometeorological methods offers significant advantages over chamber-based methods that are commonly used in N_2O flux studies. Large field plots allow for better quantification and coverage of fluxes as field variability that could be potentially missed using small plots gets captured (Chadwick et al., 2014; Hutchinson and Livingston, 1993). Further, continuous monitoring allows for capturing sporadic N_2O emission episodes that could be missed using chamber-based methods (Glenn et al., 2012; Hutchinson and Livingston, 1993).

In this study, N_2O fluxes were collected from the Trace-Gas Manitoba (TGAS-MAN) long-term research site in Glenlea, Manitoba, Canada, in the Red River Valley. The site has been monitoring CO_2 and N_2O fluxes for over a decade and has conducted numerous studies on the effects of different management strategies utilized in the region, such as perennial forages incorporated into crop rotations, reduced tillage, and fertilizer application timing, on N_2O fluxes (Glenn et al., 2012; Maas et al., 2013; Tenuta et al., 2016). The most recent study at the site conducted by Tenuta et al. (2019) looked at the effects of these management strategies and crop rotations on N_2O fluxes over a decade. This study looked at the effect of a fall rye cover crop no-till cropping system on spring-thaw and post-fertilizer N_2O fluxes compared to a conventional cropping system that managed soils with conventional tillage practices for the region. N_2O fluxes were combined with CO_2 flux data from two of the study years to assess the effect of the cover crop on net GHG balance by harvest for each of the systems and if there was an impact on cash crop grain yields. Flux data was collected from January 1 to August 15 from 2019 to 2022. Weather data, biomass samples from the cover crop and cash crop, and soil samples were collected from the site to support and explain measured fluxes. The objectives of this study were to (1) assess the effect of a no-till fall rye cover crop on spring-thaw and post-fertilizer N_2O emissions compared to conventionally managed soils, (2) assess the effect of a no-till fall rye cover crop on net GHG balance, and (3) assess the effect of the no-till fall rye cover crop on subsequent cash crop grain yields.

3.3 Materials and Methods

3.3.1 Site Description

The study was conducted in Glenlea, Manitoba (49.64N 97.16W, 235m a.s.l), approximately 16km south of Winnipeg, Manitoba, at the University of Manitoba's Trace-Gas Manitoba (TGAS-MAN) research site. The site, located in the Red River Valley floodplain, was situated on flat (<2% slope) glaciolacustrine clay with an extreme humid-continental climate on soils that consisted of gleyed humic vertisols (Canadian system) or typic humicryerts (U.S. system) of the Red River and Osborne Series (Ehrlich et al., 1953; Michalyna et al., 1975). Soil texture was approximately 60% clay, 35% silt, and 5% sand. Soil drainage ranged from poorly to imperfectly and the site experienced poor to imperfect drainage under saturated soil conditions and formed large cracks under drought conditions.

3.3.2 Site Design and Agronomic History

Details of the previous agronomic history and layout of the site were given in Chapter 2, Section 2.3.2. The agronomic practices for this study from fall 2018 to fall 2022 follow herein. The site consisted of four 200 m by 200 m (4 ha each, 16 ha total) fields arranged in a 2x2 grid inside a larger 30 ha field. For each year of the study, two fields received no-tillage and were seeded with fall rye in the fall following harvest, and two fields were treated as controls managed with conventional tillage practices for the region and left in fallow during non-cropping periods following harvest and prior to seeding in spring. The cover crop was terminated with an herbicide application, ideally at or shortly after seeding.

On August 29 and August 30, 2018, fall rye was direct seeded at a rate of 63 kg ha^{-1} into canola residue with a Case IH SDx30 seeder on the two east fields (Fields 2 and 3) and the two west fields (Fields 1 and 4) were cultivated to approximately 13cm depth with a JD 1610 deep tiller. On May 13, 2019, all fields were seeded with oats (*Avena sativa,* cv 'AC® Summit') at 108 kg ha^{-1}. A granular fertilizer blend (N-P-K-S) of 78 kg ha^{-1} ESN®, 17 kg ha^{-1} P, 6 kg ha^{-1} K, and 17 kg ha^{-1} S was banded with the seed. The site was sprayed with Roundup Transorb (1.65 L ha^{-1}; a.i. glyphosate) the day after seeding on May 14 to terminate the fall rye cover crop on the east fields and volunteer weeds on the west fields. The east fields were resprayed with Roundup Transorb (1.65 L ha^{-1}) on May 20 to terminate the remaining cover crop. All fields were sprayed with Outshine (applied according to the product label, a.i. florasulam/fluroxypyr + MCPA ester) and Twinline (applied according to the product label; a.i. pyraclostrobin and metconazole) on June

5 and July 1 respectively. The oats were desiccated on August 19 with an application of Roundup Transorb (1.65 L ha^{-1}) and harvested on September 9, 2019. The oat straw was not removed from the field. Following harvest, the east fields were cultivated with a JD 1610 deep tiller to approximately 13 cm depth on September 16, and the west fields were seeded no-till with fall rye at 63 kg ha^{-1} with a Case IH SDx30 seeder on September 17, 2019. Unfortunately, high precipitation in the fall of 2019 drowned most of the cover crop, leading to the poor establishment in the spring of 2020.

On May 21, 2020, the site was seeded with canola (*Brassica napus*, cv 'L233P' (InVigor®), BASF) at 4.7 kg ha^{-1} and was banded with a starter fertilizer (N-P-K-S) of 22 kg ha^{-1} ESN®, 22 kg ha^{-1} P, 0 kg ha^{-1} K, and 11 kg ha^{-1} S. UAN (28%) was applied on May 21 with a Case IH 3230 patriot sprayer with 100' boom with tri-nozzle streamers at 145.5 kg ha^{-1} and 168 kg ha^{-1} for the west and east fields, respectively. Roundup Transorb (1.65 L ha^{-1}) was applied to the west fields on June 5 to terminate the fall rye cover crop. A herbicide mix of Liberty (3.34 L ha^{-1}; a.i. glufosinate) and Centurion (124 ml ha^{-1}; a.i. clethodim) was applied on June 16 and fungicide Cotegra (0.605 ml ha^{-1}; a.i. boscalid and prothioconazole) was applied on July 15 to all fields. The canola was desiccated on August 27 with Roundup Transorb (1.65 L ha^{-1}) and harvested on September 8, 2020. On September 9, the west fields were seeded no-till with fall rye at 63 kg ha^{-1} with a Case IH SDx30 seeder and the east fields were cultivated with a Summers chisel plow to approximately 13 cm depth.

On May 11, 2021, the site was seeded with spring wheat (*Triticum aestivum* L., cv 'AAC Starbuck VB' Canadian Western Red Spring) at 148 kg ha^{-1}. A starter fertilizer blend (N-P-K-S) of 22 kg ha^{-1} N, 22 kg ha^{-1} P, 0 kg ha^{-1} K, and 11 kg ha^{-1} S was banded with the seed and urea was deep banded on all fields at 111 kg ha^{-1}. On May 14, the cover crop was terminated on the west fields with an application of Roundup Transorb (1.65 L ha^{-1}). The wheat was sprayed with a mix of Buctril M (applied according to the product label; a.i. bromoxynil/MCPA ester) and Axial (applied according to the product label; a.i. pinoxaden) on June 15. On August 16, the site was harvested. No straw was removed from the site following harvest. On August 30, the east fields were seeded no-till with fall rye with a Case IH SDx30 seeder at 63 kg ha^{-1}. The west fields were cultivated on September 1 and October 5 with a Summers chisel plow to approximately 13 cm depth. An additional cultivation pass was made with a disc cultivator on November 9 on the west fields to terminate small patches of volunteer wheat that were growing underneath micrometeorological equipment in the field.

On June 10, 2022, the cover crop was terminated on the east fields with an herbicide application of Roundup Transorb (1.65 L ha^{-1}). Due to saturated soil conditions following a precipitation event shortly after spraying the cover crop, seeding was delayed until June 20. On June 20, the site was seeded with wheat (*Triticum aestivum* L. cv 'AAC Viewfield' semi-dwarf Canadian Western Red Spring) at 135 kg ha^{-1} and banded with a starter fertilizer blend (N-P-K-S) of 22 kg ha^{-1} N, 22 kg ha^{-1} P, 0 kg ha^{-1} K, and 11 kg ha^{-1} S. Two different fertilizers were applied at the site in 2022 for a subsequent fertilizer study. The south fields (Fields 3 and 4) were deep banded with urea at 118 kg ha^{-1} on June 20. On June 20, the north fields (Fields 1 and 2) were deep banded with eNtrench™-coated urea. The intended rate for the eNtrench™ fertilizer was 118 kg ha^{-1}. However, flowability issues caused approximately half the rate, or 56 kg ha^{-1}, to be applied. Consequently, an additional fertilizer was applied to the north fields to make up for the half rate. On June 22, 56 kg ha^{-1} UAN (28%) treated with Centuro® was applied to the north fields with a Case IH 3230 patriot sprayer with 100' boom and tri-tip streamers. The herbicide Velocity (988 ml ha^{-1}; a.i. thiencarbazone, bromoxynil and pyrasulfotole) was applied on July 13. On October 5, 2022, the wheat was harvested.

3.3.3 Micrometeorological Instrumentation and Nitrous Oxide Flux Measurements

A detailed description of the site and equipment used to measure fluxes can be found in Chapter 2, Section 2.3.3. An abbreviated version follows here. N_2O fluxes were measured using the micrometeorological flux gradient method. The center of each study field had micrometeorological equipment used to measure net N_2O fluxes. A temperature-controlled trailer at the junction of the four fields housed a Tunable Diode Laser absorption spectrophotometer (Model TGA100A, Campbell Scientific Inc., Logan, UT, USA) trace gas analyzer (TGA) and associated hardware and electronics to continuously measured CO_2 and N_2O concentrations from gas samples collected from each of the fields. The lead-salt tunable diode laser100A (Model IR-N_2O/CO_2, Laser Components GmbH., Olching, Germany) was operated at 84K (-189°C) in dual-ramp, jump scanning mode to measure both N_2O and CO_2 concentrations simultaneously at 10Hz frequency. The ramps of the TGA laser were set to scan absorption line peaks at 2243.110 cm^{-1} and 2243.585 cm^{-1} frequency for $^{14}N_2O$ and $^{13}CO_2$, respectively. This was achieved by applying a DC current of ~563 mA for N_2O and ~589 mA for CO_2. A beam splitter was used to deflect a non-reflecting laser beam onto two detectors, one located in a reference cell and one located in a sample cell. Reference gas containing approximately 2000 ppm N_2O and 300,000 ppm CO_2 was continuously passed through the TGA100A reference cell at 10 ml min^{-1}. Sample pressure was maintained at 30 mb to analyze the gas samples.

The flux gradient micrometeorology method was used to determine the net exchange of N_2O between the cropping systems and the lower atmosphere. The N_2O flux (F_N) was determined as:

$$F_N = -K \frac{\Delta[N_2O]}{\Delta z}$$

where, K is the turbulent transfer coefficient, $\Delta[N_2O]$ is the vertical concentration gradient of N_2O, and Δz is the vertical height difference between the sampling heights.

3-D sonic anemometer-thermometers (CSAT-3, Campbell Scientific Inc.) mounted at 2 m height were used to determine K. Sonics were located in the two south fields (Fields 3 and 4) for the duration of the study. A third sonic was added to the northwest field (Field 1) in the summer of 2022. The data collected from each sonic were averaged to give one K value used for flux calculations. Corrections to K during unstable and stable atmospheric conditions were determined as:

$$K = u_* k\, (z_2 - z_1) / [\ln (z_2 / z_1) - \varphi_2 + \varphi_1]$$

where, u_* is the friction velocity, k is the von Karmann constant (0.4), z_2 and z_1 are the upper intake and lower intake heights above the zero-plane displacement (d), φ_2 is the stability correction factor for the upper intake, and φ_1 is the stability correction factor for the lower intake (Amiro et al., 2017). During the growing season following crop emergence, crop heights were measured approximately once every two weeks to estimate d, which was presumed to be 0.66 of the crop height (Amiro et al., 2017; Denmead, 2008; Garratt, 1992; Glenn et al., 2010). During the non-growing season, d was assumed to be at the soil or snow surface (Glenn et al., 2010). Snow depth measurements were taken approximately once every two weeks when snow was present. Snow depth and crop heights were interpolated between measurements. Micrometeorological towers at the center of each field and large experimental field size allowed fetch to effective observation height ratios of approximately 100:1 to be maintained in all directions for all fields for the study (Glenn et al., 2010).

To measure *$\Delta[N_2O]$* and *Δz* for the flux calculations, two gas sample intakes were mounted at different heights separated by 50 cm to a tower at the center of each experimental field. The height of the lower intake was determined as 0.66 the crop height plus 60 cm, and the upper intake was 50 cm above the lower intake. The intakes were moved up the tower during the growing season when crop height measurements were taken and in winter if snow was starting to approach the lower intake. Until November 2019, the experimental site used the sampling system and hardware described by Glenn et al. (2010). In November 2019, upgrades were made to the sampling system and data collection equipment. The two systems were described in Chapter 2, Section 2.3.3. Briefly, gas samples were taken using gas sample intakes at each tower located in the center of each experimental field to determine *$\Delta[N_2O]$*. Fields were sampled for 30 minutes before moving to the next field in the sampling sequence, yielding an average of 12 half-hour gradients from each field per day. Further descriptions of the equipment used and the sampling system are reported in Chapter 2.

3.3.4 Supporting Environmental, Soil, and Biomass Data

A weather station located that the junction of the four fields on an undisturbed grass area south of the instrumentation trailer monitored the environmental conditions for the duration of the study. Instrumentation to measure air temperature and relative humidity (Model HMP45C, Vaisala Inc., Woburn, Massachusetts, USA), incoming solar radiation (Model SP-LITE Silicon Pyranometer, Kipp & Zonen, Delft, the Netherlands), photosynthetic photon flux density (PPFD) (Model PAR LITE, Kipp & Zonen), barometric pressure (Model 61205, R.M. Young Company, Traverse City, Michigan, USA), and wind speed and direction (Model 05103-10 Wind Monitor, R.M. Young Company) was mounted to a tripod. Soil temperature and volumetric moisture content (VMC) were measured using equipment installed at the tripod's base. Soil temperature was measured at 2, 5, 10, 20, 50 and 100 cm depths using thermistors (Model 107 and 107B Thermistors, Campbell Scientific Inc.) and VMC was measured at 10 and 30 cm depths using VMC probes (Model EC-10 ECH2O Dielectric Aquameter, Decagon Devices Inc., Pullman, WA, USA). A precipitation gauge (Model T-200B Series Precipitation Gauge, Geonor, Inc., Milford, PA, USA) located approximately 3 m from the weather station tripod measured total precipitation at the site. Data from the weather station was recorded at 0.1 Hz using a datalogger (Model CR1000, Campbell Scientific Inc.). Data was stored at 30-minute, 60-minute, and daily intervals in TOB5 format. 30-year climate normals for Glenlea, Manitoba, from 1981-2010 were obtained from Environment Canada (Environment Canada, 2023*a*).

Soil samples were taken from six randomly selected predetermined sampling locations approximately once a month from soil thaw in spring until freeze up in fall. The sampling locations were repeatedly sampled (± 5 m radius) during each sampling campaign. Four 0-15 cm and 15-30 cm samples were taken at each sampling location and combined into a composite sample representing each sampling location. Soil samples were stored on ice in an insulated cooler while being collected from the site and were transferred and stored in a walk-in freezer at approximately -20°C until they were ready to be analyzed. Before analysis, samples were thawed, broken down until soil particle size was approximately ≤ 1 cm in diameter, and homogenized. Samples were then analyzed for ammonium (NH_4^+), nitrate (NO_2^-/NO_3^-) and gravimetric moisture content (GMC). A 2 M KCl extraction at a 1:5 soil-to-extractant ratio was used to determine NO_2^-/NO_3^- and NH_4^+ of samples, which were analyzed fresh without drying before extraction. Extractions were analyzed by a Technicon Autoanalyzer II colorimetry (Pulse Instrumentation Ltd., Saskatoon, SK, Canada). Minimum reportable limits were set at 0.02 mg L^{-1} for NH_4^+ and 0.2 mg L^{-1} for NO_2^-/NO_3^-. Sample results were set to 0 mg L^{-1} when determining averages for a field if results were below the reportable limit. Samples were oven dried at 105°C for 24 hours to determine GMC.

Cover crop biomass, cash crop grain yield and harvest removals for each field were determined by taking hand-clipped aboveground biomass samples. Plants were clipped approximately 2 cm from the soil surface from two adjacent rows, 1 m in length, twice at each of the six random sampling locations used to collect soil samples, yielding 4 m of biomass from each location. Cover crop biomass samples were taken prior to its termination in spring. Cash crop biomass samples were taken prior to harvest in the fall. After samples were collected in the field, they were weighed and stored in a drying room at approximately 32.2°C until they reached an equilibrium air-dry weight. Once an equilibrium weight was reached, the cash crop biomass was stationary combined (Wintersteiger Classic Combine, Ried, Austria) to determine the straw weight and the air-dry grain weight. Grain, straw, and cover crop biomass samples were then dried in an oven for 24 hours at approximately 60°C to determine their oven dry weight. Samples were then ground until they passed through a 2 mm screen using a Wiley mill (Wiley Laboratory Mill, Model 4 3375-E10, Thomas Scientific, Swedesboro, NJ, USA) and were analyzed with a vario MAX cube analyzer (vario MAX cube, Elementar, Langenselbold, Germany) to determine the total carbon (TC), total nitrogen (TN), and carbon to nitrogen ratio (C/N) for each of the samples.

3.3.5 Data Quality Control and Gap-Filling

Data collected during the study were processed in Matlab (Mathworks Inc., Natick, MA, USA). Multiple quality control parameters were implemented to ensure that only high-quality data was used to determine fluxes. Parameters were set during data collection in the manifold logger program so that station flags were issued and data was eliminated if the bypass and sample pressure were ± 10 mb from the set point, and the TGA pressure was ± 1 mb from the set point. After data collection, half-hourly data was removed when field operations (seeding, spraying, harvesting, cultivating), site visits, power interruptions, or human interference occurred. Data from the 30 minutes and the following 30 minutes after liquid nitrogen fills were removed to prevent inaccurate measurements of gas concentrations from possible temperature changes and vibrations of the analyzer (Edwards et al., 2003).

Parameters were set when processing fluxes and data was discarded if they left the acceptable range. The u_* threshold utilized in previous research at the site (Amiro et al., 2017; Glenn et al., 2010; Maas et al., 2013; Tenuta et al., 2019) was used and flux data were discarded if $u_* < 0.15$ m s^{-1}, as insufficient atmospheric mixing caused unreliable *K* data. Data was removed if the sample flow >250 ml min^{-1} or < 135 ml min^{-1} or if the excess flow < 30 ml min^{-1} or > 90 ml min^{-1} during sample collection, or if the TGA temperature was > 84.5K or < 83.5K. Fluxes were discarded if the standard deviation over the 30 minutes for the N_2O concentrations were greater than 20 ppb (Maas et al., 2013).

30-minute fluxes from each field were averaged daily to give mean daily flux values. Gaps in daily N_2O fluxes up to ten days in duration were filled by linear interpolation (Tenuta et al., 2019). 5 cm soil temperature data was gap-filled using provincial weather station data provided by the Government of Manitoba from their St. Adolphe weather station, located approximately 7 km from the site. Missing air temperature data was gap-filled using the air temperature data from the 3-D sonic anemometer thermometers. Missing precipitation data was gap-filled using Environment Canada's Winnipeg A CS weather station at Winnipeg's James Armstrong Richardson International Airport (Environment Canada, 2023*b*).

3.3.6 Flux Bias Corrections and Data Uncertainty

A brief description of the flux bias observed at the site following the system upgrades in 2019 was described in Chapter 2, section 2.3.5. Following the bias corrections that were made following the protocol set by Amiro (2021), which can be found in APPENDIX B, abnormal N_2O flux behaviour was still observed from Fields 1 and 3 for 2020 and 2021. The data from those fields have thus been excluded from this study. Additional data from other study years was removed as uncertainty in data quality was too high. Data from Fields 1 and 2 in 2019 were excluded as abnormal N_2O uptake at those fields, greater than those observed in previous research at the site (Glenn et al., 2012; Tenuta et al., 2016; Tenuta et al., 2019), resulted in high uncertainty in data quality. Data from Fields 1 and 2 following fertilizer application in 2022 was also excluded as a subsequent fertilizer study was being conducted in those fields. The flux data used for this study came from Fields 3 and 4 in 2019, Fields 2 and 4 in 2020 and 2021, all fields prior to seeding in 2022, and Fields 3 and 4 after seeding in 2022.

3.3.7 Cumulative Nitrous Oxide Fluxes and Net Greenhouse Gas Flux

N_2O fluxes were assessed over three different periods during the study. Periods were divided into spring-thaw N_2O flux ($F_{N\text{-}SPRING\text{-}THAW}$), post-fertilizer N_2O flux ($F_{N\text{-}FERTILIZER}$), and F_N for each study year. Spring-thaw was defined as the first date of daily average air temperature > 0°C until the first date of daily average 5 cm soil temperature > 5°C (Tenuta et al., 2019). Post-fertilizer emissions were defined as the period following fertilizer application until August 15. A study year was defined as January 1 to August 15 for each year, respectively. Cumulative fluxes for spring-thaw ($\sum F_{N\text{-}SPRING\text{-}THAW}$), post-fertilizer ($\sum F_{N\text{-}FERTILIZER}$), and study year ($\sum F_N$) were determined to assess the difference in treatments on cumulative N_2O fluxes. $\sum F_N$ for 2019 and 2022 was converted to CO_2 equivalents (CO_2-eq) using a global warming potential (GWP) of 265 (Tenuta et al., 2019) and was removed from the C balance ($F_{ECOSYSTEM}$) as a loss to give cumulative net greenhouse gas flux equivalents ($\sum F_{GHG}$) for those years respectively.

3.3.8 Statistical Analysis

Statistical analysis was performed in Matlab. To compare the difference in spring 0-30 cm soil NO_2^-/NO_3^- prior to seeding, an analysis of variance (Matlab, "anova1") was performed. Significance was set at P < 0.05. The distribution of data was tested for normality using the Anderson-Darling test (Matlab, "adtest"). Data from the conventional fields did not meet normal distribution from samples taken on May 13, 2019 (P = 0.007), April 23, 2021 (P = 0.003), and May 11, 2022 (P = 0.008). Data from the cover crop fields did not meet normality on May 11, 2022 (P = 0.0005). All other data were not different from normal distribution (P = 0.09 – 0.85). Linear regression analysis (Matlab, "regstats") was used to test the relationship between biomass accumulation and biomass C/N ratio. Analysis of variance (Matlab, "anova1") was performed to assess treatment effect on grain yield, using biomass sample locations as replicates from all treatment fields, yielding 12 samples total each year for the cover crop and conventional treatments, respectively. Significance was determined as P < 0.05. An Anderson-Darling test

(Matlab, “adtest”) determined that the yield data from all study years was not different from normal distribution (P = 0.18 – 0.98).

3.4 Results

3.4.1 Weather and Soil Conditions

The average air temperature from the month of cover crop seeding until December was above the 30-year normal in 2020 and 2021 and below the 30-year normal in 2018 and 2019 (Table 3.1). Precipitation from the month of cover crop seeding until December was lower than normal in 2018, 2020 and 2021 and above normal in 2019 (Table 3.1). A significant precipitation event in September 2019 resulted in more than twice the normal amount of precipitation accumulated in September for that year, which subsequently affected the cover crop growth and establishment in the fall of 2019. The site only received 40 mm of precipitation from cover crop seeding from September 2020 until December, which was 29% of the normal amount of precipitation for that period (Table 3.1). While the site received lower than normal precipitation during the cover crop seeding and establishment in three study years, it only drastically affected cover crop growth in the fall of 2020.

Average air temperature from January to August during flux measurements for each study year was above the 30-year normal of 4.4°C in 2020 and 2021, at 4.9°C and 5.7°C for each, respectively, and below the 30-year normal in 2019 and 2022 at 2.9°C and 2.4°C for each, respectively (Table 3.1). Precipitation was below the 30-year normal of 403 mm from January to August in 2019, 2020, and 2021 by approximately 200 mm each year and above the 30-year normal in 2022 by approximately 200 mm (Table 3.1).

Table 3.1 Air temperature and precipitation from the on-site weather station from January to August for each study year compared with the 30-year (1981-2010) Canadian Climate Normal for Glenlea, Manitoba (Environment Canada, 2023*a*).

	Jan	Feb	Mar	Apr	May	Jun	Jul	Aug
Average Air Temperature (°C)								
2019	-17.9	-20.0	-8.3	4.2	10.0	17.6	19.6	17.9
2020	-12.6	-13.8	-5.4	1.6	11.1[a]	19.2[a]	20.4	18.6
2021	-10.6	-17.9	-0.5	3.3	11.1	19.7	21.5	18.8
2022	-19.5[a]	-20.1	-8.4	-0.3	10.3[a]	17.8[a]	20.0[a]	19.0
30 Year Normal	-17.2	-13.3	-6	4.4	12.2	17	19.4	18.8
Total Precipitation (mm)								
2019	1	0	0	6	28	47	119	53
2020	0	1	2	6	25[b]	25[b]	72	90
2021	0	1	11	22	17	54	15	80
2022	21[b]	36	40	98	147[b]	85[b]	112[b]	85
30 Year Normal	16	13	21	28	62	100	92	72

[a] Missing temperature data from the weather station was gap-filled with air temperature data from the site's sonic anemometer thermometers

[b] Missing precipitation data from the weather station was gap-filled using data from the Winnipeg A CS weather station located at Winnipeg's James Armstrong Richardson International Airport, approximately 35km from the site (Environment Canada, 2023*b*)

Soil NO_3^-/NO_2^- concentrations in spring before seeding were lower for the cover crop fields than the conventional fields in 2019, 2021 and 2022 (Figure 3.1). Soil sampling was not performed prior to seeding in 2020. Differences in soil NO_3^-/NO_2^- concentrations prior to seeding were significant at all samplings in 2019 and 2022 (P = 0.02 – 0.00007). Differences were not significant in 2021 (P = 0.73). Soil NO_3^-/NO_2^- increased in all years following fertilizer application. NO_3^-/NO_2^- and NH_4^+ concentrations were similar for both the conventional and the cover crop fields in all years except during the sampling on May 19, 2021, and June 18, 2021 (Figure 3.1). NH_4^+ was 25 mg kg^{-1} for the cover crop field and 35 mg kg^{-1} for the conventional field on May 19, 2021.

NO_3^-/NO_2^- was 40 mg kg^{-1} for the conventional field and 79 mg kg^{-1} for the cover crop field on June 18, 2021. The average GMC was slightly lower from April to July 2019 for the cover crop field and approximately the same as the conventional field after that (Figure 3.1). GMC was approximately the same at all samplings for each treatment in 2020 and higher at all samplings in 2021 for the cover crop field compared to the conventional field (Figure 3.1). Average GMC was lower at all samplings in 2022 for the cover crop fields than the conventional fields. Differences in soil GMC from the different treatments were not statistically significant for all samplings in all study years ($P = 0.058 – 0.98$).

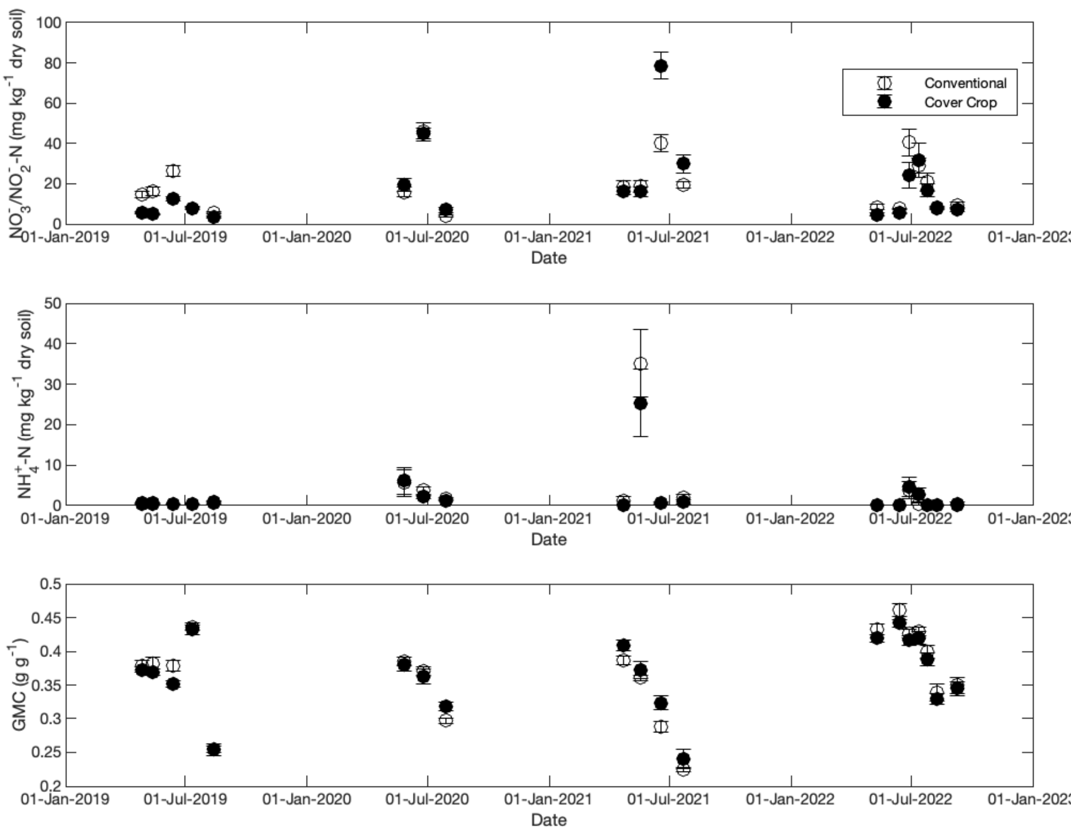

Figure 3.1 Concentrations of NO_3^-/NO_2^-, NH_4^+, and gravimetric moisture content (GMC) from 0 to 0.3m soil depth from the conventional and cover crop treatments from 2019 to 2022. Open circles correspond to the conventional treatment; closed circles correspond to the cover crop treatment. Soil samples were collected from six locations in each field. Data from Field 3 and 4 is shown for 2019, Field 2 and 4 for 2020 and 2021, and all Fields in 2022 prior to seeding and Fields 3 and 4 following seeding, giving a mean of a minimum of six locations per treatment per year ($n \geq 6$). Bars represent ±1 standard error of the mean.

3.4.2 Nitrous Oxide Fluxes

3.4.2.1 Temporal Coverage of Nitrous Oxide Fluxes

The percent of N_2O fluxes captured by flux measurements for each study year was 24% in 2019, 23% in 2020, 27% in 2021, and 36% in 2022. Spring-thaw length during the study varied from a minimum of 38 days to a maximum of 69 days. Post-fertilizer measurement length ranged from 57 days to 97 days. Large data gaps were experienced in 2019 (maximum gap of 25 days from February 16 to March 12, 2019), 2020 (maximum gap of 34 days from January 1 to February 3, 2020), and 2022 (gaps of 11 and 13 days from January 1 to 11, and January 14 to 26, 2022). The average gap length prior to gap filling was 3.6 days for the conventional fields and 3.8 days for the cover crop fields. Total gaps before gap filling with linear interpolation were 143 days for the cover crop system and 146 days for the conventional system out of 909 total days measured for the study. Only gaps greater than ten days remained after gap-filling, resulting in 83 days missing from the cover crop and conventional flux measurements, all of which occurred prior to the start of spring-thaw each year, respectively.

3.4.2.2 Cover Crop Biomass Accumulation

Varying environmental conditions at cover crop seeding and establishment in fall resulted in different amounts of cover crop biomass being accumulated the following spring. Environmental conditions at establishment were ideal in fall of 2018 and 2021, resulting in good cover crop growth the following spring. Drought conditions at cover crop seeding and establishment in 2020 caused low cover crop growth in spring 2021 and flooding caused by high levels of precipitation in September of 2019 during cover crop establishment resulted in most of the cover crop drowning in the fall of 2019 and little growth in 2020, resulting in no sampling occurring in spring of 2020.

The duration of biomass accumulation from spring-thaw until cover crop termination was the longest in 2021 and 2022, at 82 and 83 days for 2021 and 2022, respectively, and 49 days in 2019. Biomass accumulation was lowest in 2021 at 337 kg dry weight ha^{-1}, slightly higher in 2019 at 452 kg dry weight ha^{-1}, and highest in 2022 at 1,761 kg dry weight ha^{-1} (Table 3.2). C/N ratio of the cover crop was lowest in 2021 at 14.0 and highest in 2022 at 26.9 (Table 3.2). Linear regression analysis showed that the C/N ratio of the cover crop increased with increased biomass accumulation ($R^2 = 0.72$).

Table 3.2 Cover crop biomass and C/N ratio in spring at termination. Cover crop biomass was not collected in 2020 as flooding the fall before establishment killed most of the cover crop. Biomass was collected from six locations in each field, yielding at least six samples per treatment per year ($n > 6$). Biomass samples from both cover crop fields were used in 2022 ($n = 12$).

Year	Cover Crop Biomass (kg dry weight ha^{-1})	Biomass S.D.	C/N ratio	C/N ratio S.D.
2019	452	215	19.1	1.9
2020	-	-	-	-
2021	337	110	14.0	1.1
2022	1,761	948	26.9	4.3

3.4.2.3 Spring-Thaw Nitrous Oxide Fluxes

Both cropping systems experienced N_2O emission events of varying magnitudes during spring-thaw in each study year (Figure 3.2). The cover crop treatment saw lower peak N_2O emissions in all study years with cover crop biomass accumulation, except for 2020, where cover crop establishment was poor (Figure 3.2). Daily average fluxes before spring-thaw varied between cropping systems and study years. In 2019, the daily average flux before spring-thaw was 10 g N_2O-N ha^{-1} day^{-1} for the conventional system and -3 g N_2O-N ha^{-1} day^{-1} for the cover crop system. In 2020, the daily average flux before spring-thaw was approximately the same for both systems at 3 g N_2O-N ha^{-1} day^{-1}. In 2021, the daily average flux before spring-thaw was approximately 0 g N_2O-N ha^{-1} day^{-1} for the conventional system and 1 g N_2O-N ha^{-1} day^{-1} for the cover crop system. In 2022, the daily average flux before spring-thaw was approximately the same for both cropping systems at 3 g N_2O-N ha^{-1} day^{-1}.

In 2019, the spring-thaw started on March 27 and finished on May 12. Daily average N_2O and peak N_2O fluxes were lower from the cover crop field than the conventional field (Figure 3.2 a). Peak emissions occurred on April 13, 2019, at 135 g N_2O-N ha^{-1} for the conventional system, and on April 9, 2019, for the cover crop system at 78 g N_2O-N ha^{-1} (Figure 3.2 a). In 2020, spring-thaw began on March 24 and abated on April 30. Daily average and peak N_2O fluxes were similar for the two cropping systems, with peak emissions of 65 g N_2O-N ha^{-1} occurring on April 5 in the cover crop field and peak emissions of 61 g N_2O-N ha^{-1} occurring on April 12 for the conventional field (Figure 3.2 b). Peak N_2O emissions were lower for the cover crop fields in 2021 and 2022 (Figure 3.2 c, d). In 2021, spring-thaw started on February 22, 2021, and finished on May 1, 2021. Peak N_2O emissions occurred in March for both cropping systems, with the cover crop field having peak emissions on March 13, 2021, at 90 g N_2O-N ha^{-1}, and the conventional field having peak emissions on March 8, 2021, at 146 g N_2O-N ha^{-1} (Figure 3.2 c). In 2022, spring-thaw started on March 20 and ended on May 4. Peak N_2O emissions occurred on April 11 and May 3 for the conventional and cover crop fields, respectively (Figure 3.2 d). The conventional system had peak emissions of 149 g N_2O-N ha^{-1}, and the cover crop system had peak emissions of 60 g N_2O-N ha^{-1} (Figure 3.2 d). Cumulative fluxes for the spring-thaw period were lower for the cover crop fields than the conventional fields in 2019 and 2022 and similar for the two systems in 2020 and 2021 (Table 3.3).

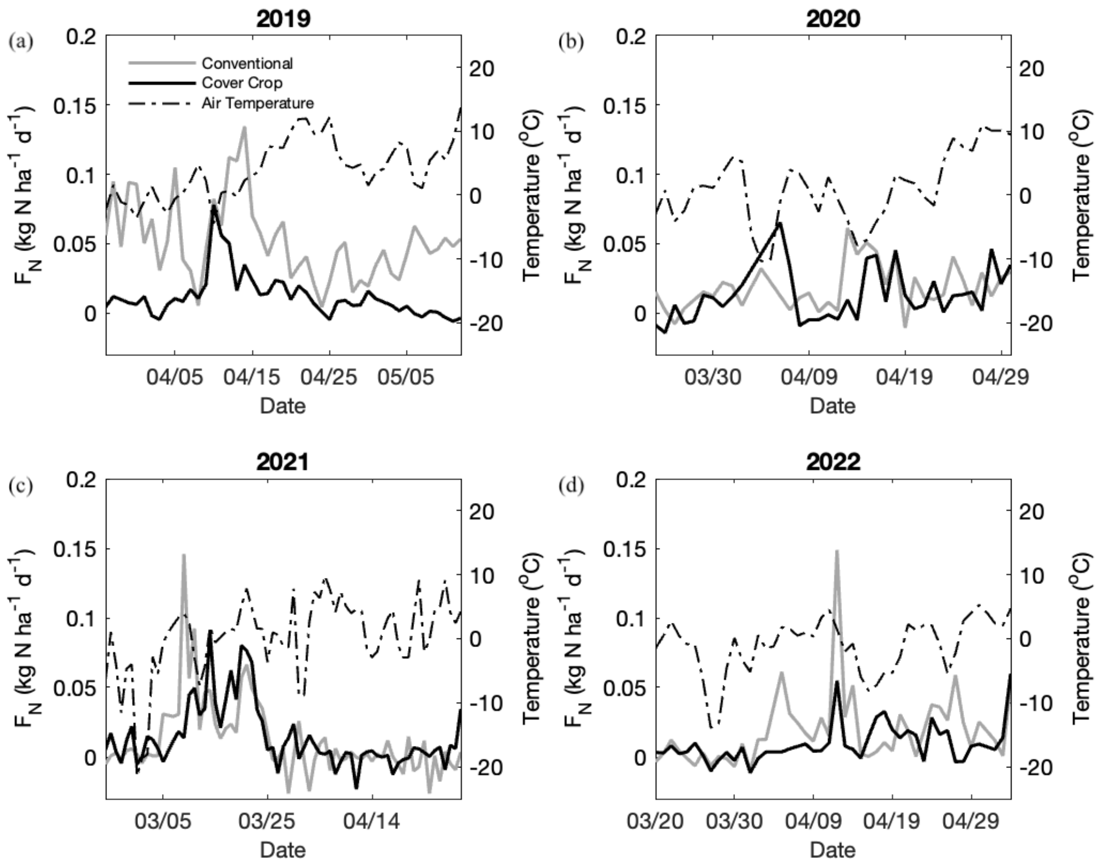

Figure 3.2 Gap-filled daily average N_2O flux (F_N) and gap-filled daily average air temperature during spring-thaw for (a) 2019, (b) 2020, (c) 2021, and (d) 2022.

3.4.2.4 Post-Fertilizer Nitrous Oxide Fluxes

N_2O fluxes for both cropping systems following fertilizer application were associated with precipitation events. Peak post-fertilizer N_2O fluxes were lowest in 2019 and highest in 2022. In 2019, two emission events occurred following fertilizer application on May 13, the first starting at the end of May following a 3-day precipitation event of 14 mm starting on May 24, and the second occurring at the beginning of July following a 3-day precipitation event of 89 mm that started on July 8. During the first emission event, emissions peaked on May 28, with the conventional system emitting 102 g N_2O-N ha^{-1} and the cover crop system emitting 54 g N_2O-N ha^{-1} (Figure 3.3 a).

Peak emissions were higher during the second emission event in 2019, with peak emissions of 146 g N_2O-N ha^{-1} and 113 g N_2O-N ha^{-1} occurring for the cover crop and conventional systems, respectively, on July 10.

Two emission events occurred in 2020 approximately one month after fertilizer application on May 21. The first emission event occurred in early June after the site received 21 mm of rain from June 6 to 7. Emissions peaked on June 8, with the cover crop field emitting 570 g N_2O-N ha^{-1} and the conventional field emitting 643 g N_2O-N ha^{-1} (Figure 3.3 b). The second emission event occurred at the beginning of July following 28 mm of rain from June 30 to July 1, with peak emissions occurring on July 1. The cover crop had higher peak emissions of 245 g N_2O-N ha^{-1} during this event than the conventional system, which emitted 208 g N_2O-N ha^{-1} (Figure 3.3 b).

In 2021, fertilizer was applied on May 11 and a single prolonged emission event occurred starting on May 23 after the site received 13 mm of rain from May 20 to 22 and lasting until June 19. The second and third rain events occurred on June 5, 6 and 9, followed by increased N_2O fluxes at the site. Peak emissions occurred on June 10 and 11 for the cover crop and conventional systems, respectively, during which the cover crop field emitted 584 g N_2O-N ha^{-1} and the conventional field emitted 703 g N_2O-N ha^{-1} (Figure 3.3 c).

Multiple precipitation events in 2022 resulted in three emission events following fertilizer application on June 20. Approximately a week after the fertilizer application, the first emission event started after the site received 28 mm of rain on June 24 and 25. Peak emissions for the cover crop field happened on June 26, with 768 g N_2O-N ha^{-1} being emitted (Figure 3.3 d). Peak emissions for the conventional field occurred the following day on June 27, with 1189 g N_2O-N ha^{-1} being emitted (Figure 3.3 d). The second emission event occurred in early July after the site received 32 mm of rain on July 4. Peak emissions during the second event occurred on July 7 and were higher for both cropping systems than the first emission event, with the cover crop field emitting 1,704 g N_2O-N ha^{-1} and the conventional field emitting 2,436 g N_2O-N ha^{-1} (Figure 3.3 d). The third emission event occurred mid-July after the site received 53 mm of rain on July 19. Peak emissions were similar for both cropping systems, with the cover crop field emitting 430 g N_2O-N ha^{-1} on July 21 and the conventional field emitting 422 g N_2O-N ha^{-1} on July 23 (Figure 3.3 d). Cumulative fluxes for the post-fertilizer application period were lower for the cover crop fields in all study years than the conventional fields (Table 3.3).

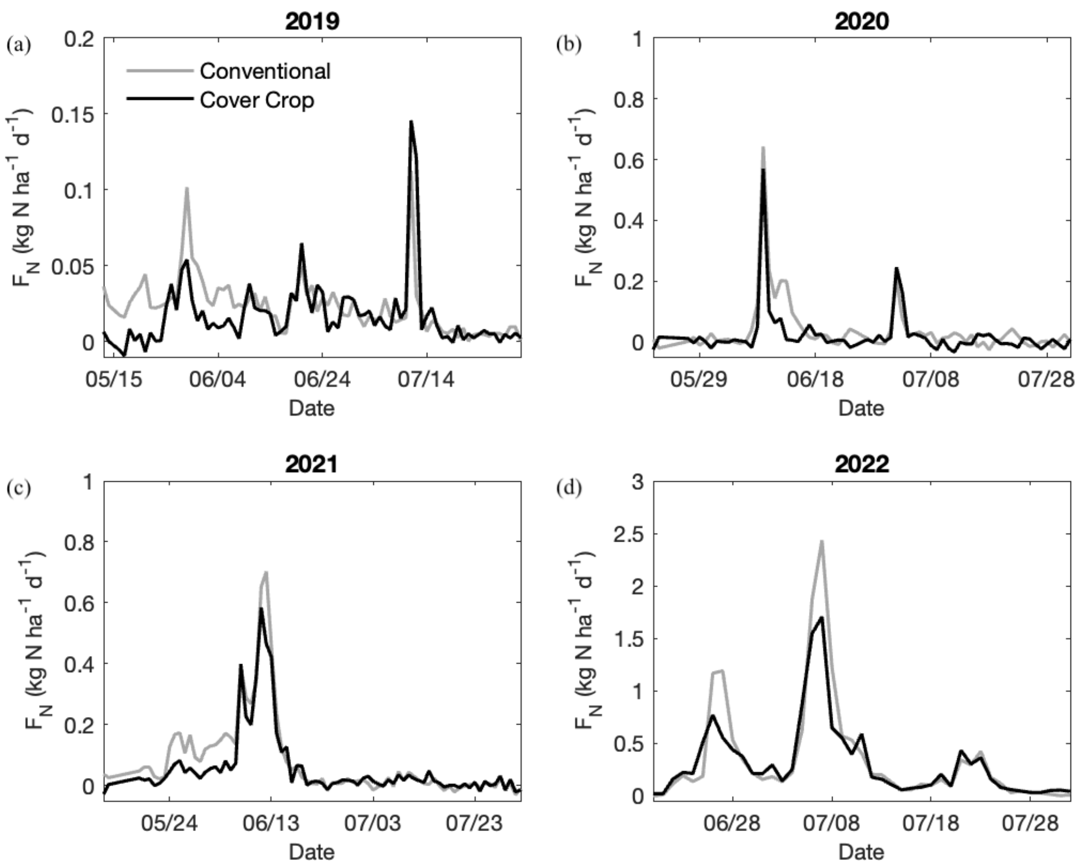

Figure 3.3 Gap-filled daily average N_2O flux (F_N) from fertilizer application until August 15 for (a) 2019, (b) 2020, (c) 2021, and (d) 2022.

3.4.2.5 Cumulative Nitrous Oxide Fluxes

Daily average fluxes for each study year varied but were consistently lower for the cover crop fields in all study years than the conventional fields. The average N_2O flux for the cover crop fields was 10 g ha^{-1} day^{-1} in 2019 and 2020, 25 g ha^{-1} day^{-1} in 2021, and 74 g ha^{-1} day^{-1} in 2022. The daily average N_2O flux for the conventional fields was 25 g ha^{-1} day^{-1} in 2019, 18 g ha^{-1} day^{-1} in 2020, 32 g ha^{-1} day^{-1} in 2021, and 83 g ha^{-1} day^{-1} in 2022. Both cropping systems experienced sporadic periods of N_2O uptake in each study year. Daily N_2O uptake during the study ranged from 4 g ha^{-1} day^{-1} to 37 g ha^{-1} day^{-1} for the conventional fields and 29 g ha^{-1} day^{-1} to 42 g ha^{-1} day^{-1} for the cover crop fields. There was no consistent time of the year when maximum uptake of N_2O occurred.

Contributions of spring-thaw and post-fertilizer N_2O fluxes to cumulative N_2O fluxes varied between study years and between the cropping systems (Table 3.3). In 2019, spring-thaw accounted for 48% and 29% of the N_2O emissions for the conventional and cover crop systems, respectively. Post-fertilizer fluxes accounted for 40% of the emissions, and the other periods accounted for 12% of the emissions of the conventional system. 71% of the emissions could be attributed to post-fertilizer emissions for the cover crop system and slight cumulative uptake of N_2O of approximately 200 g N_2O-N ha^{-1} occurred during the remaining periods. Contributions of spring-thaw and post-fertilizer N_2O fluxes to cumulative fluxes were similar for the two cropping systems in 2020, 2021 and 2022. However, the contribution varied by year. In 2020, spring-thaw accounted for 20-30% of the cumulative flux, post-fertilizer contributed 65-71%, and the remaining periods contributed 5-9%. In 2021, spring-thaw contributed 11-18% of the cumulative N_2O flux and post-fertilizer emissions contributed 82-89%. Contributions from post-fertilizer N_2O

fluxes were greatest in 2022 at 89% for both cropping systems, with spring-thaw contributing 3-5% of the fluxes and 6-8% coming from the remaining period.

Cumulative N_2O emissions from January to August 15 were lower in the cover crop fields in all study years than in conventionally managed fields (Table 3.3). The highest cumulative emissions occurred in 2022 for both the cover crop and conventional systems and the lowest in 2019 from the cover crop field (Table 3.3). Cumulative emissions from the cover crop fields were 62% lower in 2019, 43% lower in 2020, 21% lower in 2021, and 11% lower in 2022 (Table 3.3). Combining the N_2O fluxes from the two cropping systems from all four study years, the conventional system emitted 32.6 kg N_2O-N ha^{-1} and the cover crop system emitted 24.6 kg N_2O-N ha^{-1}. Cumulative N_2O fluxes for each field used during the study can be found in the Appendix (APPENDIX A Table 5.2).

Table 3.3 Nitrogen fluxes of the two cropping systems from the four study years: cumulative gap-filled spring-thaw N_2O flux ($\sum F_{N\text{-}SPRING\text{-}THAW}$), cumulative gap-filled post-fertilizer N_2O flux ($\sum F_{N\text{-}FERTILIZER}$), and cumulative gap-filled net N_2O flux ($\sum F_N$) for each study year (January 1 to August 15).

		Year			
Cropping System		**2019**	**2020**	**2021**	**2022**
Conventional	$\sum F_{N\text{-}SPRING\text{-}THAW}$, kg N ha^{-1}	2.4	0.7	0.8	0.9
	$\sum F_{N\text{-}FERTILIZER}$, kg N ha^{-1}	2.0	2.5	6.4	15.0
	$\sum F_N$, kg N ha^{-1}	5.0	3.5	7.2	16.9
Cover Crop No-Till	$\sum F_{N\text{-}SPRING\text{-}THAW}$, kg N ha^{-1}	0.6	0.6	1.0	0.4
	$\sum F_{N\text{-}FERTILIZER}$, kg N ha^{-1}	1.5	1.3	4.7	13.3
	$\sum F_N$, kg N ha^{-1}	1.9	2.0	5.7	15.0

3.4.3 Net Greenhouse Gas Emissions

When combining the N_2O emissions with the carbon fluxes from the two cropping systems from 2019 and 2022 (Chapter 2), both systems were a significant GHG sources (Table 3.4). In

2019, the cover crop system was a slight GHG source at 231 kg CO_2-eq ha^{-1} due to high $\sum F_{NEP}$ and lower $\sum F_N$, while the conventional system was a significant GHG source of approximately 1,700 kg CO_2-eq ha^{-1} (Table 3.4). Both systems had a negative carbon balance ($F_{ECOSYSTEM}$) in 2022, resulting in both being carbon sources before factoring in N_2O fluxes. Once $\sum F_N$ was factored in, both systems were significant GHG sources, with the conventional system being a source of 5,956 kg CO_2-eq ha^{-1} and the cover crop system being a source of 5,434 kg CO_2-eq ha^{-1} (Table 3.4). When combining the two study years, the conventional system was a source of 7,653 kg CO_2-eq ha^{-1} and the cover crop system was a source of 5,665 kg CO_2-eq ha^{-1}.

Table 3.4 2019 and 2022 cumulative ecosystem carbon and nitrogen fluxes from the two cropping systems: cumulative gap-filled net N_2O flux ($\sum F_N$) from January 1 to August 15 for each year, respectively, gap-filled cumulative net ecosystem production ($\sum F_{NEP}$) from January 1 to harvest for each study year respectively, C harvest removal ($F_{HARVEST}$), C balance ($F_{ECOSYSTEM} = \sum F_{NEP} - F_{HARVEST}$), and cumulative net greenhouse gas flux equivalents ($\sum F_{GHG}$). A global warming potential of 265 was used to convert $\sum F_N$ to CO_2-eq. Only flux data from fields 3 and 4 were used for flux determinations.

	Cropping System			
	Conventional		**Cover Crop**	
	2019	**2022**	**2019**	**2022**
$\sum F_N$, kg N ha^{-1}	5.0	17.0	1.9	15.0
$\sum F_{NEP}$, kg C ha^{-1}	1,444	-66	1,820	-128
$F_{HARVEST}$, kg C ha^{-1}	1,815	1,385	1,547	1,331
$F_{ECOSYSTEM}$, kg C ha^{-1}	-372	-1,451	273	-1,459
$\sum F_{GHG}$, kg CO_2-eq ha^{-1}	-1,697	-5,956	-231	-5,434

3.4.4 Cover Crop Impact on Grain Yield

Grain biomass from all four fields at the site was used to assess the impact of the cover crop on cash crop grain yield. The mean grain yield was higher for the cover crop system in all study years except 2019, where the mean yield was higher for the conventional system (Table 3.5). In 2019, the grain yield from the conventional fields was approximately 100 kg ha^{-1} higher than the average oat yield of 3,860 kg ha^{-1} for Manitoba in 2019 (Government of Manitoba, 2023*a*).

The mean grain yield for the cover crop system in 2019 was approximately 300 kg ha$^{-1,}$ lower than the mean provincial yield in 2019. In 2020, the mean grain yield from the cover crop system was approximately 300 kg ha^{-1} higher than the provincial average canola yield of 2,321 kg ha^{-1} for Manitoba in 2020 (Government of Manitoba, 2023*b*). Grain yield from the conventional system was approximately the same as the provincial grain yield for canola in 2020. The mean grain yield for both cropping systems in 2021 and 2022 was lower than the provincial average for spring wheat of 3,222 kg ha^{-1} in 2021 and 3,910 kg ha^{-1} in 2022 (Government of Manitoba, 2023*b*). However, the cover crop fields yielded higher than the conventional fields in 2021 and 2022 (Table 3.5). While the cover crop fields generally yielded higher than the conventionally managed fields, differences in yield were not statistically significant in all study years (P = 0.18 – 0.98).

Table 3.5 Air dry grain yield from each field and mean grain yield for each cropping system for each study year. Biomass samples were collected from six locations in each field (n=6).

Year	Location	Field 1	Field 2	Field 3	Field 4	Mean Conventional	Mean Cover Crop
2019	Grain Yield (kg ha^{-1})	3,667	3,496	3,616	4,247	3,957	3,556
	Standard Deviation	1,251	639	782	701	1,013	684
2020	Grain Yield (kg ha-^{1})	2,344	2,464	2,261[a]	2,907	2,363	2,625
	Standard Deviation	583	533	430[a]	812	480	735
2021	Grain Yield (kg ha^{-1})	3,018	2,579	2,681	2,578	2,630	2,798
	Standard Deviation	430	301	554	524	428	512
2022	Grain Yield (kg ha^{-1})	2,287	3,382	3,101	3,213	2,750	3,242
	Standard Deviation	1,756	1,192	1,678	1,139	1,492	1,395

[a] average grain yield and standard deviation of four grain samples (n=4)

3.5 Discussion

3.5.1 Cover Crop Impacts on Soil Nitrate and Moisture

Soil NO_3^-/NO_2^- concentrations were lower in the cover crop fields in spring prior to cash crop seeding in 2019, 2021, and 2022 and were significantly lower in 2019 and 2022. Reductions in NO_3^-/NO_2^- were greatest in 2019, with the cover crop fields having approximately 6 mg NO_3^-/NO_2^- kg^{-1} dry soil compared to 15 mg NO_3^-/NO_2^- kg^{-1} dry soil for the conventional fields (Figure 3.1). In 2019 and 2022, the cover crop appeared to reduce soil NO_3^-/NO_2^- up to 5 mg NO_3^-/NO_2^- kg^{-1} dry soil, after which soil NO_3^-/NO_2^- stayed approximately the same (Figure 3.1). Significance in soil NO_3^-/NO_2^- reductions appeared to result from biomass accumulation, as biomass accumulation was lowest in 2021. However, reductions in soil NO_3^-/NO_2^- did not continue with increased biomass accumulation, as concentrations were similar in 2019 and 2022, with different amounts of biomass accumulated before seeding (Table 3.2). Similar reductions in soil nitrate from cover crop growth were observed by Reicks et al. (2021), who found that soil nitrate was more than 50% lower in the top 30 cm of soil in cover crop fields than in non-cover cropped fields.

Differences in soil GMC between the two cropping systems were observed in different years of the study. Soil GMC from the cover crop system was lower in spring and the early growing season in 2019, the same as the conventional system in 2020, higher than the conventional system in 2021, and lowered compared to the conventional system in 2022. Differences were likely the result of cover crop maturity in spring, water usage by the cover crop, and snow trapping by the cover crop and previous cash crop residue (Acharya et al., 2019; Chakraborty et al., 2022; Kahimba et al., 2008; Liu and Lobb, 2021). In 2019 and 2022, with good cover crop establishment, the cover crop would have utilized available soil moisture, decreasing soil GMC. Other studies have observed lowered soil moisture by cover crops (Chakraborty et al., 2022; Kahimba et al., 2008).

Cover crop establishment was very poor and precipitation in winter and early spring was very low in 2020, with less than 10 mm of total precipitation accumulated from January to May (Table 3.1), likely resulting in the minimal difference in GMC observed. In 2021 however, cover crop establishment was better and slightly more precipitation was received over winter, potentially increasing the snow trapping and water conservation in 2021. Intact crop stubble and cover crop biomass can trap more snow, increasing water conservation (Liu and Lobb, 2021), and water percolation has been seen to improve with no-till practices (Acharya et al., 2019), which may have increased water conservation and retention under dry conditions in 2021 compared to the conventional fields.

3.5.2 Cover Crop Effects on Nitrous Oxide Fluxes

3.5.2.1 Spring-Thaw N_2O Fluxes

The cover crop fields saw lower peak N_2O emissions during spring-thaw in study years with cover crop biomass establishment and lower cumulative emissions in 2019 and 2022. Reductions in spring-thaw N_2O emissions were likely the result of reduced soil nitrate from cover crop growth (Dietzel et al., 2011; Reicks et al., 2021) compared to the conventional fields. Cover crop biomass establishment was good in the fall of 2018 and 2021, which reduced soil NO_3^-/NO_2^- concentrations in those fields the following spring compared to the conventional fields, resulting in less NO_3^-/NO_2^- available for denitrification by soil microbes. Peak N_2O emissions from the cover crop field were lower than the conventional field in the spring of 2021, however, cumulative spring-thaw N_2O emissions in 2021 were similar to the conventional field. Soil NO_3^-/NO_2^- was lower in the cover crop field compared to the conventional field in 2021, with NO_3^-/NO_2^- concentrations of approximately 16 mg NO_3^-/NO_2^- kg^{-1} dry soil for the cover crop field compared to approximately 18 mg NO_3^-/NO_2^- kg^{-1} dry soil for the conventional field. However, NO_3^-/NO_2^- concentrations were not as low as concentrations in 2019 and 2022, where soil NO_3^-/NO_2^- in spring was approximately 5 mg NO_3^-/NO_2^- kg^{-1} dry soil. Thomas et al. (2017) found that NO_3 concentrations less than 6 mg NO_3-N kg^{-1} limited N_2O fluxes. Therefore, the difference in spring-thaw N_2O reductions in 2019 and 2022 versus 2021 was likely the result of reductions in soil nitrate from cover crop establishment. Reductions in spring-thaw N_2O emissions could have also been from cover crops delaying soil freezing in the fall prior from improved soil insulation (Kahimba et al., 2008) and reduced freezing intensity (Wagner-Riddle et al., 2007), which may not have occurred in 2021 as biomass establishment was poor from drought conditions and precipitation in winter months was lower than normal, reducing the amount of snow available to insulate the soil. Differences in peak emissions were not observed in 2020 when cover crop biomass establishment was poor and no-till of the cover crop field did not impact spring-thaw emissions. Wagner-Riddle et al. (2007) found that no-till significantly decreased spring-thaw N_2O emissions due to reduced soil freezing from increased insulation from better snow cover. Precipitation was limited in our study in 2020 from January to April, likely limiting the ability of the intact crop residue of the cover crop field to trap snow and reduce freezing intensity. However, reduced tillage has been seen to have no effect on spring-thaw emissions at the site in the past and soil nitrate going into winter was a better determinant of spring-thaw emissions at the site (Glenn et al., 2012).

3.5.2.2 Post-Fertilizer N_2O Fluxes

Post-fertilizer N_2O emissions followed fertilizer application and rainfall in all study years regardless of the fertilizer applied, which has been observed at the site in previous studies (Glenn et al., 2012; Maas et al., 2013; Tenuta et al., 2019). 2019 N_2O emissions peaked later in the growing season compared to other study years. Later peak emissions with ESN were also observed by Sistani et al. (2011), who saw delayed N_2O emissions from ESN fertilizer compared to other N fertilizer sources. N_2O emissions following fertilizer application were highest in 2022 due to high soil moisture conditions and increased temperatures following application due to delayed seeding operations. Seeding and fertilizer application in the 2019-2021 study years occurred in May with average air temperatures between 10-11°C for each year, respectively, while in 2022, seeding occurred in June and average air temperatures for the month were 17.8°C (Table 3.1). N_2O emissions can increase exponentially with increases in temperature as increased temperature increases microbial activity and oxygen consumption, resulting in increased anaerobic conditions in soil (Smith et al., 2018). Further, increased WFPS increases N_2O production as anaerobic conditions increase (Smith et al., 2018). Precipitation in 2022 was higher than average every month from January to August, except in June, where it was slightly below normal, resulting in prolonged saturated soil conditions during the growing season (Table 3.1). The combination of warmer air temperatures and high soil moisture at fertilizer application likely resulted in the high N_2O emissions observed following fertilizer application in 2022.

The cover crop fields had lower primary peak emissions following fertilizer application compared to the conventional fields in all years and then similar or slightly higher peak emissions during emissions events later in the growing season in some years (Figure 3.3). The response of N_2O emissions following fertilizer application on cover-cropped soils has seen varying results, with some studies reporting increased N_2O emissions from non-legume cover-cropped fields following fertilizer application and others reporting decreased N_2O emissions (Basche et al., 2014; Han et al., 2017; Mitchell et al., 2013; Muhammad et al., 2019). The reduction in primary peak emissions in our study could have been the result of cover crop impacts on soil moisture

(Chakraborty et al., 2022) and the effect of cover crop residues on soil mineral N availability during residue decomposition (Fiorini et al., 2020). The cover crop lowered soil moisture in 2019 and 2022 compared to the conventional fields, which could have resulted in increased aerobic conditions and reduced N_2O production compared to the conventional fields following fertilizer application. Cover crop residues may have also altered soil mineral N availability, affecting N_2O emissions. We would expect that the C additions from the cover crop would increase N_2O production by providing increased C substrates to soil microorganisms, increasing microbial activity and N_2O production (Mitchell et al., 2013; Tenuta et al., 2019). However, C/N ratio and termination method may have affected C substrate availability and subsequent N_2O emissions following fertilizer application. Cover crop residues with higher C/N ratios can promote the immobilization of soil N by soil microorganisms (Fiorini et al., 2020). Muhammad et al. (2019) found that increased C/N ratio of cover crop residues decreased N_2O emissions. The C/N ratio of cover crop biomass in our study ranged from 14.0 in 2021 with low biomass accumulation to nearly 27 in 2022 with high biomass accumulation (Table 3.2), which may have resulted in increased immobilization. Further, microbial access to residues was restricted as cover crops were terminated with an herbicide application and left intact on the soil surface rather than being incorporated. Incorporating cover crop residues increases residue mineralization and N_2O emissions as tillage increases aeration and microbial access to residues (Muhammad et al., 2019). Therefore, the reduced soil moisture in some years, C/N ratio of residues, and restricted microbial access to residues may have resulted in decreased N_2O emissions compared to the conventional fields in our study.

Differences in N_2O emissions in 2020 following fertilizer application were likely the result of the N rate applied at seeding and not cover crop residues, as biomass accumulation was very poor and the cover crop field received 145.5 kg ha^{-1} UAN compared to 168 kg ha^{-1} for the conventional field. Tenuta et al. (2019) found that N_2O emissions increased exponentially with N fertilizer application rate after N application rates exceeded 150 kg N ha^{-1} y^{-1}. The higher N_2O emissions observed in 2020 from the conventional field were likely a result of an increased N rate compared to the cover crop field.

3.5.3 Cumulative N_2O Fluxes and Net Greenhouse Gas Emissions

Daily average N_2O and cumulative N_2O fluxes from January to mid-August were lower in all study years from the cover crop no-till fields than from the conventional fields. N_2O uptake was observed from both cropping systems in all study years. However, there was no consistent time of the year when maximum N_2O uptake occurred. Since N_2O consumption primarily occurs during denitrification (Liu et al., 2022), we can deduce that consumption occurred when production rates of N_2O decreased past consumption rates under anaerobic conditions.

Contributions of spring-thaw emissions to cumulative N_2O emissions ranged from 3 to 48% depending on the cropping system and year. Cumulative spring-thaw emissions were lower than those reported by Wagner-Riddle et al. (1997), who observed N_2O emissions during spring-thaw ranging from 1.5 to 4.3 kg N ha^{-1} but were similar to spring-thaw emissions reported by other studies conducted at the site (Maas et al., 2013; Tenuta et al., 2016; Tenuta et al., 2019). Post-fertilizer N_2O emissions accounted for the majority of the N_2O emissions during the study period at the site, which was also observed by Tenuta et al. (2019), who reported post-planting N_2O emissions contributed more than 50% to annual N_2O emissions when analyzing a decade of N_2O emissions from the site. Contributions of post-fertilizer application N_2O emissions to cumulative N_2O emissions were higher in our study than those reported in Tenuta et al. (2019), as our study only covered emissions from January to mid-August and not annual N_2O fluxes. Combining the N_2O fluxes from the four study years, the cover crop fields emitted 25% less N_2O than the conventional fields.

While the cover crop reduced N_2O emissions in our study, combining the N_2O fluxes with the CO_2 fluxes measured in 2019 and 2022 (reported in Chapter 2), both cropping systems were GHG sources (Table 3.4). The combination of C assimilation by the cover crop and reduced N_2O emissions resulted in the cover crop system being only a slight source of GHGs in 2019 and was considerably lower than the conventional system, which emitted over 1400 kg CO_2-eq ha^{-1} more than the cover crop fields (Table 3.4). Negative $F_{ECOSYSTEM}$ for both cropping systems in 2022 due to saturated soil conditions and high N_2O emissions from both systems resulted in both systems being a significant source of GHGs in 2022. However, the cover crop fields emitted approximately 500 kg CO-eq ha^{-1} less than the conventional system in 2022 due to lowered N_2O emissions (Table 3.4). Abdalla et al. (2019) reported that cover crops could mitigate net GHG balances by 2.06 +- 2.10 Mg CO_2 -eq ha^{-1} $year^{-1}$ from increases in soil organic carbon in the soil, decreases in nitrogen leaching and indirect N_2O emissions, without significant increases in N_2O emissions. The difference in net GHG emissions in 2019 indicates that there is potential for cover crops to mitigate GHG production from agricultural soils. However, there is no guarantee that cover crops can mitigate GHG emissions every year as growing season conditions can affect crop growth, C balance, and N_2O emissions, illustrated by the 2022 growing season as the majority of CO-eq emitted in 2022 resulted from N_2O emissions following fertilizer application.

3.5.4 Cover Crop Impacts on Cash Crop Yield

Cover crops have seen varying impacts on subsequent cash crop grain yields, with some studies reporting maintained yields with cover crops, some reporting increased yields, and others reporting decreased yields (Abdalla et al., 2019; Acharya et al., 2019; Bourgault et al., 2022; Finney et al., 2016; Fiorini et al., 2020; Han et al., 2017; Hunter et al., 2019; Liebman et al., 2018). In our study, yields between the cover crop and conventional cropping systems were not statistically significant, resulting in yields maintained under the cover crop no-till system. Mean yields were higher in 2019 in the conventional system, which resulted from increased yields from Field 4 compared to the other fields at the site (Table 3.5). Amiro et al. (2017) observed higher yields from Field 4 in many years from observations over a decade at the site. Higher yields were also observed from Field 4 in 2020, under the cover crop no-till treatment that year (Table 3.5). Yields were generally similar between Fields 1, 2 and 3 in 2019 and 2020. Yields were highest in 2021 from Field 1 as dry growing conditions and lower elevation at Field 1 increased yields compared to the other fields under drought conditions. Alternatively, saturated soil conditions in 2022 resulted in Field 1 having the lowest yields as high moisture in areas caused bare patches in the field from the wheat drowning.

Yields were generally maintained close to the provincial average grain yield in 2019 and 2020. In 2021 and 2022, drier and wetter years than normal, respectively, grain yields were lower than the provincial average. However, the mean cover crop yield was higher than the mean conventional yield in both years. Improvements in yields from the cover crop fields in 2021 and 2022 could have resulted from increased moisture from improved snow trapping in 2021 and lowered soil moisture in 2022 from cover crop utilization of soil moisture in spring (Figure 3.1).

3.5.5 Uncertainty

Limited measurements at the site due to the removal of N_2O data from specific fields in different study years resulted in flux measurements only capturing 23 to 36% of N_2O fluxes during the study, approximately half of what was captured by Tenuta et al. (2019) looking at a decade of N_2O emissions from the site. Only one field was measured per treatment in each study year, except 2022, where fluxes were measured from all four fields until fertilizer application, which may have caused under or overestimations of N_2O fluxes of treatments as peak emissions have been seen to vary by year and by field at the site (Tenuta et al., 2019). However, site analysis by Amiro (2022), which can be found in APPENDIX C, on the field variability at the site found that Field 2 and 4, and Field 3 and 4 were the best field comparisons if other field data were unavailable from the site. In 2019 and 2022, data from Field 3 and 4 was used, and in 2020 and 2021, data from Fields 2 and 4 was used, providing some confidence in the field comparisons made in the study. Further, the location of the cover crop no-till and conventional treatments changed locations in different years of the study, with the east fields being the cover crop no-till treatment in 2019 and 2022 and the west fields being the cover crop no-till treatment in 2020 and 2021, reducing the uncertainty in observations caused by field effect rather than treatment effect.

There is uncertainty in measurements from missing data due to site maintenance, field operations or power interruptions that caused data to be removed. The average gap size during the study was 3.6 and 3.8 days for the conventional and cover crop fields. Gaps of less than ten days were filled with linear interpolation. However, large data gaps remained after gap-filling in three of the four study years. While the large gaps occurred in the winter months, where N_2O fluxes are minimal and other gaps were relatively short, fluxes may have been missed as emission events were episodic and unpredictable, which could have led to an underestimation of fluxes.

Uncertainty in flux measurements may have occurred from gradient measurements and from *K* values. In early research at the site, Glenn et al. (2012) estimated gradient measurement uncertainty of ± 1.2 g N ha^{-1} day^{-1} (Glenn et al., 2012). Long-term analysis of N_2O fluxes at the site from 2006-2016 estimated an average N_2O flux of 5 kg N ha^{-1} y^{-1} (Tenuta et al., 2019). This corresponds to uncertainty from gradient measurements for our study of approximately 5%, based on the long-term measurements by Tenuta et al. (2019). Error from *K* values may have been introduced during flux calculations as a single *K* value, the average of the *K* values from sonics at the site, was used for flux calculations. Time-of-day bias may have been introduced to fluxes calculated in 2020 onward as the system upgrades in late 2019 did not have a time lag at midnight to avoid time-of-day bias like the system in 2019 did. There is also uncertainty in the flux data from 2020 and 2021 as bias corrections were made to correct data bias from mechanical issues in the field. Uncertainty in the bias corrections increased with temperature (Amiro, 2021, see APPENDIX B), increasing the uncertainty in N_2O emission events at warmer temperatures, such as those following fertilizer application.

There is also uncertainty in yield data as grain yield was determined from hand-clipped biomass samples that were threshed using different equipment than what was used to harvest the grain from the field. Further, yield, cover crop biomass, and soil samples were only obtained from six locations within each field, increasing uncertainty as only a few samples represented a much larger area and variability within each field may have been missed.

3.5.6 Cover Crops and Climate Change

Our study demonstrates that fall rye cover crops seeded no-till can effectively reduce N_2O emissions from soils in the Red River Valley region of the Canadian Prairies while maintaining cash crop yields. The fall rye no-till cover crop system effectively reduced peak and cumulative N_2O emissions during spring-thaw by reducing soil nitrate when adequate cover crop biomass was accumulated. Further, the cover crop no-till system did not increase N_2O emissions following cover crop termination and fertilizer application and reduced peak emissions during primary emission periods, which resulted in lower cumulative N_2O fluxes from the no-till cover crop fields compared to the conventionally managed fields.

However, flux data obtained in 2019 and 2022 illustrated that the effectiveness of cover crops in reducing cumulative GHG emissions is complex and is greatly affected by environmental conditions. In 2019 with good cover crop establishment and ideal conditions during the growing season, the no-till cover crop system was only a slight GHG source (-231 kg CO_2-eq ha^{-1}) compared to the conventional system, which was a considerable GHG source (-1,697 kg CO_2-eq ha^{-1}). In 2022 however, even with high levels of cover crop biomass accumulated in spring, delayed seeding due to wet soil conditions and saturated soil conditions for most of the growing season resulted in both cropping systems being a C source after harvest removals and a considerably higher GHG source once N_2O emissions were factored in which was driven by high post-fertilizer emissions. Cumulative post-fertilizer N_2O fluxes were more than double the next highest cumulative emissions measured at the site in our study due to warmer air temperatures and saturated soil conditions following fertilizer application, highlighting the importance of the contribution of GHG emissions from synthetic N fertilizer use. Combining the two years however, the cover crop system emitted nearly 2,000 kg CO_2-eq ha^{-1} less than the conventional system over the two years, demonstrating that cover crops can reduce cumulative GHG emissions. Producers may want to consider modifying crop rotations under wet growing conditions and delayed seeding like those that were experienced in our study in 2022 to reduce fertilizer use, N_2O emissions, and overall GHG emissions.

A whole year of continuous GHG monitoring will be necessary to fully understand the effects of no-till fall rye cover crops on N_2O fluxes and what happens if the practice is discontinued. Tenuta et al. (2019) found that more than 50% of N_2O emissions from 10 years of fluxes from the site came from early growing season post-fertilizer emissions and that 15-20% came from spring-thaw, with the remaining N_2O emissions coming from other times of the year, which we did not cover in our study. To understand if cover crops make a difference in N_2O emissions annually compared to conventional systems, whole-year fluxes must be monitored. Further, we did not assess the effect of discontinuing the practice of no-till cover cropping on N_2O emissions, which should be considered as reductions in N_2O emissions during spring-thaw and the growing season could be potentially lost if the practice is stopped and residues are incorporated into the soil.

While our study did not find that the use of cover crops resulted in agricultural soils being a net GHG sink, there are other benefits to growing cover crops which should also be considered going into the future with climate change. Cover crops can provide numerous benefits in agricultural production, such as improved soil structure, reduced land degradation, reduced soil erosion, provide weed suppression, breaking pest and disease cycles, provide habitat for beneficial insects, and reduced nitrogen leaching, to name a few, which will become increasingly important with climate change (Basche et al., 2014; Basche et al., 2016; Blesh, 2018; Burke et al., 2021; Darapuneni et al., 2021; De Baets et al., 2011; Finney et al., 2016; Hartwig and Ammon, 2002; Hudek et al., 2022; Kabelka et al., 2021; Liebman et al., 2018; Muhammad et al., 2019). In our study, fall rye was selected as a cover crop but can also be harvested as a cash crop if allowed to reach maturity, providing an economic benefit if a cash crop cannot be seeded due to environmental conditions. As the severity and frequency of extreme weather events continue with climate change, the stability of agricultural and food production will be challenged (IPCC, 2022). Improving the resiliency of agricultural production systems will be essential going into a future with climate change. Cover crops offer a mitigation strategy to reduce GHG emissions from agricultural soils in the Canadian Prairies by reducing N_2O emissions, which was observed in this study. Further research into combining cover cropping and no-till with other agronomic practices will be required to determine how to make agricultural soils in the Canadian Prairies a net GHG sink.

3.6 Conclusion

A fall rye cover crop no-till cropping system reduced cumulative spring-thaw N_2O emissions when cover crop establishment was adequate and nitrate uptake by the cover crop reduced soil nitrate levels in spring. Following fertilizer application, the cover crop no-till fields saw lower initial peak N_2O emissions and lower cumulative emissions than conventional fields. In 2020, reductions in N_2O emissions following fertilizer application were suspected to be from lower fertilizer application rates than from the cover crop, as cover crop establishment was very poor in 2020. In all study years, the cover crop system did not significantly affect cash crop yields compared to the conventional system. Both cropping systems were a net GHG source when combining CO_2 fluxes from January to cash crop harvest from 2019 and 2022 with N_2O fluxes from January to mid-August each year. However, the cover crop system did have lower cumulative net GHG emissions in both years, resulting in the cover crop no-till system emitting over 2,000 kg

CO_2-eq ha^{-1} less than the conventional system from the two years. Further research into the effect of cover crops on annual N_2O fluxes and annual net GHG emissions will be required to fully understand the effect of fall rye no-till cover crop systems on GHG emissions.

3.7 References

Abdalla, M., Hastings, A., Cheng, K., Yue, Q., Chadwick, D., Espenberg, M., Truu, J., Rees, R.M., and Smith, P. 2019. A critical review of the impacts of cover crops on nitrogen leaching, net greenhouse gas balance and crop productivity. Global Change Biology. **25**: 2530-2543.

Acharya, B.S., Dodla, S., Gaston, L.A., Darapuneni, M., Wang, J.J., Sepat, S., and Bohara, H. 2019. Winter cover crops effect on soil moisture and soybean growth and yield under different tillage systems. Soil and Tillage Research. **195**: 104430.

Amiro, B.D. 2021. Corrections for bias in gradients caused by mis-matched lines in 2020 and 2021 at TGAS-MAN. APPENDIX B.

Amiro, B.D. 2022. Field Variability at TGAS. APPENDIX C.

Amiro, B.D., Tenuta, M., Gervais, M., Glenn, A.J., and Gao, X. 2017. A decade of carbon flux measurements with annual and perennial crop rotations on the Canadian Prairies. Agricultural and Forest Meteorology. **247**: 491-502.

Basche, A.D., Archontoulis, S.V., Kaspar, T.C., Jaynes, D.B., Parkin, T.B., and Miguez, F.E. 2016. Simulating long-term impacts of cover crops and climate change on crop production and environmental outcomes in the Midwestern United States. Agriculture, Ecosystems and Environment. **218**: 95-106.

Basche, A.D., Miguez, F.E., Kaspar, T.C., and Castellano, M.J. 2014. Do cover crops increase or decrease nitrous oxide emissions? A meta-analysis. Journal of Soils and Water Conservation. **69**: 471-482.

Blesh, J. 2018. Functional traits in cover crop mixtures: Biological nitrogen fixation and multifunctionality. Journal of Applied Ecology. **55**: 38-48.

Bourgault, M., Wyffels, S.A., Dafoe, J.M., Lamb, P.F., and Boss, D.L. 2022. Introducing cover crops as fallow replacement in the Northern Great Plains: II. Impact on following wheat crops. Renewable Agriculture and Food Systems. **37**: 303-312.

Burke, J.A., Lewis, K.L., Ritchie, G.L., DeLaune, P.B., Keeling, J.W., Acosta-Martinez, V., Moore, J.M., and McLendon, T. 2021. Net positive soil water content following cover crops with no tillage in irrigated semi-arid cotton production. Soil and Tillage Research. **208**: 104869.

Chadwick, D.R., Cardenas, L., Misselbrook, T.H., Smith, K.A., Rees, R.M., Watson, C.J., McGeough, K.L., Williams, J.R., Clow, J.M., Thorman, R.E., and Dhanoa, M.S. 2014. Optimizing chamber methods for measuring nitrous oxide emissions from plot-based agricultural experiments. European Journal of Soil Science. **65**: 295-307.

Chakraborty, P., Singh, J., Singh, N., and Kumar, S. 2022. Assessing the influence of cover crop on soil water dynamics using soil moisture measurements and hydrus-1D simulations. Soil Science Society of America Journal. **86**: 1538-1552.

Darapuneni, M.K., Idowu, O.J., Sarihan, B., DuBois, D., Grover, K., Sanogo, S., Djaman, K., Lauriault, L., Omer, M., and Dodla, S. 2021. Growth characteristics of summer cover crop grasses and their relation to soil aggregate stability and wind erosion control in arid southwest. Applied Engineering in Agriculture. **37**: 11-23.

De Baets, S., Poesen, J., Meersmans, J., and Serlet, L. 2011. Cover crops and their erosion-reducing effects during concentrated flow erosion. Catena. **85**: 237-244.

Denmead, O.T. 2008. Approaches to measuring fluxes of methane and nitrous oxide between landscapes and the atmosphere. Plant and Soil. **309**: 5-24.

Dietzel, R., Wolfe, D., and Thies, J.E. 2011. The influence of winter soil cover on spring nitrous oxide emissions from an agricultural soil. Soil Biology and Biochemistry. **43**: 1989-1991.

Edwards, G.C., Thurtell, G.W., Kidd, G.E., Dias, G.M., and Wagner-Riddle, C. 2003. A diode laser based gas monitor suitable for measurement of trace gas exchange using micrometeorological techniques. Agricultural and Forest Meteorology. **115**: 71-89.

Ehrlich, W.A., Poyser, E.A., Pratt, L.E., and Ellis, J.H. 1953. MB-5 Report of Reconnaissance Soil Survey of Winnipeg and Morris Map Sheet Areas. Manitoba Soil Survey, Winnipeg, MB. https://sis.agr.gc.ca/cansis/publications/surveys/mb/mb5/mb5_report.pdf (accessed March 21, 2022).

Environment Canada. 2018. National Inventory Report 1990-2016: Greenhouse Gas Sources and Sinks in Canada. Environment and Climate Change Canada. https://publications.gc.ca/collections/collection_2018/eccc/En81-4-2016-3-eng.pdf (Accessed April 3, 2023).

Environment Canada. 2023*a*. Canadian Climate Normals 1981-2010 Station Data. Government of Canada. https://climate.weather.gc.ca/climate_normals/results_1981_2010_e.html?searchType=stnName&txtStationName=Glenlea&searchMethod=contains&txtCentralLatMin=0&txtCentralLatSec=0&txtCentralLongMin=0&txtCentralLongSec=0&stnID=3599&dispBack=1 (accessed March 25, 2023).

Environment Canada. 2023*b*. Historical Data. Government of Canada. https://climate.weather.gc.ca/climate_data/hourly_data_e.html?hlyRange=2013-12-10%7C2023-01-03&dlyRange=1996-10-01%7C2023-01-03&mlyRange=1996-10-01%7C2007-11-01&StationID=27174&Prov=MB&urlExtension=_e.html&searchType=stnName&optLimit=yearRange&StartYear=1840&EndYear=2023&selRowPerPage=25&Line=0&searchMethod=contains&txtStationName=Winnipeg+A+CS&timeframe=1&time=LST&time=LST&Year=2022&Month=8&Day=28# (accessed March 25, 2023).

Finney, D.M., White, C.M., and Kaye, J.P. 2016. Biomass production and carbon/nitrogen ratio influence ecosystem services from cover crop mixtures. Agronomy Journal. **108**: 39-52.

Fiorini, A., Maris, S.C., Abalos, D., Amaducci, S., and Tabaglio, V. 2020. Combining no-till with rye (*Secale cereale L.*) cover crop mitigates nitrous oxide emissions without decreasing yield. Soil and Tillage Research. **196**: 104442.

Garratt, J.R. 1992. The atmospheric boundary layer. Cambridge Atmospheric and Space Science Series. Cambridge University Press. New York, NY.

Glenn, A.J., Amiro, B.D., Tenuta, M., Stewart, S.E., and Wagner-Riddle, C. 2010. Carbon dioxide exchange in a northern Prairie cropping system over three years. Agricultural and Forest Meteorology. **150**: 908-918.

Glenn, A.J., Tenuta, M., Amiro, B.D., Maas, S.E., and Wagner-Riddle, C. 2012. Nitrous oxide emissions from an annual crop rotation on poorly drained soil on the Canadian Prairies. Agricultural and Forest Meteorology. **166-167**: 41-49.

Government of Manitoba. 2023*a*. Manitoba Markets – November Estimates of Crop Production 2019. Government of Manitoba. https://www.gov.mb.ca/agriculture/markets-and-statistics/pubs/estimates-of-production.pdf (accessed March 29, 2023).

Government of Manitoba. 2023*b*. Manitoba Markets – Estimates of Field Crop Production 2022. Government of Manitoba. https://www.manitoba.ca/agriculture/markets-and-statistics/crop-statistics/pubs/estimates_of_field_crop_production-2022.pdf (accessed March 29, 2023).

Han, Z., Walter, M.T., and Drinkwater, L.E. 2017. N_2O emissions from grain cropping systems: a meta-analysis of the impacts of fertilizer-based and ecologically-based nutrient management strategies. Nutrient Cycling in Agroecosystems. **107**: 335-355.

Hartwig, N.L. and Ammon, H.U. 2002. Cover crops and living mulches. Weed Science. **50**: 688-699.

Hudek, C., Putinica, C., Otten, W., and De Baets, S. 2022. Functional root trait-based classification of cover crops to improve soil physical properties. European Journal of Soil Science. **73**: e13147.

Hunter, M.C., Schipanski, M.E., Burgess, M.H., LaChance, J.C., Bradley, B.A., Barbercheck, M.E., Kaye, J.P., and Mortensen, D.A. 2019. Cover crop mixture effects on maize, soybean, and wheat yield in rotation. Agricultural and Environmental Letters. **4**: 180051.

Hutchinson, G.L. and Livingston, G.P. 1993. Use of chamber systems to measure trace gas fluxes. *In*: Harper, L.A., Mosier, A.R., Duxbury, J.M., and Rolston, D.E. (Eds.). Agricultural Ecosystem Effects on Trace Gases and Global Climate Change. Agronomy Society of America, Inc. ASA Special Publication Number 55. Madison, WI. pp. 63-78.

IPCC. 2022. Summary for Policymakers. Pörtner, H.-O., Roberts, D.C., Poloczanska, E.S., Mintenbeck, K., Tignor, M., Alegría, A., Craig, M., Langsdorf, S., Löschke, S., Möller, V., and Okem, A. (eds.). *In*: Climate Change 2022: Impacts, Adaptation and Vulnerability. Contribution of Working Group II to the Sixth Assessment Report of the Intergovernmental Panel on Climate Change. Pörtner, H.-O., Roberts, D.C., Tignor, M., Poloczanska, E.S., Mintenbeck, K., Alegría, A., Craig, M., Langsdorf, S., Löschke, S., Möller, V., Okem, A., and Rama, B. (Eds.). Cambridge University Press. Cambridge, UK and New York, NY, USA. pp. 3-33, doi:10.1017/9781009325844.001.

Kabelka, D., Kincl, D., Vopravil, J., and Vráblík, P. 2021. Impact of cover crops in inter-rows of hop gardens on reducing soil loss due to water erosion. Plant, Soil and Environment. **67**: 230-235.

Kahimba, F.C., Sri Ranjan, R., Froese, J., Entz, M., and Nason, R. 2008. Cover crop effects on infiltration, soil temperature, and soil moisture distribution in the Canadian Prairies. Applied Engineering in Agriculture. **24**: 321-333.

Larsen, R.J., Beres, B.L., Blackshaw, R.E., and Graf, R.J. 2018. Extending the growing season: winter cereals in western Canada. Canadian Journal of Plant Science. **98**: 267-277.

Liebman, A.M., Grossman, J., Brown, M., Scott Wells, M., Reberg-Horton, S.C., and Shi, W. 2018. Legume cover crops and tillage impact nitrogen dynamics in organic corn production. Agronomy Journal. **110**: 1046-1057.

Liu, H., Li, Y., Pan, B., Zheng, X., Yu, J., Ding, H., and Zhang, Y. 2022. Pathways of soil N_2O uptake, consumption, and its driving factors: a review. Environmental Science and Pollution Research. **29**: 30850-30864.

Liu, J. and Lobb, D.A. 2021. An overview of crop and crop residue management impacts on crop water use and runoff in the Canadian Prairies. Water. **13**: 2929.

Maas, S.E., Glenn, A.J., Tenuta, M., and Amiro, B.D. 2013. Net CO_2 and N_2O exchange during perennial forage establishment in an annual crop rotation in the Red River Valley, Manitoba. Canadian Journal of Soil Science. **93**: 639-652.

Michalyna, W., Gardiner, W.M., and Podolsky, G. 1975. Soils of the Winnipeg Region Study Area. Canada-Manitoba Soil Survey. Prepared for: Province of Manitoba, Department of Municipal Affairs Municipal Planning Branch. https://sis.agr.gc.ca/cansis/publications/surveys/mb/mbd14/mbd14_report.pdf (accessed March 21, 2022).

Mitchell, D.C., Castellano, M.J., Sawyer, J.E., and Pantoja, J. 2013. Cover crop effects on nitrous oxide emissions: role of mineralizable carbon. Soil Science Society of America Journal. **77**: 1765-1773.

Muhammad, I., Sainju, U.M., Zhao, F., Khan, A., Ghimire, R., Fu, X., and Wang, J. 2019. Regulation of soil CO_2 and N_2O emissions by cover crops: A meta-analysis. Soil and Tillage Research. **192**: 103-112.

Reicks, G.W., Clay, D.E., Clay, S.A., Joshi, D.R., Moriles-Miller, J., Westhoff, S., Daigh, A.L.M., and Bruggeman, S.A. 2021. Winter cereal rye cover crop decreased nitrous oxide emissions during early spring. Agronomy Journal. **113**: 3900-3909.

Sistani, K.R., Jn-Baptiste, M., Lovanh, N., and Cook, K.L. 2011. Atmospheric emissions of nitrous oxide, methane, and carbon dioxide from different nitrogen fertilizers. Journal of Environmental Quality. **40**: 1797-1805.

Smith, K.A., Ball, T., Conen, F., Dobbie, K.E., Massheder, J., and Rey, A. 2018. Exchange of greenhouse gases between soil and atmosphere: interactions of soil physical factors and biological processes. European Journal of Soil Science. **69**: 10-20.

Snyder, C.S., Bruulsema, T.W., Jensen, T.L., and Fixen, P.E. 2009. Review of greenhouse gas emissions from crop production systems and fertilizer management effects. Agriculture, Ecosystems and Environment. **133**: 247-266.

Tenuta, M., Amiro, B.D., Gao, X., Wagner-Riddle, C., and Gervais, M. 2019. Agricultural management practices and environmental drivers of nitrous oxide emissions over a decade for an annual and an annual-perennial crop rotation. Agricultural and Forest Meteorology. **276-277**: 107636.

Tenuta, M., Gao, X., Flaten, D.N., and Amiro, B.D. 2016. Lower nitrous oxide emissions from anhydrous ammonia application prior to soil freezing in late fall than spring pre-plant application. Journal of Environmental Quality. **45**: 1133-1143.

Thomas, B.W., Hao, X., Larney, F.J., Goyer, C., Chantigny, M.H., and Charles, A. 2017. Non-legume cover crops can increase non-growing season nitrous oxide emissions. Soil Science Society of America Journal. **81**: 189-199.

Wagner-Riddle, C., Congreves, K.A., Abalos, D., Berg, A.A., Brown, S.E., Ambadon, J.T., Goa, X., and Tenuta, M. 2017. Globally important nitrous oxide emissions from croplands induced by freeze-thaw cycles. Nature Geoscience. **10**: 279-283.

Wagner-Riddle, C., Furon, A., McLaughlin, N.L., Lee, I., Barbeau, J., Jayasundara, S., Parkin, G., von Bertoldi, P., and Warland, J. 2007. Intensive measurement of nitrous oxide emissions from a corn-soybean-wheat rotation under two contrasting management systems over 5 years. Global Change Biology. **13**: 1722-1736.

Wagner-Riddle, C., Thurtell, G.W., Kidd, G.K., Beauchamp, E.G., and Sweetman, R. 1997. Estimates of nitrous oxide emissions from agricultural fields over 18 months. Canadian Journal of Soil Science. **77**: 135-144.

Zhang, X., Davidson, E.A., Mauzerall, D.L., Searchinger, T.D., Dumas, P., and Shen, Y. 2015. Managing nitrogen for sustainable development. Nature. **528**: 51-59.

4. OVERALL SYNTHESIS

4.1 Study Findings and Implications

Research into the short-term and cumulative seasonal effects of a no-till fall rye (*Secale cereale* L.) cover crop on trace gas fluxes has been limited in the Canadian Prairies. Adding to the growing body of micrometeorological flux data collected at the Trace Gas Manitoba (TGAS-MAN) long-term research site, this thesis looked at the effect of a no-till fall rye cover crop cropping system on seasonal carbon dioxide (CO_2) and nitrous oxide (N_2O) fluxes compared to soils managed with conventional tillage practices in the Red River Valley region of Manitoba, Canada. Continuous monitoring of trace gases during each study period provided insight into the changes in emission trends at different stages during cover crop growth and following its termination. Changes in trace gas fluxes from environmental drivers and following agronomic activities were also observed.

Net ecosystem production (*NEP*) varied between the two cropping systems and the two study years and was mainly driven by environmental conditions during the growing season (Chapter 2). In both study years, the cover crop affected spring *NEP* by assimilating carbon (C) during spring before seeding, while the conventional system was a C source since it was left fallow. The cover crop increased respiration (*R*) following its termination compared to the conventional fields. However, the source of the increase in respiration differed between the two study years, with the increase in 2019 resulting from increased heterotrophic *R* and the increase in 2022 resulting from increased autotrophic *R* when $GPP < 40$ and heterotrophic *R* when $GPP > 40$. The cumulative effects of the cover crop by harvest varied between the two study years. In 2019, both the conventional and the cover crop systems were a cumulative C sink from January to harvest. However, only the cover crop system was a C sink after harvest removals were accounted for. In

2022, both cropping systems were a cumulative C source by harvest and were approximately the same, which resulted from prolonged saturated soil conditions in spring and during the growing season. After harvest removals were accounted for, the cover crop system was a larger C source than the conventional system due to higher yields from the cover crop fields in that year.

Nitrous oxide emission episodes occurred in spring during soil thawing and following fertilizer application, accounting for most N_2O emissions during the study (Chapter 3). The cover crop effectively reduced spring-thaw N_2O emissions when the establishment was good by reducing soil nitrate concentrations and leaving less nitrate available for denitrification during soil thaw in spring. The cover crop no-till system also saw lower primary peak N_2O emissions and cumulative N_2O emissions than the conventional system following fertilizer application in all study years. This resulted in an average of 25% lower cumulative N_2O emissions from the cover crop system than the conventional system across all study years. Determining cash crop grain yields at the end of the growing season found that the cover crop did not significantly affect yields, which concerns producers interested in adopting the practice. Monitoring CO_2 and N_2O simultaneously allowed for quantifying cumulative greenhouse gas (GHG) fluxes in 2019 and 2022. Both systems were GHG sources after converting N_2O emissions to CO_2-equivalents (CO_2-eq). However, most of the GHGs emitted by each cropping system occurred in 2022 due to high N_2O emissions and net C loss by harvest. The cover crop did reduce cumulative GHG emissions from 2019 and 2022 by over 2000 kg CO_2-eq ha^{-1} compared to the conventional system.

Data obtained during this thesis will help further the understanding of cover cropping on trace gas fluxes in the Canadian Prairies. Data from both studies determined that there is enough time for fall rye cover crops to establish in fall and affect CO_2 and N_2O fluxes the following year. Data obtained from monitoring CO_2 fluxes provided insight into the differences in C dynamics between the two cropping systems and how C balances can be altered to increase C sequestration using cover crops on the Canadian Prairies. In particular, C assimilation during cover crop growth and changes in respiration following cover crop termination could be helpful to GHG models in predicting the C balance of cropping systems that utilize cover crops under different weather conditions. Data obtained from monitoring N_2O fluxes help understand cover crop impacts on N_2O emissions in northern latitude soils, which experience emission events during spring-thaw and following fertilizer application. Similar to what has been found in numerous other N_2O studies, N_2O emissions following fertilizer application were overall the largest contributor of N_2O emissions in our study, highlighting the importance of managing N_2O emissions from synthetic nitrogen fertilizer application in crop production.

This study's GHG emissions analysis should be considered incomplete as trace gas data only covered part of each year and did not cover annual CO_2 and N_2O fluxes. To fully understand the effect of fall rye cover crops on trace gas fluxes, multiple years of continuous measurements of trace gases need to be performed to determine the annual and multiyear effects of fall rye cover crops on GHG emissions. Further, this study did not include emissions from field activities, manufacturing of fertilizers and transportation, underestimating GHG budgeting and life cycle analysis of each cropping system.

4.2 Study Recommendations, Improvements, and Future Work

Although the data collected for this thesis provides valuable information on the effect of no-till fall rye cover crops on CO_2 and N_2O fluxes in spring and during the growing season, a better understanding of the effect of cover crops on trace gas fluxes would have been determined with continuous annual monitoring of fluxes. Keeping the treatments on the same fields instead of alternating them every few years could have allowed for multiyear changes in CO_2 and N_2O fluxes to be determined and keeping the nitrogen fertilizer type consistent throughout the study could have provided better insights into cover crop impacts on N_2O emission behaviour following fertilizer application, as ESN which was used in 2019 altered emission behaviour compared to the other fertilizer types used during the study.

Additional improvements could have been made with supporting environmental data to understand better the effect of the cover crop no-till system on water dynamics and changes in soil structure. Continuous measuring of volumetric moisture content from each field could have provided a better understanding of the cover crop effects on soil moisture in spring and during the growing season. Snow depth measurements in each field would have helped to determine the effect of the intact crop residue and cover crop on snow trapping and water conservation into spring. Measuring water infiltration rates during the growing season and assessing changes in soil structure between the two systems could have helped to determine the effect of the cover crop no-till system on soil structure and N_2O emissions.

Directly pertinent to the studies conducted for this thesis is the effect of discontinuing cover cropping and no-till with tillage on CO_2 and N_2O fluxes, as the incorporation of cover crop and crop residues may increase trace gas fluxes which have been seen with the termination of perennial forage crops (Amiro et al., 2017; Basche et al., 2014; Tenuta et al., 2019). There is little understanding of what changes to CO_2 and N_2O fluxes would occur with the cessation of no-till cover cropping, which warrants investigation.

Future work at the site started during the 2022 growing season, with the subsequent study at the site aiming to assess the effect of an enhanced efficiency fertilizer on N_2O fluxes compared to urea nitrogen fertilizer which is commonly used in crop production. Synthetic nitrogen fertilizer use is a significant source of N_2O emissions and enhanced efficiency fertilizers have been suggested as a way to decrease N_2O emissions from fertilizer application (Snyder et al., 2009). However, N_2O is often the only GHG monitored in fertilizer studies and emissions are often determined using chamber techniques, which could result in N_2O fluxes being underestimated if emissions are missed. Further, the effect of enhanced efficiency fertilizers on CO_2 fluxes in different cropping systems is limited, and changes in CO_2 fluxes from enhanced efficiency fertilizers will be important in determining net GHG emissions from cropping systems with enhanced efficiency fertilizers (Watts et al., 2015).

Future work relating to cover crops and GHG fluxes could look at the effects of inter-seeding annual cover crops into cash crop stands and fall and winter species cover crops following harvest to increase C assimilation in both fall and spring. Also of value would be to investigate the effects of livestock integration in cropping systems on CO_2 and N_2O fluxes as livestock integration has been suggested as a way to increase soil organic carbon accumulation (Brewer and Gaudin, 2020) and Manitoba is a large producer of livestock in Canada (Government of Manitoba, 2023).

The benefit of long-term flux monitoring at the TGAS-MAN site is that the effect of numerous management strategies often utilized in the Canadian Prairies on CO_2 and N_2O fluxes have been able to be assessed and their effect in the short-term and the long-term has been able to be determined. Information gathered for this thesis will help to quantify better GHG emissions from agricultural soils under different agronomic practices in Manitoba and help better determine national GHG budgets from agricultural production in Canada.

4.3 References

Amiro, B.D., Tenuta, M., Gervais, M., Glenn, A.J., and Gao, X. 2017. A decade of carbon flux measurements with annual and perennial crop rotations on the Canadian Prairies. Agricultural and Forest Meteorology. **247**: 491-502.

Basche, A.D., Miguez, F.E., Kaspar, T.C., and Castellano, M.J. 2014. Do cover crops increase or decrease nitrous oxide emissions? A meta-analysis. Journal of Soils and Water Conservation. **69**: 471-482.

Brewer, K.M. and Gaudin, A.C.M. 2020. Potential of crop-livestock integration to enhance carbon sequestration and agroecosystem functioning in semi-arid croplands. Soil Biology and Biochemistry.**149**: 107936.

Government of Manitoba. 2023. Manitoba markets – Livestock on farms in Manitoba and Canada. https://www.gov.mb.ca/agriculture/markets-and-statistics/livestock-statistics/pubs/livestock-on-farms-in-manitoba-and-canada-on-farms-january-2023.pdf (Accessed April 15, 2023).

Snyder, C.S., Bruulsema, T.W., Jensen, T.L., and Fixen, P.E. 2009. Review of greenhouse gas emissions from crop production systems and fertilizer management effects. Agriculture, Ecosystems and Environment. **133**: 247-266.

Tenuta, M., Amiro, B.D., Gao, X., Wagner-Riddle, C., and Gervais, M. 2019. Agricultural management practices and environmental drivers of nitrous oxide emissions over a decade for an annual and an annual-perennial crop rotation. Agricultural and Forest Meteorology. **276-277**: 107636.

Watts, D.B., Runion, G.B., Nannenga, K.W.S., and Torbert, H.A. 2015. Impacts of enhanced-efficiency nitrogen fertilizers on greenhouse gas emissions in a coastal plain soil under cotton. Journal of Environmental Quality. **44**: 1699-1710.

5. APPENDIX A

5.1 Appendix Tables

Table 5.1 Detailed agronomic information over the study period.

Date	Event	Location	Detail
29-Aug-18	seeding - cover crop	fields 2 and 3	Fall rye seeded at 63 kg ha^{-1} with Case IH SDx30 seeder
30-Aug-18	cultivation	fields 1 and 4	Cultivated with JD 1610 deep tiller to 13 cm depth
13-May-19	seeding	all fields	Summit Oats seeded at 108 kg ha^{-1}
13-May-19	fertilizing	all fields	Fertilizer blend (N-P-K-S) of 78 kg ha^{-1} ESN®, 17 kg ha^{-1} P, 6 kg ha^{-1} K, and 17 kg ha^{-1} S
14-May-19	spraying - herbicide	all fields	Roundup Transorb (a.i. glyphosate) at 1.65 L ha^{-1}
20-May-19	spraying - herbicide	fields 2 and 3	Roundup Transorb (a.i. glyphosate) at 1.65 L ha^{-1}, extra application to terminate remaining cover crop
05-Jun-19	spraying - herbicide	all fields	Outshine (a.i. florasulam/fluroxypyr + MCPA ester) [a]
01-Jul-19	spraying - fungicide	all fields	Twinline (a.i. pyraclostrobin and metconazole) [a]
19-Aug-19	spraying - desiccant	all fields	Roundup Transorb (a.i. glyphosate) at 1.65 L ha^{-1}
09-Sep-19	harvest	all fields	
16-Sep-19	cultivation	fields 2 and 3	Cultivated with JD 1610 deep tiller to 13 cm depth
17-Sep-19	seeding - cover crop	fields 1 and 4	Fall rye seeded at 63 kg ha^{-1} with Case IH SDx30 seeder
21-May-20	seeding	all fields	Invigor L233P at 4.7 kg ha^{-1} banded with starter fertilizer (N-P-K-S) of 22 kg ha^{-1} ESN®, 22 kg ha^{-1} P, 0 kg ha^{-1} K, and 11 kg ha^{-1} S
21-May-20	fertilizing	fields 1 and 4	145.5 kg ha^{-1} UAN 28% applied with Case IH 3230 patriot sprayer with 100' boom with tri nozzle streamer
21-May-20	fertilizing	fields 2 and 3	168 kg ha^{-1} UAN 28% applied with Case IH 3230 patriot sprayer with 100' boom with tri nozzle streamer
05-Jun-20	spraying - herbicide	fields 1 and 4	Roundup Transorb (a.i. glyphosate) at 1.65 L ha^{-1}, terminating cover crop
16-Jun-20	spraying - herbicide	all fields	Liberty (a.i. glufosinate) at 3.34 L ha^{-1} with Centurion (clethodim) at 124 ml ha^{-1}
15-Jul-20	spraying - fungicide	all fields	Cotegra (a.i. boscalid and prothioconazole) at 0.605 ml ha^{-1}
27-Aug-20	spraying - desiccant	all fields	Roundup Transorb (a.i. glyphosate) at 1.65 L ha^{-1}
08-Sep-20	harvest	all fields	
09-Sep-20	seeding - cover crop	fields 1 and 4	Fall rye seeded at 63 kg ha^{-1} with Case IH SDx30 seeder
09-Sep-20	cultivation	fields 2 and 3	Cultivated with Summers chisel plow to 13 cm depth
11-May-21	fertilizing	all fields	111 kg ha^{-1} urea
11-May-21	seeding	all fields	Starbuck wheat seeded at 148 kg ha^{-1} banded with starter fertilizer (N-P-K-S) of 22 kg ha^{-1} N, 22 kg ha^{-1} P, 0 kg ha^{-1} K, and 11 kg ha^{-1} S
14-May-21	spraying - herbicide	fields 1 and 4	Roundup Transorb (a.i. glyphosate) at 1.65 L $ha^{-1,}$ terminating cover crop
15-Jun-21	spraying - herbicide	all fields	Buctril M (a.i. bromoxynil/MCPA ester) and Axial (a.i. pinoxaden) [a]
16-Aug-21	harvest	all fields	
30-Aug-21	seeding - cover crop	fields 2 and 3	Fall rye seeded at 63 kg ha^{-1} with Case IH SDx30 seeder
01-Sep-21	cultivation	fields 1 and 4	Cultivated with Summers chisel plow to 13 cm depth
05-Oct-21	cultivation	fields 1 and 4	Cultivated with Summers chisel plow to 13 cm depth
09-Nov-21	cultivation	fields 1 and 4	Cultivating volunteer wheat underneath lines to towers with disc cultivator
10-Jun-22	spraying - herbicide	fields 2 and 3	Roundup Transorb (a.i. glyphosate) at 1.65 L ha^{-1}, terminating cover crop
20-Jun-22	fertilizing	fields 1 and 2	56 kg ha^{-1} eNtrench™ coated urea (118 kg ha^{-1} intended but flowability issues caused half rate)
20-Jun-22	fertilizing	fields 3 and 4	118 kg ha^{-1} urea
20-Jun-22	seeding	all fields	Viewfield wheat at 135 kg ha^{-1} banded with starter fertilizer (N-P-K-S) of 22 kg ha^{-1} N, 22 kg ha^{-1} P, 0 kg ha^{-1} K, and 11 kg ha^{-1} S
22-Jun-22	fertilizing	fields 1 and 2	56 kg ha^{-1} UAN (28%) treated with Centuro® applied with Case IH 3230 patriot sprayer 100' boom with tri-tip streamers
13-Jul-22	spraying - herbicide	all fields	Velocity (t a.i. hiencarbazone, bromoxynil and pyrasulfotole) at 988 ml ha^{-1}
05-Oct-22	harvest	all fields	

[a] applied according to product label

Table 5.2 Nitrous oxide fluxes for each field and cropping system from the four study years: Spring-thaw ($\sum F_{N\text{-}SPRING\text{-}THAW}$), post-fertilizer ($\sum F_{N\text{-}FERTILIZER}$), and cumulative gap-filled net N_2O flux ($\sum F_N$) for each year of the study (January 1 to August 15).

Year		Field 1	Field 2	Field 3	Field 4	Mean F_N Conventional	Mean F_N Cover Crop
2019	$\sum F_{N\text{-}SPRING\text{-}THAW}$, kg N ha^{-1}	-	-	0.56	2.44	2.44	0.56
	$\sum F_{N\text{-}FERTILIZER}$, kg N ha^{-1}	-	-	1.52	2.02	2.02	1.52
	$\sum F_N$, kg N ha^{-1}	-	-	2.08	4.46	4.46	2.08
2020	$\sum F_{N\text{-}SPRING\text{-}THAW}$, kg N ha^{-1}	-	0.70	-	0.56	0.70	0.56
	$\sum F_{N\text{-}FERTILIZER}$, kg N ha^{-1}	-	2.50	-	1.34	2.50	1.34
	$\sum F_N$, kg N ha^{-1}	-	3.20	-	1.90	3.20	1.90
2021	$\sum F_{N\text{-}SPRING\text{-}THAW}$, kg N ha^{-1}	-	0.85	-	0.98	0.85	0.98
	$\sum F_{N\text{-}FERTILIZER}$, kg N ha^{-1}	-	6.38	-	4.70	6.38	4.70
	$\sum F_N$, kg N ha^{-1}	-	7.23	-	5.68	7.23	5.68
2022	$\sum F_{N\text{-}SPRING\text{-}THAW}$, kg N ha^{-1}	0.58	0.40	0.47	1.16	0.87	0.44
	$\sum F_{N\text{-}FERTILIZER}$, kg N ha^{-1}	-	-	13.34	15.03	15.03	13.34
	$\sum F_N$, kg N ha^{-1}	-	-	13.82	16.19	16.19	13.82

6. APPENDIX B

Draft Appendix: Corrections for bias in gradients caused by mis-matched lines in 2020 and 2021 at TGAS-MAN

Brian Amiro

December 22, 2021

Background:

We have observed a bias in the N2O gradient: during periods of expectation of a zero gradient, we observe either positive or negative gradients, depending on the Site. This bias increases with ambient temperature. Our working hypothesis is that the different types of tubing used in the paired sets have expanded differentially to temperature, altering flows and pressure, creating a false difference between intakes. Note that the difference in sample flow between upper and lower lines is also correlated with temperature, but has more scatter. Ambient air temperature appears to be the best predictor of the bias. However, ambient radiation and wind speed both affect heat transfer, and filtering for these does reduce the scatter. We also note that the CO2 gradient also has a bias, but it is more difficult to model because we almost always have some CO2 flux, which makes it hard to identify the bias.

Paired Line Installations:

The new paired-line installation occurred in fall of 2019, following many years of a single-line system. Reliable data with the new system began in 2020. The mis-match in the paired lines was corrected on October 29, 2021. Hence, we need to develop reliable bias corrections for 2020 and for 2021 from January 1 to October 28.

All four sites had pairs of line that were not of the identical type. The lines were of the same internal dimension (nominally) and of close to the same length. The difference was in the material construction. The line types were:

HP= Eaton Synflex HP type, 1/4" O.D. X.040 Wall. 1015314. Tube material is nylon. (https://www.autolow.com/9ft-eaton-synflex-hp-1-4-od-general-use-nylon-tubing-air-hydraulic-pneumatic-sd00018036)

1300 = Synflex Type "1300" - 1/4" O.D. Saint Gobain - 0405170 (this is the line type with the metal core). Tube material is aluminum (https://www.eaton.com/tw/en-us/skuPage.1300-06603.specifications.html).

1219FR = Eaton Synflex "1219 FR" (94V-2) - 1/4" O.D. X.040 Wall - Plenum Tubing, Classified for flame and smoke only - NFPA 90A - 1989 - 1010813. Tube material is polyethylene. (https://www.eaton.com/tw/en-us/skuPage.1219-44005.specifications.html).

The line types for each site are listed in the Tables below.

Site 1 Dates	**Upper line**	**Lower line**	**Reversed in code**
2020 Jan 1-May 20	1219FR	HP	no
2020 May 21- Sept 8 (0900)	HP	1219FR	yes
2020 Sept 8 (0900)- 2021 Oct 29	1219FR	HP	no

Site 2 Dates	**Upper line**	**Lower line**	**Reversed in code**
2020 Jan 1-May 21	?	?	yes*
2020 May 21-Sep 9	1219FR	HP	yes*
2020 Sept 9-Dec 31	HP	1219FR	yes*
2021 Jan 1 - May 17 (0600)	HP	1219FR	no
2021 May 17(0600)- June 16 (1500)	1219FR	HP	yes
2021 June 16 (1500)- 2021 Oct 29	HP	1219FR	no

Site 3 Dates	**Upper line**	**Lower line**	**Reversed in code**
2020 Jan 1-May 20	HP	1300	no
2020 May 21- Sept 8 (0900)	1300	HP	yes
2020 Sept 8 (0900)- 2021 Oct 29	HP	1300	no

Site 4 Dates	**Upper line**	**Lower line**	**Reversed in code**
2020 Jan 1-May 21	1219FR	HP	yes
2020 May 21- Sept 9	HP	1219FR	no
2020 Sept 9 - 2021 May 17	1219FR	HP	yes
2021 May 17 - Oct 29	HP	1219FR	no

A direction check of the intakes on April 23, 2021 confirmed the directions: Site 4 was reversed, and the lines were switched on May 17, 2021 to make it correct.

The Site 2 directions in 2020 were likely incorrect (marked in the above Table with *). It seems likely that there was a reversal of lines at seeding; so, the reversal in the code should not have been done for the period 2020 Jan 1-May 21. The N_2O gradient between seeding and harvest in 2020 appears to be correct (showing the fertilizer emission) for Site 2 when the code reversal is used. Also, there was no opportunity for the intakes to be switched between Sept harvest 2020 and April 23, 2021 when the directions were checked; hence, we assume that the code should not have reversed the gradient for the Sept 9 to Dec 31, 2020 period. Overall summary for Site 2 in 2020: for 2020 Jan 1-May 21 ignore the data because of too much uncertainty; for 2020 May 21-Sep 9 use the data with the code reversal; for 2020 Sept 9-Dec 31 use the data but flip the gradients back to be consistent with the 2021 Jan-2021 Jan 1 - May 17 period.

It is important to note that the temperature bias stays with the line pairs. This means that flipping the gradient in post-processing will result in the reverse response to temperature. Hence, all sites require some additional care to establish the relationships because we did not have a consistent configuration throughout the period. After August 8, 2021, the system was subjected to multiple tests, so data after August 8, 2021 were not used for the regressions.

Conceptual Method

To develop our regressions, we only include data when ustar> 0.15 m/s, which is the nominal ustar threshold that we use for the TGAS-Man site. Note that lower windspeeds would likely increase the variability in the regression data because we would have less heat transfer between the lines and the air. Although we expect line heating to be a function of air temperature, solar radiation and convection (wind), we do not get improved regressions when we include either PPFD or ustar as additional predictors for the bias. It seems that air temperature alone works best, likely because of the large variability in line placements with respect to both radiation and wind exposure over the year. We can get improved regressions if we only look at windy nights (i.e., we remove the radiation and convective factors), but we need to have a model to correct the bias in all data.

We have also tried filtering, lagging and weighting the temperature and gradient data with the assumption that the actual line temperature has some memory based on the recent temperature. There really is no improvement with moving averages and running means (in history) for periods out to several hours.

We calculate the relationships for time periods when there are no N2O emissions. This means excluding the following periods:

2020 June 7 to 10 inclusive; and July 1 to 2 inclusive. These are fertilizer emissions (note that we cannot discern a large thaw emission in 2020).

2021 March 1 to 25, inclusive (thaw emissions) and May 15 to June 20, inclusive (fertilizer emissions).

Note that the meteorological station at TGAS was not operating for an extended period in spring 2020. We have replaced the air temperature data with the mean of the sonic anemometer temperatures for this period.

Setting the line pairs to be consistent as 1219FR/HP for Upper/Lower for Sites 1, 2 and 4; and HP/1300 for Upper/Lower for Site 3, we see a consistent pattern between apparent N_2O gradient and air temperature (Figure 1). Both Sites 2 and 4 show some positive outliers in 2020; we have left these in the analyses, but they will need some filtering when the final dataset is developed. Note that the gradients are defined as the upper-intake concentration minus the lower-intake concentration.

Figure 1. N2O gradient (upper-lower) increases with air temperature for both 2020 and 2021. The line pairs are 1219FR/HP for Upper/Lower for Sites 1, 2 and 4; and HP/1300 for Upper/Lower for Site 3.

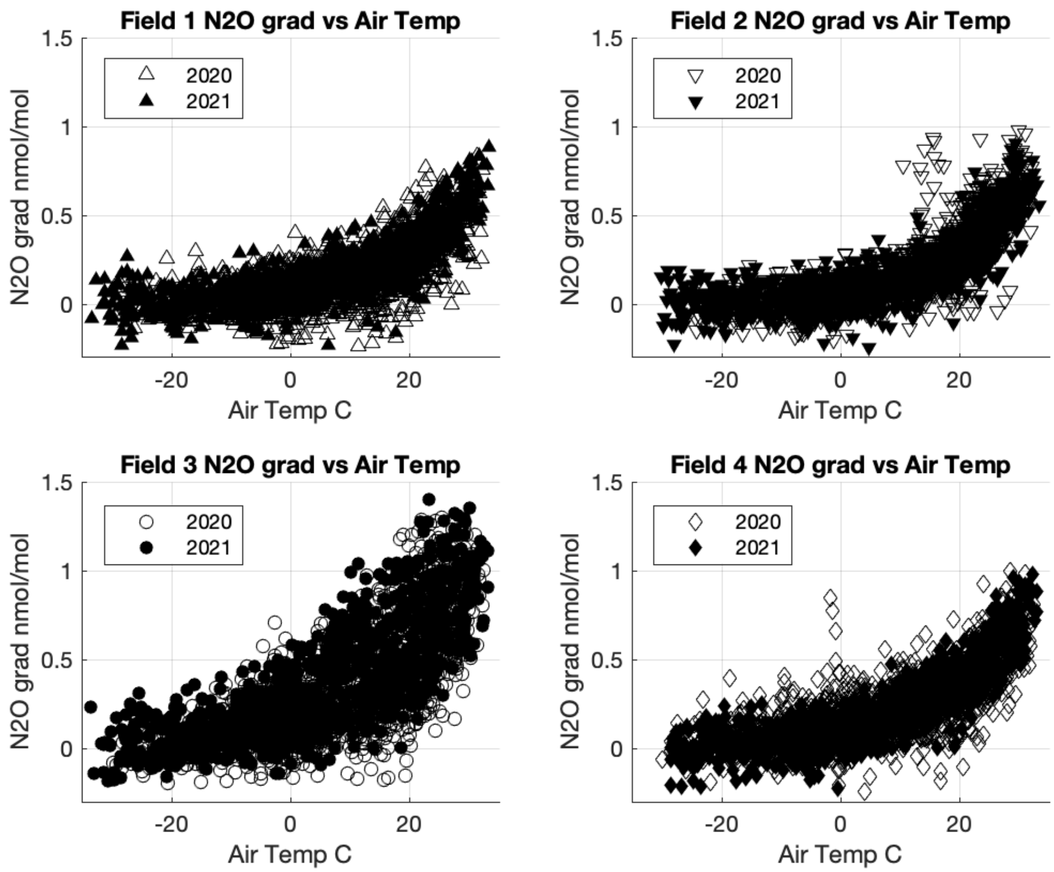

There is sufficient scatter to make it difficult to see if there are differences among sites and years. If we average the data into bins of 150 points, the pattern is much clearer (Figure 2). We also see that 2020 and 2021 data are similar (note that 2021 only had data until August so it is missing the fall and winter period, which affects the range of points available for the bins). We have two combinations of line pairings. In principle, this should mean that only two regression relationships are required; this would be a reasonable outcome for the goal of developing general relationships. However, we find some subtle differences among sites, possibly caused by slight differences in line lengths or the number of repairs. Our goal is to develop the best correction for each site, so we will approach the bias correction by site, but combine both 2020 and 2021 for each site.

Figure 2. N2O gradient (upper-lower) with air temperature as mean data binned in groups of 150 points.

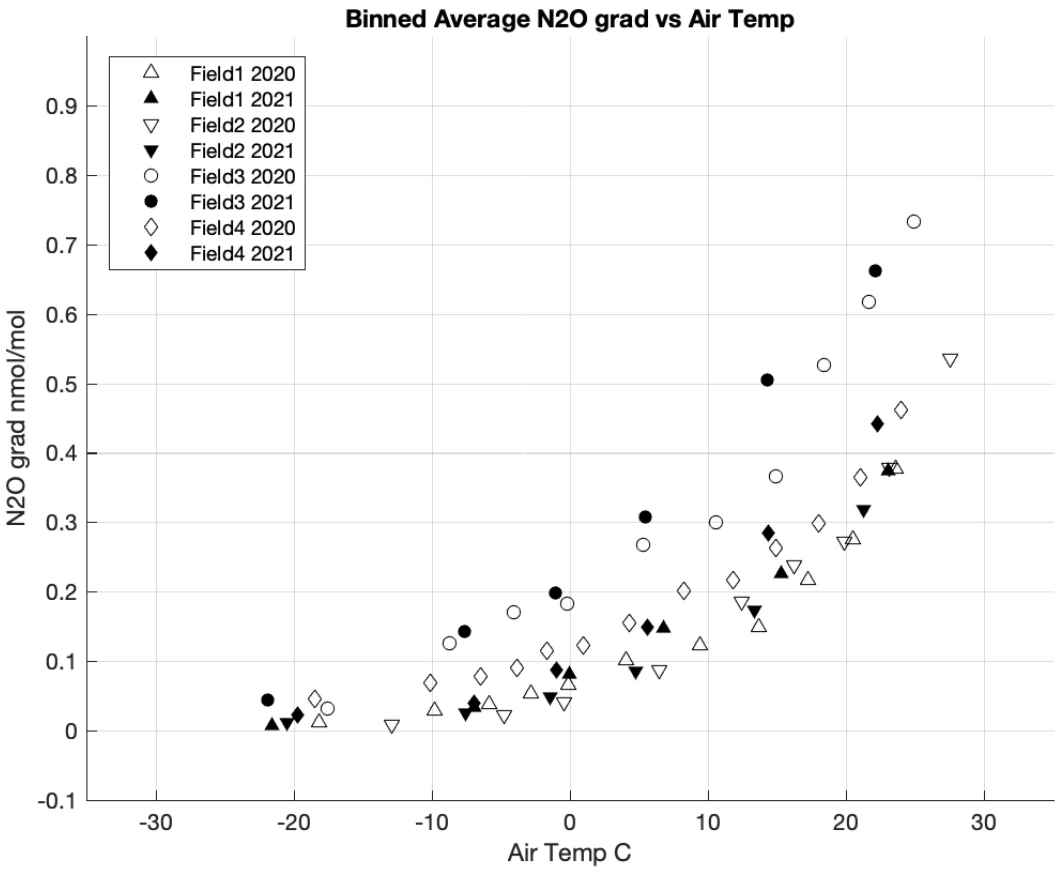

Regression Development

The patterns in Figures 1 and 2 suggest an exponential relationship; i.e., the N2O gradient increases exponentially (or perhaps with a power) with temperature. Such a relationship will have an asymptote, which appears to approach a zero N2O gradient at cold temperatures. Hence, we will develop relationships of the general form:

N2O gradient + offset = exp(air temperature),

where we need to include an offset to only work with positive N2O gradients when we log-transform the N2O gradient when developing the regression.

The regressions were developed using Matlab. Although we tested regressions using the full dataset for each site, these regressions tend to under-estimate the response at higher temperatures because of a smaller number of data points. Hence, we calculated bin-averages of the data based on bins of a width of 5C, and regressed the natural logarithm of the (N2O gradient + offset) against the air temperature for these bins. We found that the curves tend to be sensitive to the magnitude of the offset and fit the data best when the offset was relatively small but still resulted in a positive net N2O gradient for the regression.

Regression Results:

The regression results are shown in Figure 3 including both the bin-averaged points and the raw data. We see good fits, with r-square values for the regression of the bin-averages for Sites 1, 2, 3, and 4 being 0.91, 0.99, 0.99, and 0.98, respectively. Plots of the residuals defined as the mean difference of standard deviation using the range of the raw N2O gradient data for each temperature bin are shown in Figure 4. Here, we see that overall mean bias is small with generally no pattern with temperature. However, we do see that the variability (standard deviation) is larger at higher temperatures, so that our uncertainty increases with temperature. This variability is greatest for Site 3.

Figure 3. Regressions of the N2O gradient with air temperature showing both the bin-averaged points and the raw data for each site with data for both 2020 and 2021.

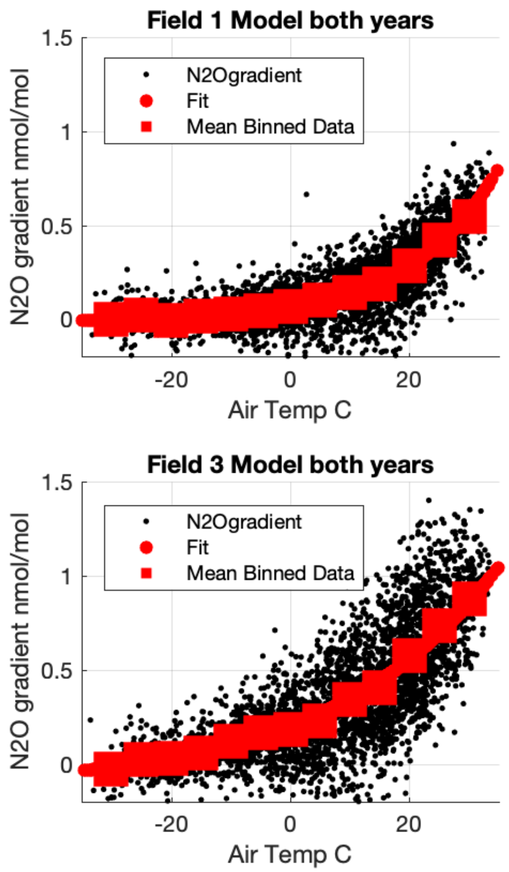

Figure 4. Residuals of the mean data per temperature bin minus the regression curve fit. Both the mean difference and Standard deviation of the difference are shown.

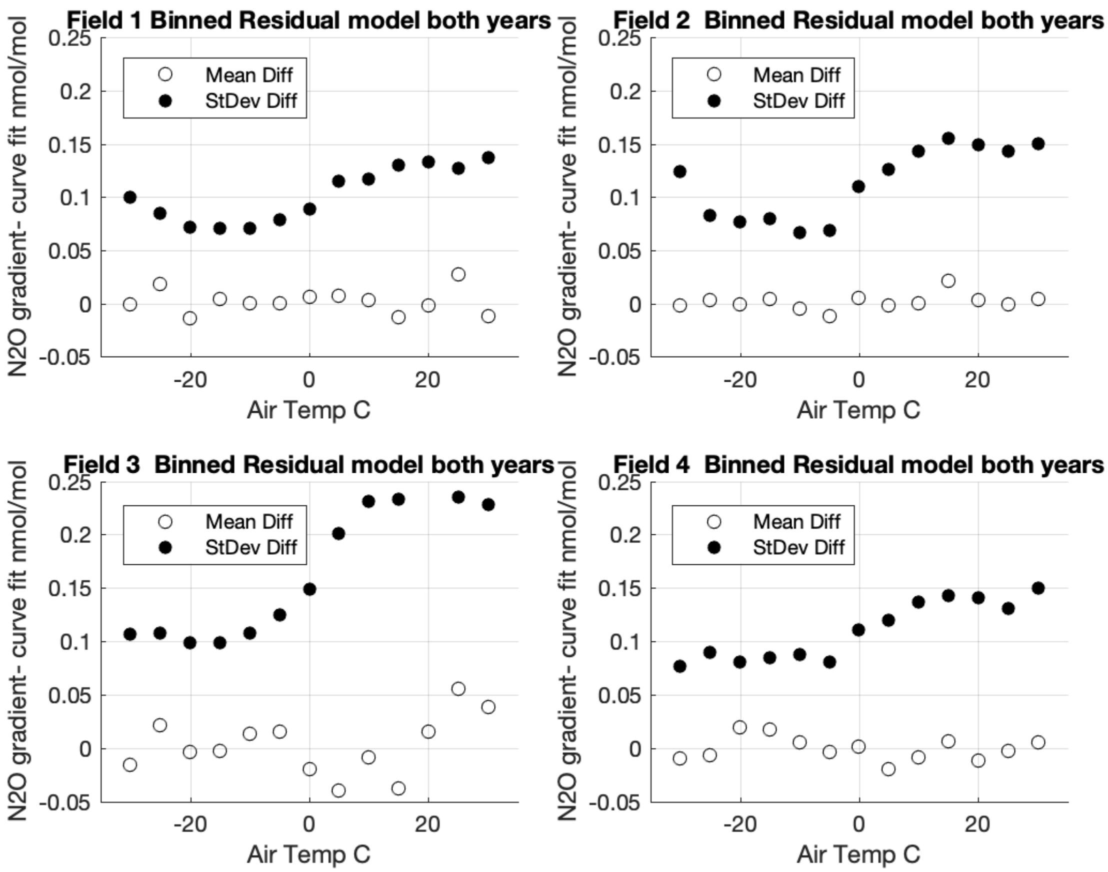

A comparison of the regression curves among sites shows that Sites 1 and 2 have almost identical responses with temperature, and Site 4 has a slight departure between about 0 and 25C (Figure 5). This close agreement among these three sites is consistent with the identical line pairs that were used. Site 3 is clearly different; it also tends to maintain a gradient different at sub-freezing temperatures whereas the other sites plateau at about -5C.

Figure 5. Comparison of the regression line fits for the four sites. Data from both 2020 and 20201 were used in the curve fit.

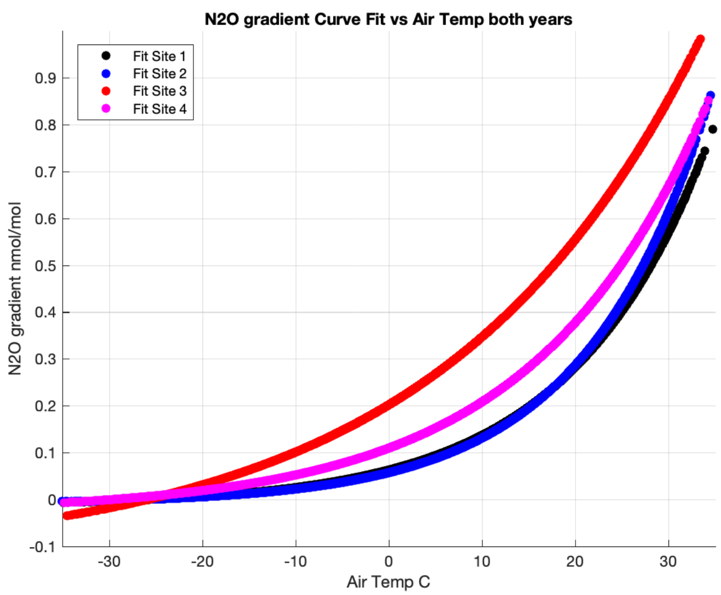

Implications of the Corrections for Concentration Gradients and Fluxes:

N2O:
The bias corrections were developed using periods when N2O fluxes were expected to be near zero. There is some risk that small upward or downward fluxes were included in the regressions, and that these will be cancelled out by the corrections. This is not likely to be a large issue, because the regressions are based on a large dataset, and we would expect periods of small transient fluxes (in either direction) to be preserved, assuming that the overall mean flux for the regression period was zero. N2O emission events tend to be large, and the bias corrections will have minimal effect on these.

To investigate the impact of the bias correction on the N2O fluxes, it is often easier to investigate cumulative fluxes through the year. We do this using the corrected N2O gradients and the K values calculated in our standard way. For this illustration, we have not done additional quality controls that are usually employed in our standard outputs; we have not filled gaps; and have calculated the cumulative N2O flux based on the daily average flux (Figures 6 and 7). Hence, our comparison of cumulative N2O fluxes are for illustration only, and the final dataset will differ when gaps are filled and data quality is checked. Two post-fertilizer emission events occurred in 2020 but a thaw event is not evident. In 2021, both a thaw event and post-fertilizer event occurred.

Figure 6. Cumulative N2O fluxes 2020. Data prior to May 22 for Site 2 have been ignored because of quality-control issues.

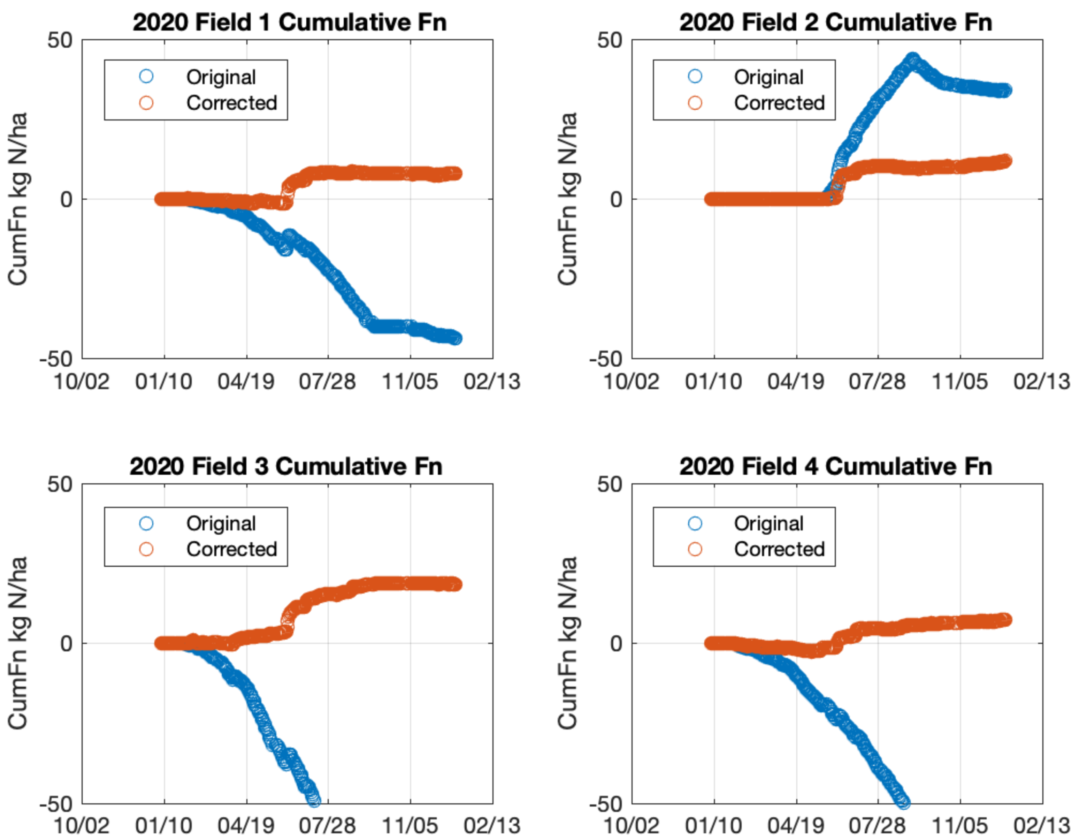

Figure 7. Cumulative N2O fluxes 2021. The January and February 2021 period had problems with sample flow irregularities, and data have been omitted prior to March 1.

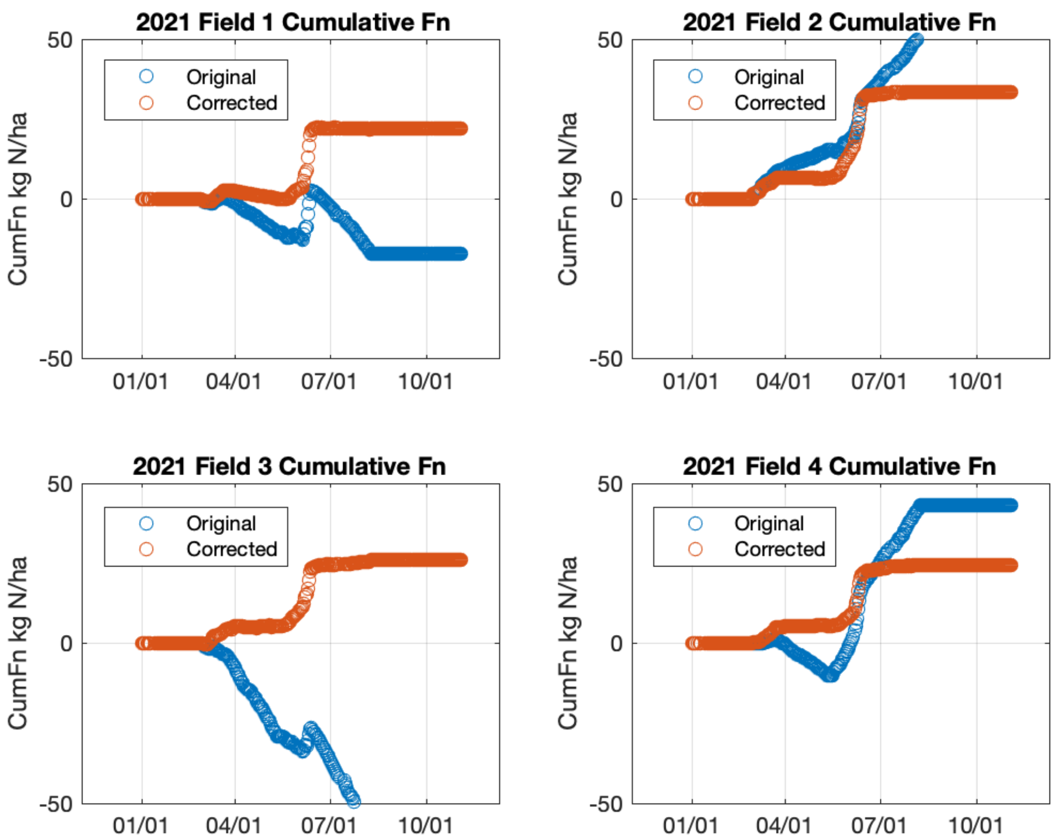

CO2:

We assume that the bias caused by the temperature response of the differential lines will affect the CO2 concentrations in the same way as for N2O. Hence, we scale the bias correction regressions by the ratio of the measured concentrations of CO2 to N2O at the top intakes for each 30-minute period. Figures 8 and 9 show the expected response of respiration in the spring and fall and net uptake during the summer. The unusual behaviour at Site 2 in 2020 is caused by the exclusion of all data pre-seeding; and all 2021 data were omitted after August 8, 2021 because of system checks (hence no period of fall respiration). Note that the CO2 daily average flux data will be biased during the summer because we have excluded data when ustar<0.15 m/s, which tends to exclude more night (respiration) data. The NEE gap-filling model will result in different magnitudes of these cumulative fluxes for the final dataset.

Figure 8. Cumulative CO2 fluxes 2020. Data prior to May 22 for Site 2 have been ignored because of quality-control issues (flat line). The unusual directional change for the original data for Field 2 happened when the line orientation was switched at seeding and harvest.

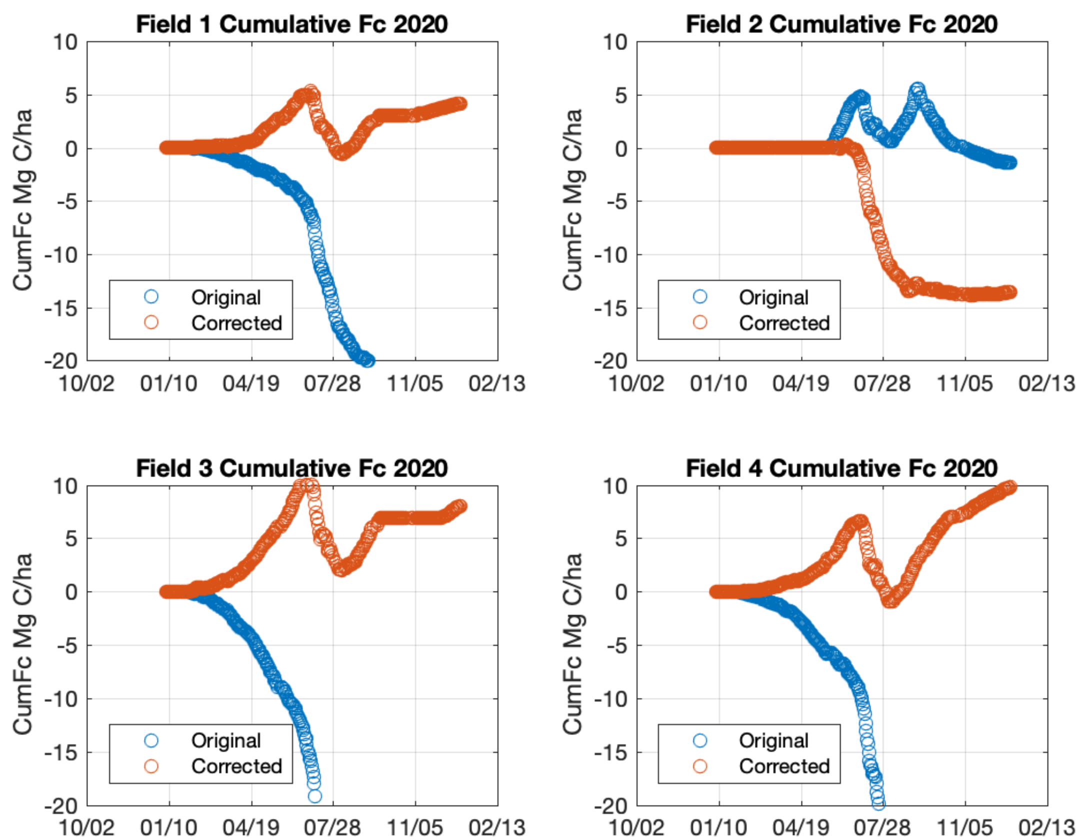

Figure 9. Cumulative CO2 fluxes 2021. The January and February 2021 period had problems with sample flow irregularities, and data have been omitted prior to March 1 (flat curve). The unusual directional change for the original data for Field 4 happened when the line orientation was switched at seeding.

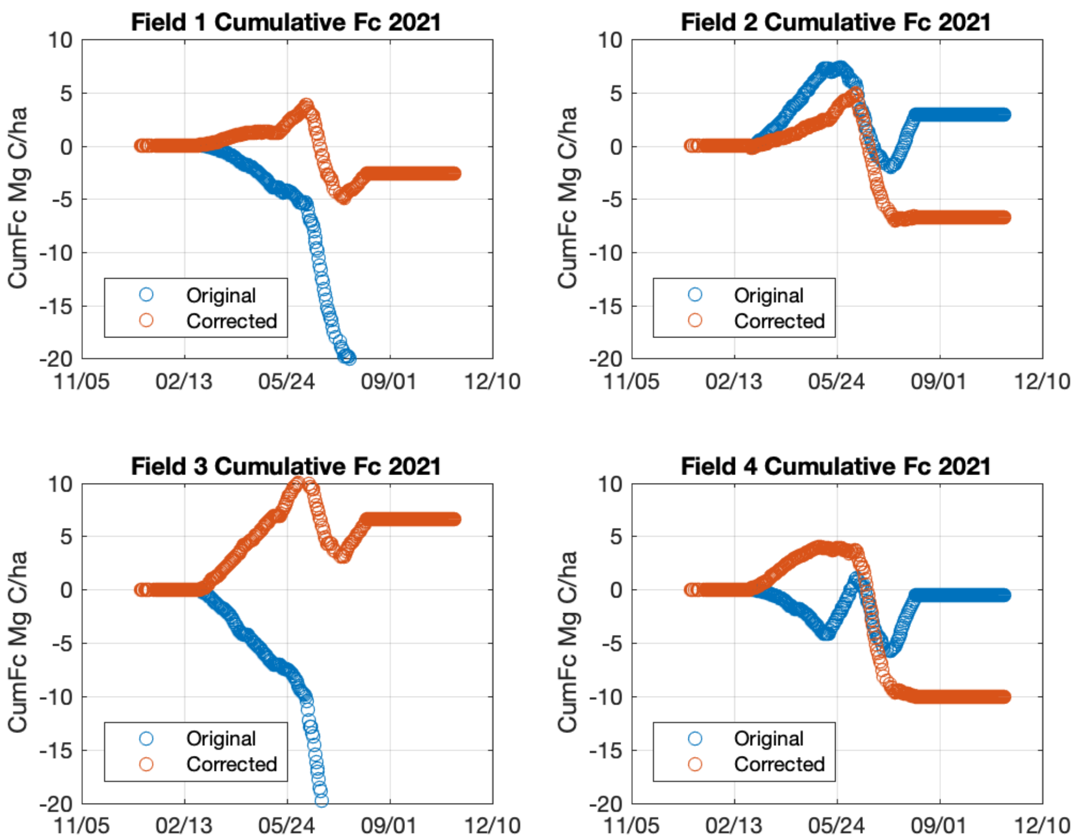

Recommendations:

1. The mis-matched lines from installation of the new system in Fall 2019 until the line replacement on October 29, 2021 has created a bias in concentration measurements. Although we have developed a correction for this bias, the correction adds additional uncertainty. The data can be used for scientific analyses providing that the corrections are reported in a transparent fashion (e.g., an appendix to a paper or thesis). There should be some caution about including these data in an open database for outside users.

2. Removal of the bias in the measured concentrations gradients for both N_2O and CO_2 appears to be feasible through development of a regression based on air temperature. The uncertainty is larger for warmer temperatures, with a maximum standard deviation of about 0.15 nmol N_2O/mol air for Sites 1, 2, and 4; and slightly larger for Site 3.

3. For the line pair of 1219FR/HP for Upper/Lower for Sites 1, 2 and 4; and HP/1300 for Upper/Lower for Site 3, we recommend the following bias corrections to be subtracted from the N_2O gradient (the bias should be added if the lines are reversed):
Site 1: Bias=exp(-2.576+0.0679(Ta))-0.0133,
Site 2: Bias=exp(-2.706+0.0745(Ta))-0.0095,
Site 3: Bias=exp(-1.103+0.0362(Ta))-0.13,
Site 4: Bias=exp(-1.985+0.0541(Ta))-0.0278,
where Ta is the air temperature (C) and the Bias is in units of nmol N_2O/mol air.
The bias needs to be scaled for application to the CO_2 gradient by the ratio of the CO_2/N_2O concentrations (i.e., umol/umol).

4. Implementation of the bias corrections might best be done in the coding where the fluxes are calculated. We also recognize that some additional quality-control may be needed before the final fluxes are determined.

7. APPENDIX C

Field Variability at TGAS
Brian Amiro. October 6, 2022

Goal: Evaluate the differences among the TGAS individual fields to help make decisions related to field averaging when comparing treatments.

Approach: Look at the carbon dioxide fluxes among the fields during years when we have a common crop and treatment. We will select **2014 (spring wheat), 2015 (soybean),** and **2016 (soybean).** This allows for a minimum of 2 years following the differential perennial (alfalfa) and annual crop comparisons. We will evaluate years individually, recognizing potential weather and crop differences. Note that the flux data are staggered so that we have no simultaneous measurements among the sites; hence, we will work with daily averages of the carbon fluxes to allow a common timeframe and to reduce some variability. Typically, missing data within a daily period affects all sites similarly (we do not fill gaps). We choose the carbon flux data because the nitrous oxide flux data are highly episodic and do not lend themselves well to a variability comparison.

Compare Individual Fields to the Mean of All Fields.

First, look at scatter plots of each field against the mean of all four fields by year. The 1:1 line is also plotted. This gives us some feeling for the differences among sites against a common average.

2014 Spring Wheat

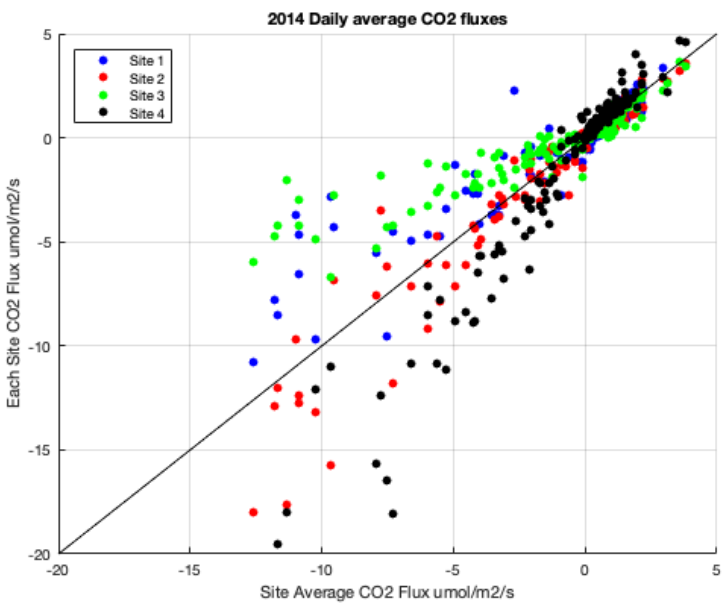

2015 Soybean

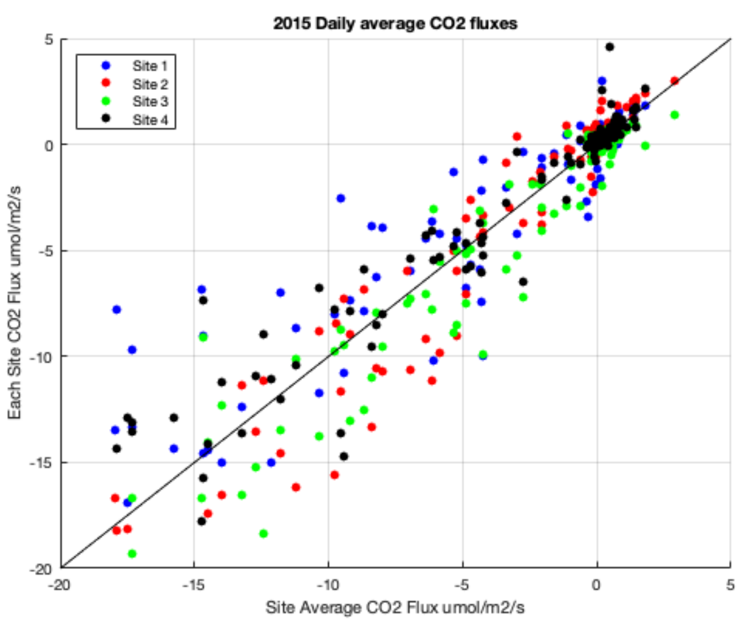

2016 Soybean

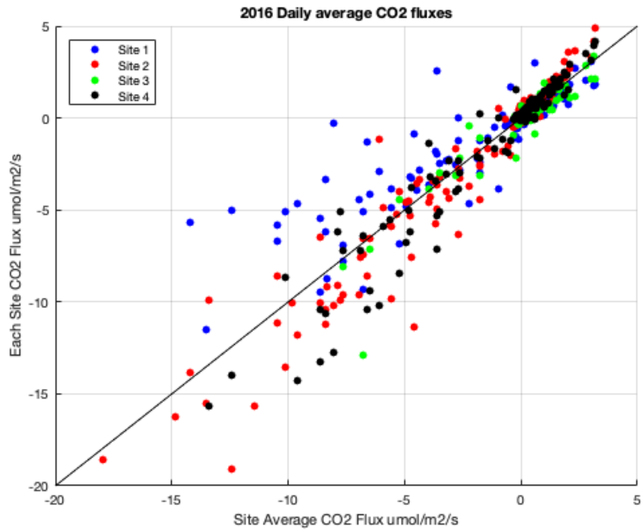

Now let's look at the statistics for the comparisons of each field to the mean of all fields.

Compared to Field Mean	**Field 1**	**Field 2**	**Field 3**	**Field 4**
2014 Spring Wheat				
r-square	0.85	0.93	0.84	0.91
Equation (x is mean; units umol/m2/s)	y=0.67x+0.082	y=1.13x-0.112	y=0.47x+0.205	y=1.72x-0.177
Field Mean (umol/m2/s)	-0.20	-0.71	-0.03	-1.06
2015 Soybean				
r-square	0.83	0.92	0.95	0.91
Equation (x is mean; units umol/m2/s)	y=0.78x+0.059	y=1.27x+0.084	y=1.18x-0.149	y=1.02+0.220
Field Mean (umol/m2/s)	-1.46	-2.25	-2.51	-2.05
2016 Soybean				
r-square	0.80	0.94	0.86	0.93
Equation (x is mean; units umol/m2/s)	y=0.64x+0.030	y=1.12x+0.042	y=1.07x-0.181	y=1.26x+0.030
Field Mean (umol/m2/s)	-0.87	-1.63	-0.08	-1.21

Compare East and West sides

Our ideal strategy is to have full measurements at all sites. Treatment differences are typically comparisons between the east (Fields 2 and 3) and west (Fields 1 and 4) sides. Let's look at how the sides differ, comparing the CO2 flux averages for each pair of fields.

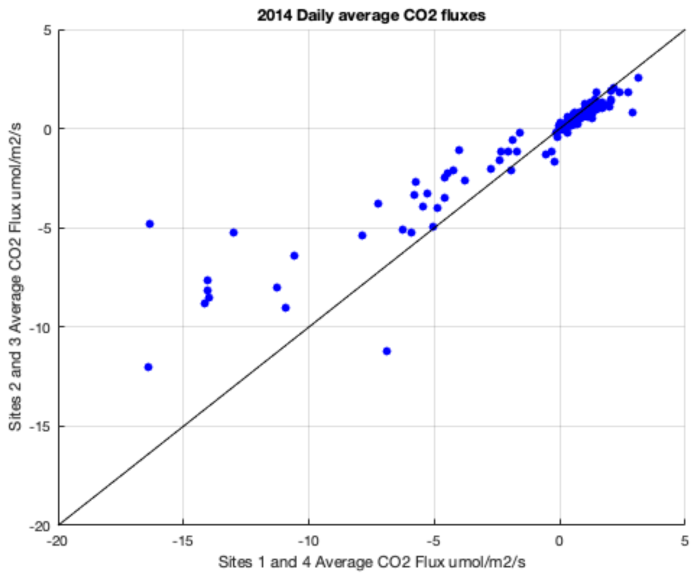

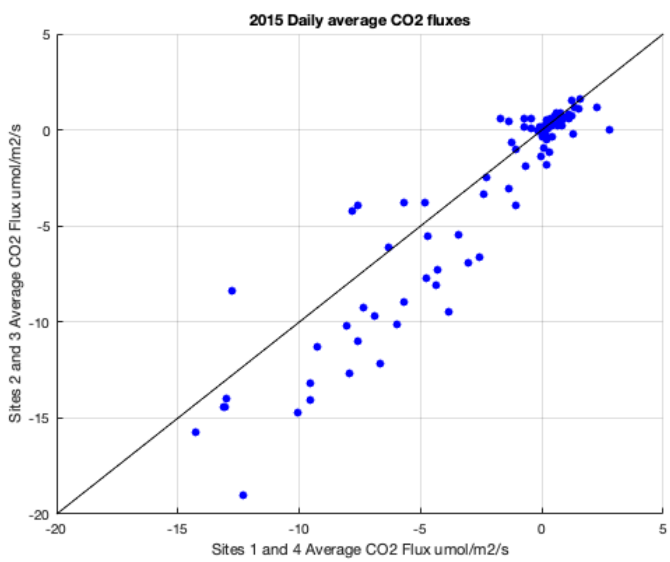

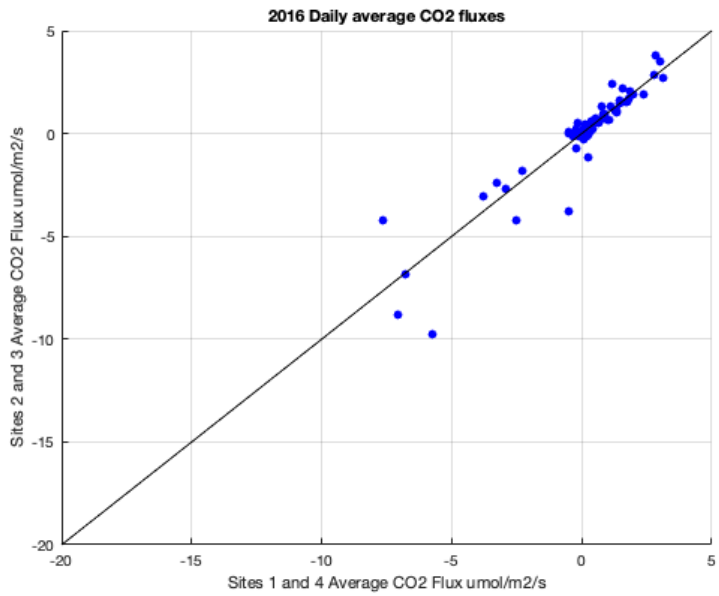

Table of East-West comparison

	2014	2015	2016
r-square	0.86	0.92	0.86
Equation (x is West side; units umol/m2/s)	y=0.61x+0.0264	y=1.37x -0.226	y=1.03x-0.047

Intercompare the Replicate Fields

Let's now look at the relative coherence between the pair of fields.

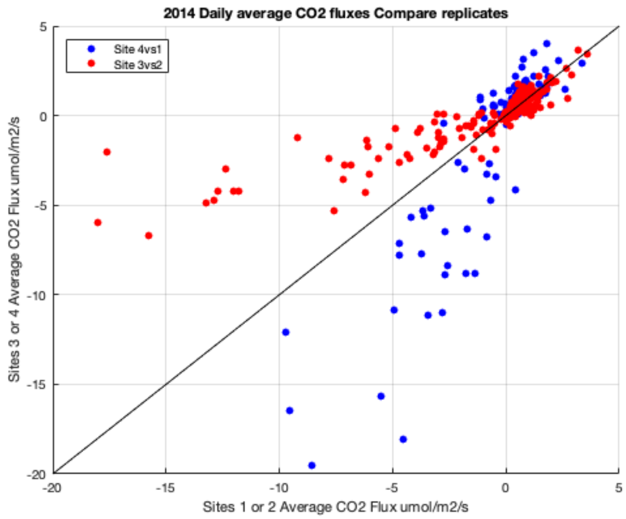

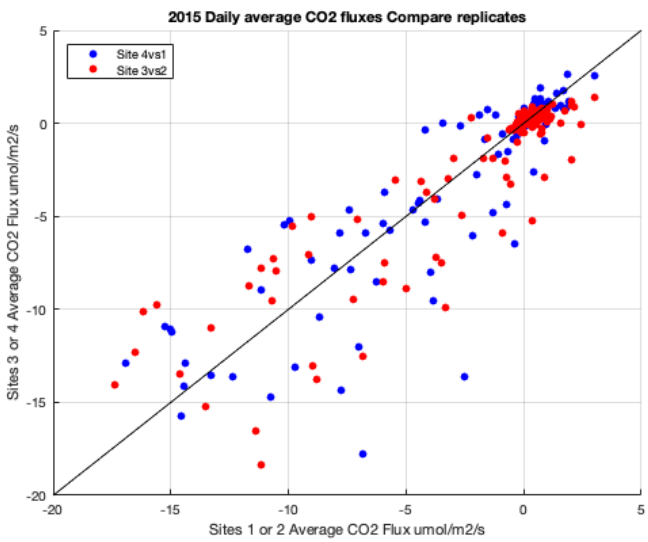

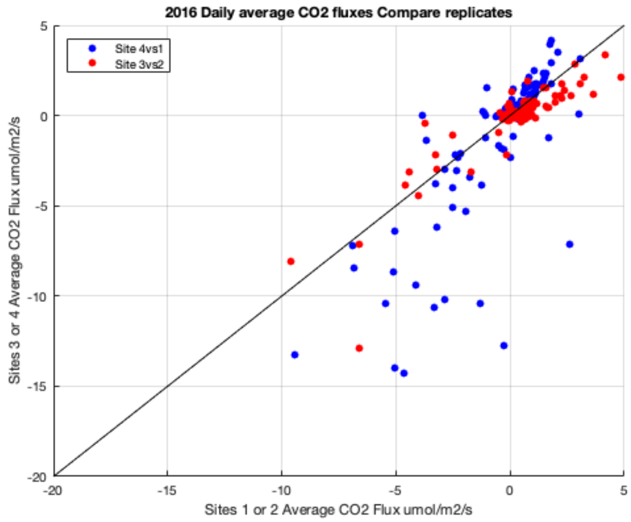

Table: Comparison of replicate fields

	2014	2015	2016
Field 4 vs 1			
r-square	0.78	0.69	0.75
Equation (x is Field 1; units umol/m2/s)	y=2.18x-0.409	y=1.00x -0.319	y=1.82x-0.40
Field 3 vs 2			
r-square	0.77	0.81	0.71
Equation (x is Field 2; units umol/m2/s)	y=0.38x+0.229	y=0.82x-0.437	y=0.81x-0.250

Overall Observations on daily average CO fluxes by year:

1. **Field 1** is generally less than the overall TGAS mean, while the other Fields have years that are closer to the mean, or slightly greater (i.e., Field 1 brings down the mean).
2. The difference between the East and West sides of TGAS can be as much as **+/- 40%,** depending on the year. However, the two sides were quite similar in 2016.
3. In comparisons between the Field replicates, **2014 may be an anomaly**. It has poor replication for both the East and West sides, and our NEP estimates in the 2017 carbon paper show an overall low NEP. **Field 3** seems to be different in 2014. We are aware that each field has some peculiarities that are often caused by drainage.

Interpretation for decisions related to Field averaging

1. We expect to have the **most confidence** when we have measurements at all 4 fields. Averaging the 2 fields in each treatment (typically East vs West sides) gives us better temporal and spatial coverage. Comparisons of the average of the east and west sides shows good agreement in some years (2016); East > West in 2015; and West > East in 2014. The differences between East and West in 2014 and 2015 are almost 40%.

2. In cases where we do not have data from all four fields, we could consider using data only from fields that match well. Although we see that there is variation among years, our best matches can be found by looking at regressions for pairs of sites. The Table below shows the regression slopes for all carbon flux data for the combined 2014 to 2016 period. We see that **Fields 2, 3 and 4 are reasonably matched**, within 5%.

Table: Regression slopes for all data 2014-2016.

Field	2	3	4	
1	1.38	0.43	1.67	
2		0.95	0.98	
3			1.05	

Overall, the **best pair of Sites** to compare is Field 2 and Field 4. Regressing the daily averages for 2014, 2015, and 2016 yields r-square= 0.89, with equation Site 4= 0.98 (Site 2) + 0.001 (units are umol/m2/s). Both the slope and the offset suggest that these two fields are the best pairs. However, we see that there are differences among years in the plot below.

Field 4 vs Field 2	2014-2016	2014	2015	2016
r-square	0.89	0.82	0.82	0.82
Equation (x is Field 2; units umol/m2/s)	y=0.98x+0.001	y=1.38x-0.104	y=0.69x -0.110	y=1.04x-0.154

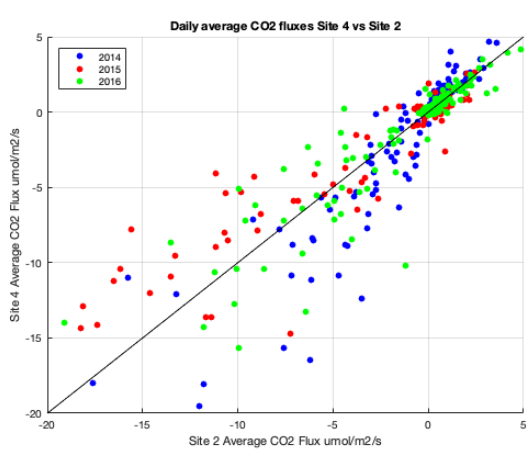

3. The agreement between Fields 2 and 4 is essentially the same as the agreement between the combined East vs West fields, even though we have half the temporal and spatial coverage. We suggest the following decision tree to be used for the carbon dioxide flux data to allow for the best treatment comparisons (East vs West fields). Although this is based on the carbon flux data, here may be some advantage to consider if this should also be applied to nitrous oxide fluxes.

Decision tree

Data Availability	**Action**
All Fields available	Average Fields 1/4 and 2/3; i.e., West vs East
Field 1 missing	Only use data from Fields 2 and 4
Field 2 missing	Only use data from Fields 3 and 4
Field 3 missing	Only use data from Fields 2 and 4
Field 4 missing	Gap in the west fields; assess impact of gap-filling
All Fields missing	True gap